UNIVERSITY OF TWENTE.

Faculty of Engineering Technology

Master Thesis

Sustainable Energy Technology

Examining the Integration of Renewable Energy and Storage Technologies in Commercial Office Buildings: A Zilverling Case Study

Torben Harm Jansen

Chair: Mathematics of Operations Research
Faculty: EEMCS

24.01.2024

Graduation Committee
Prof. Dr. Johann Hurink
Dr.ir. Gerwin Hoogsteen.
Dr.ir. Elham Shirazi

Master Graduation Assignment for the master's programme Sustainable Energy Technology

University of Twente
Enschede, January 2024

Abstract

This master's thesis introduces a method for analyzing the impact of integrating renewable energy production and storage technologies into commercial office buildings. The Zilverling building at the University of Twente serves as a case study, focusing on optimizing self-sufficiency while ensuring economic feasibility. Historical data on heating and electricity demand form the basis for incorporating renewable energy production and storage solutions. The versatile approach can be adapted at various stages to meet the specific needs of similar buildings seeking implementation solutions. The method offers insights into what can be achieved, addressing challenges such as limited data availability and data resolution. It utilizes a linear least-squares solver implemented in MATLAB. The building is represented as a block within the model, with the outer facade's surface area being a critical parameter. The impact of integrating insulation, solar panels, heat and electrical storage, and technologies like heat pumps is evaluated, proposing a combination of these technologies for advanced solutions with high self-sustainability. Economic feasibility is assessed through a multi-criteria analysis, resulting in Pareto front plots that consider self-sufficiency and self-consumption against investment costs. The payback time for the proposed solutions is also calculated. Additionally, the method allows for the evaluation of energy demand reduction and the determination of the degree of self-sufficiency. In the case of the Zilverling building, the proposed solution incorporates the installation of external wall insulation with a solar panel distribution of 2082 m^2, utilizing the facades and roof of the Zilverling, and a heat pump system with a heating capacity of 272 kW. To increase the self-sufficiency and self-consumption of this system, a battery with a capacity size of 462 kWh is proposed, achieving a total self-sufficiency of 46.29% and a self-consumption of 81.67%. The considered investment costs are in the range of 832,100€ ± 153,600€ with an estimated payback time of 5.89 years ± 1.09 years. In conclusion, this method, as presented in the thesis, can be applied to other cases and buildings, contributing to the transition from centralized to decentralized energy production and the development of smart grids by transforming buildings from passive consumers into active energy participants. The method supports realizing energy plans by examining the integration of renewable energy and storage technologies while ensuring efficient energy usage with high self-sufficiency.

Keywords: Renewable energy production, energy storage possibilities, MATLAB, self-sufficiency, economic feasibility, multi-criteria analysis, method, Pareto plots, linear least-squares solver

Acknowledgement

After five and a half years of studying at the University of Twente in Enschede, I am now writing my final piece of work, marking the end of an extraordinary period in my life – my student life. From a young man from the small village of Vrees in Germany, who completed his Abitur in 2018, I have evolved into a Master of Science. I am profoundly grateful for all the experiences I have gathered over these five and a half years and can proudly say that this period has been the time of my most significant personal development. My heartfelt thanks go out to everyone who joined me on this journey, from my Bachelor of Science in Advanced Technology to my Master of Science in Sustainable Energy Technology.

I extend my gratitude to all the friends I made along the way in Enschede, during my exchange semester at NJIT, and my childhood friends back home. Special thanks to my teammates over the years at v.v. Drienerlo and my Dispuut 2Pˆ2 , who made me feel welcome in the Netherlands and helped to make Enschede a second home. My time abroad in the United States allowed me to make many international contacts, for which I am incredibly grateful and hope to maintain.

I firmly believe that with the achievement of this degree, the knowledge acquired, and the connections made, the world is full of opportunities waiting for me.

Furthermore, I wish to express my appreciation to Prof. Dr. Johann Hurink for supervising my second study year in Sustainable Energy Technology, including planning my elective courses, overseeing my internship at CEC Haren, and being the chair of my Master Thesis. The past 1.5 years have been enriching, and I am thankful for always having someone with an open door to turn to for advice. I also extend my thanks to Dr.ir. Gerwin Hoogsteen for his guidance on this thesis. Your tolerance of my "quick questions" when passing by your office on the fifth floor of the Zilverling was much appreciated. Working on this master assignment with you has been a rewarding experience. My gratitude also goes to Dr.ir. Elham Shirazi for joining my graduation committee and taking the time to evaluate my final work.

Am Ende möchte ich meiner Familie danken. Ohne euch, Papa Gerd, Mama Silvia, Franka, Bennet, Oma Agnes und Oma Berta, hätte ich es nicht schaffen können. Danke für euer unendliches Verständnis und die Unterstützung, die ich erfahren habe. Ich weiß, dass das nicht selbstverständlich ist. Leider, können Opa Wilhelm und Opa Hermann meinen Abschluss an der Universität Twente nicht miterleben, aber ich bin sicher, sie wären genauso stolz wie ihr und ich. Dieser Abschluss ist nicht nur mein Verdienst, sondern auch euer. Jetzt werden wir sehen, was die Zukunft bringt.

In the end, I can say that the people make the experience special, and to each person involved in my time at the University of Twente, all I can say is: Thank you, Dankeschön, and Dank je wel!

Contents

Chapter 1

Introduction

Energy is an integral part of our daily lives, manifesting itself in various forms that we regularly encounter. It powers our homes and workplaces, enabling us to carry out both personal and professional activities. Whether it is the electricity that lights our homes or the heat that keeps us warm in winter, we often take the availability of energy for granted. What frequently goes unnoticed are the extensive efforts required to ensure a continuous supply of energy that meets the demands of customers.

The provision of energy involves a complex supply and demand chain. Currently, this process encompasses the extraction of fossil fuels and raw materials, which are then transported to centralized energy generation facilities. These facilities produce energy, which is transmitted and distributed by energy companies and ultimately sold to end consumers through energy service providers. The schematic representation of this value chain can be observed in Figure 1.1. However, this conventional value chain is undergoing a transformation in response to the challenges posed by climate change. We are fundamentally changing our energy sector, marked by a transition towards decarbonization and the incorporation of renewable energy sources.

This energy transition is characterized by a restructuring of our power grid, the development of policies at EU, governmental, and municipal levels, and active participation from consumers. Achieving this transition necessitates innovative solutions, among which is the reduction of centralized load on the power grid and a minimization of the utilization of transmission networks in a centralized setting. Simultaneously, it involves enhancing self-sufficiency and ensuring resource security at the local level. These transformative goals influence both the producer and consumer sides of the energy value chain. To steer the transition towards sustainable decentralized energy production, it is essential to adopt general methods that can adapt to this new type of energy production, distribution, and demand effectively.

In this broader context, the application of the three elements of the Trias Energetica [1] becomes relevant:

1. Reducing energy demand.

2. Utilizing renewable energy sources for production.

3. Using fossil fuels efficiently and with minimal environmental impact only when necessary.

Here, measures and investments are crucial in the residential, commercial, and industrial sectors, reshaping buildings and districts to contribute to achieving climate targets, aiming for a 55% reduction in greenhouse emissions by 2030 compared to 1990. The European

energy transition involves shifting from centralized fossil fuel-based energy production to renewables like wind, hydro, and solar [2]. Further, Energy reduction is also pursued through the introduction of more efficient technologies and minimizing losses, such as improved insulation in buildings. Considering the energy transition in the planning of new building projects as well as renovation of existing buildings is required to achieve the climate targets and the aimed-for reduction.

In the context of this thesis, a method is introduced specifically tailored to incorporate solar energy production and storage technologies into commercial office buildings. The chosen case is the Zilverling building, situated on the campus of the University of Twente, providing an example of the possibilities in the renovation of existing buildings.
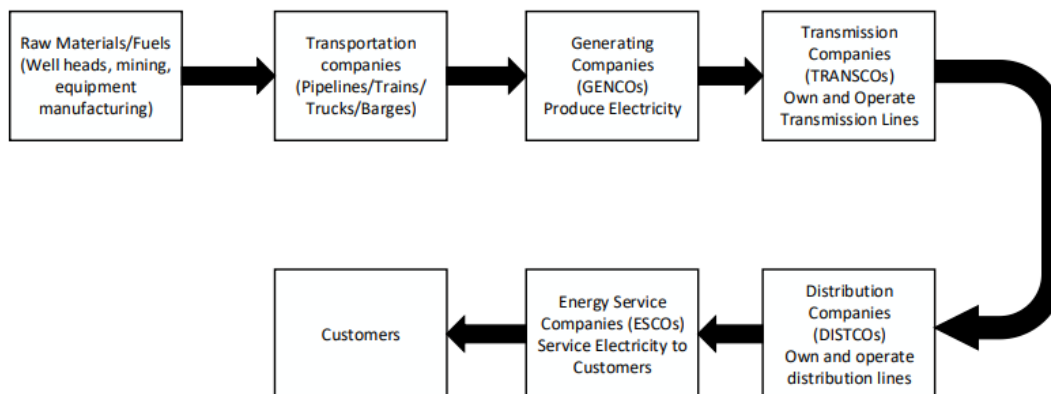

FIGURE 1.1: Supply and Demand Chain of the Modern Electricity Market [3]

1.1 Smart Grids

In the energy transition, the energy industry is shifting from centralized energy production regulated by the producer to a more decentralized and interactive energy production model involving consumers, making them active prosumers. To facilitate this change, the electricity grid is evolving into what is commonly referred to as a smart grid. This smart grid incorporates the philosophies, concepts, and technologies that also enabled the development of the internet [4]. The key characteristics of a smart grid, as outlined in [5], include:

- Distributed renewable energy resources.

- Distributed fixed & mobile energy storage.

- Distributed data sources and vast information size.

- Active demand-side contribution.

To facilitate this transition, it is essential to consider these characteristics and to bring energy production closer to the point of energy consumption. Consequently, changes have to occur on the consumer side of the energy value chain. These changes are localized and impact the daily lives of consumers.

An illuminating example of the potential benefits of a smart grid emerged on Jeju Island in South Korea [6], where the focus encompasses smart power grid infrastructure, efficient

power usage, electric vehicle adoption, reliable energy management, and innovative electricity services. This case highlights the capabilities and advantages of smart grid systems, demonstrating a significant transformation in infrastructure, usage patterns, transportation, energy management, and services within the energy sector.

Within the energy sector, buildings play a significant role in this transition, accounting alone for 43% of the overall energy consumption in the European Union, encompassing electrical, heating, and cooling demands [7]. Therefore, it becomes imperative to integrate renewable energy production and storage solutions into both residential and commercial buildings and to incorporate a decentralized energy production concept. This approach necessitates prosumer activity and aligned policies, requiring collaboration among various stakeholders to achieve the overall goal of the energy transition.

1.2 Governmental Initiatives & Policies

Current initiatives for the integration of renewable energy production are exemplified by the city of Münster, which has made it obligatory to install a photovoltaic system of at least 1 kWp per residential unit in new building projects [8]. Additionally, in Germany, there is a mandate to install heating systems that run on 65% renewable energy sources per setup in new projects. The objective is to promote the use of heat pumps and to install 500,000 heat pumps annually from 2024 onwards, focusing on both new building projects and renovation efforts for existing buildings [9].

Likewise, the Dutch government has outlined its policy and measures to achieve greenhouse gas emission reductions in the Climate Act, which includes the National Energy and Climate Plan (NECP) and the National Climate Agreement. The goal is to ensure that these reductions are both achievable and economically viable for all stakeholders. The approach prioritizes a cost-efficient transition that minimizes the financial burden on households and aims to equitably distribute the costs between citizens and businesses. The government plans to implement these measures gradually, prioritizing a methodical and sustainable approach rather than rushing through the process [10]. The sectors targeted for these measures encompass the built environment, mobility, industry, agriculture, and electricity. Furthermore, cohesion across various sectors is promoted. In addressing the built environment, the Dutch government is adopting a district-based approach. Solutions are customized and can differ from district to district, depending on factors like building density and the type of buildings, whether they are high-rise buildings or individual homes. This approach centers on achieving cost reductions through tailored insulation solutions and the installation of heat pumps, with the aim of reducing the reliance on natural gas for heating. Additionally, it seeks to enhance the financial attractiveness of local electricity production by applying lower taxation rates. Lastly, the plan is to make renovation projects appealing by offering favorable loan conditions [11].

1.3 University of Twente's Policies

The transition towards renewable energy is clearly multifaceted, spanning various sectors, and is shaped by the policies and regulations put forth by municipalities, governmental bodies, and the European Union. In the context of this thesis, a methodology for integrating renewable energy production and storage technologies into commercial office buildings is proposed, with a specific focus on the Zilverling building situated on the University of

Twente campus. Therefore, it is imperative to consider the university's energy policies. The University of Twente has established sustainability objectives for its campus. These objectives are centered around several themes, including buildings, energy, travel and mobility, waste, food and drinks, water, biodiversity, procurement and purchasing, as well as events [12]. Furthermore, the University's Shaping2030 mission aims to mold individuals, connections, and society towards an open, inclusive, entrepreneurial, and sustainable mindset, incorporating the 'High Tech Human Touch' philosophy into its vision [13]. Consequently, the University of Twente is actively engaged in the energy transition on the consumer side of the energy value chain. The university not only educates its community to actively participate but also sets defined energy transition goals in pursuit of climate targets. This proactive stance reflects the commitment of the university to sustainable and responsible energy practices.

The energy plan for the buildings at the University of Twente is illustrated in Figure 1.2. This plan outlines the overarching objective of achieving energy-neutral buildings on the campus by 2050. Specifically, there is a concerted effort to phase out the consumption of natural gas and reduce carbon dioxide (CO_2) emissions from the buildings by 49% till 2030 compared to 1990 levels. To work towards these ambitious goals, several key initiatives are underway. By 2022, buildings attained an energy label of C, signifying a certain level of energy efficiency. A sustainable maintenance plan is being implemented to ensure the long-term efficiency and sustainability of these structures. Furthermore, an energy monitoring system is being deployed across all buildings to closely track and optimize energy usage.
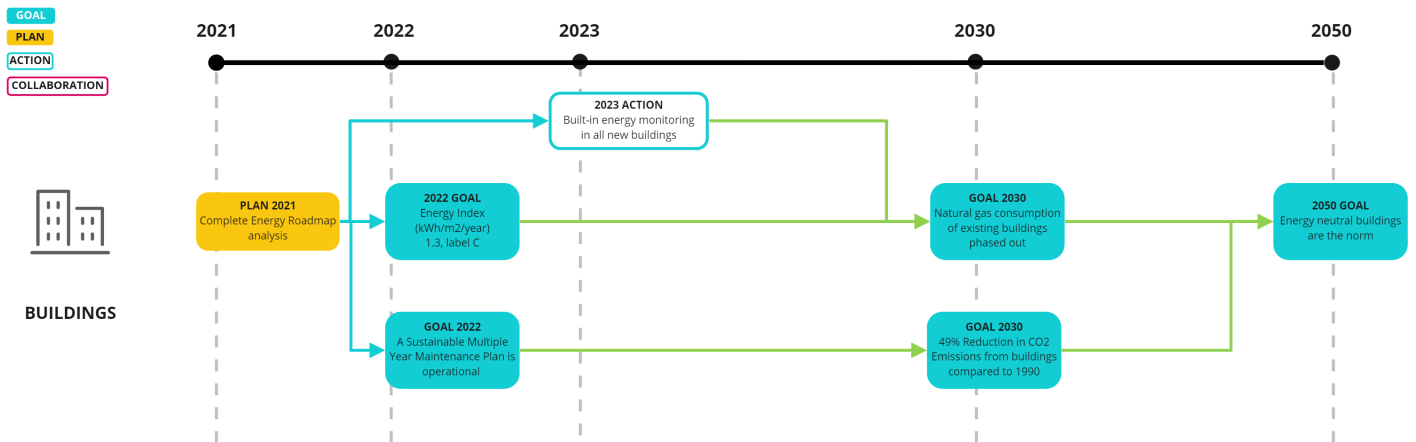
FIGURE 1.2: Energy Plan for Buildings by the University of Twente [12]

For each building, more detailed and specific plans are outlined in the "Routekaart Energietransitie Universiteit Twente" [14]. This document serves as a long-term strategic plan covering the years 2020-2030. The plan highlights the necessity of renovating existing buildings to ensure they meet the established sustainability standards. It further includes a multi-year financial framework and emphasizes the need for flexibility during the renovation process, which is why the renovations are executed in phases. For the Zilverling this plan specifies the intention to renovate it in the years 2024/2025. Therefore, this thesis aims to provide potential solutions to be incorporated into the renovation project for the building while presenting a method that can also be applied to other buildings. The

starting point of the Zilverling is here an energy certificate label of C [15].

1.4 Problem Statement

In the context of the energy transition, a restructuring of the power grid from centralized energy production to decentralized and interactive energy production in a desired smart grid is needed. In a broader context, the three elements of the Trias Energetica [1] need to be applied to buildings, along with the inclusion of the four key characteristics of a smart grid [5], to transform buildings from passive energy consumers to active energy participants. Here, governmental initiatives and policies on different levels promote the integration of renewable energy production, energy storage solutions, and energy-saving measures. This integration has to be steered, as renewable energy production is weather-dependent, to ensure resource security at a local level and to avoid centralized loads and grid congestion. It is not only important to generate sufficient amounts of energy, but also the timing and amounts of consumption are essential. Therefore, the goal is to generate and supply enough energy during the day to fulfill the current demand, increasing self-sufficiency, but also not to overgenerate too much energy and consume most of the generated energy directly, thereby increasing self-consumption. Therefore, the installation of a renewable energy production system is not necessarily targeted to provide the maximum power output. To achieve efficient, sustainable, and decentralized energy production, general methods that can adapt to this new type of energy production are required.

This thesis introduces a method to analyze the effect of incorporating solar energy production and storage technologies into commercial office buildings, using the Zilverling building situated on the University of Twente campus as a case study. The primary goal is to enhance the self-sufficiency of the building while providing a versatile approach that can be adapted at various stages to meet the specific needs of similar buildings seeking implementation solutions. The method provides insight into what can be achieved, thereby particularly addressing challenges such as limited data availability, data resolution, and lack of additional information. Further, the method is design-oriented, and ultimately, the goal is to provide an engineering-friendly and straightforward approach for estimating the impact of such implementations on self-sufficiency without relying on high-resolution data. In the case study, the architecture of the Zilverling building and its demand data are used in a simplified freestanding scenario, assuming no influence of surrounding structures like shadow falls. The example is used to demonstrate the contribution of the methodology to the broader transition toward decentralized, green energy production. The aim is to combine energy production and storage solutions within the renovation of existing buildings. The central research question is:

- **How can the integration of renewable energy and storage technologies in commercial buildings achieve a high level of self-sufficiency while remaining economically feasible?**

Throughout this research, several sub-questions emerge, including inquiries about the sequence of methodology steps, the impact of storage sizing, and the influence of algorithm flexibility and data availability. The subquestions are:

- What is the impact on self-sufficiency of a different prioritization of energy usage?

- How does the storage size influence self-sufficiency and investment costs?

- How do the resulting solutions differ with regard to larger flexibility and data availability?

1.5 Outline

In this chapter, an introduction to the energy transition with its resulting challenges and goals, smart grids, current initiatives, government policies, EU policies, the University of Twente's policies, and the problem statement with its research questions have been discussed. In Chapter 2, the specific background for this research is presented. Here, the energy transition, possible renewable energy production technologies and hybrid systems, energy storage technologies, data availability, and methods for selecting active surfaces for solar production are considered. In Chapter 3, the developed method is presented. It is applied to the Use-Case of the Zilverling, presented and defined in more detail in Chapter 4. The achieved results are presented in Chapter 5, followed by a discussion in Chapter 6 and the conclusion in Chapter 7.

Chapter 2

Background

The background of this thesis encompasses a range of crucial topics, including the energy transition, renewable energy production options, hybrid solar energy and heat pump systems, energy storage systems, data availability and active surface selection for solar energy production. These topics are connected to the first three key characteristics of a smart grid shown in Section 1.1 before. Therefore, they provide a comprehensive context for the research and analysis conducted in this thesis. A summary of the background for the case study is concluded at the end of this chapter.

2.1 Energy Transition

The energy transition aims to reduce greenhouse emissions by shifting away from fossil fuels and embracing renewable energy sources like wind, hydro, and solar power. However, it is arguable that what is happening is more of an energy addition than a true transition. While renewables are growing rapidly and making up a larger portion of overall energy production, the overall energy consumption continues to rise as well [16]. For context, the annual growth rate of renewables averaged 12.6% from 2011 to 2021 [17]. Historically, established energy sources have not seen sustained declines when new sources were introduced. Instead, overall energy consumption has continued to grow over two centuries, and a complete replacement has not yet occurred [16]. This increase in overall energy consumption can be explained by the rising population and the developed growth of new infrastructure and energy availability across the globe.

To achieve a genuine energy transition, rather than an energy addition, two key points are essential. First, there must be a focus on developing the necessary infrastructure and expanding the production of new energy sources (renewables). Second, there should be a genuine reduction in the use of more established energy sources (fossils) [16]. This approach aligns with the first two elements of the Trias Energetica [1]. A shift in market economies is necessary, placing a higher value on conservation over relentless profit pursuit. Governmental regulations play a key role in confronting the power industry and actively instigating change. This might include phasing out fossil fuels, capping the growth of overall electricity production to control the capacity of the grid, and influencing changes in consumer behavior regarding how energy is produced and consumed in society [16].

In the transition, the pace of measures and the commitment of governments are critical factors. The 2015 Paris Agreement marked a global commitment to move toward a low-carbon economy, signifying the necessary political will to facilitate a faster transition and the readiness to invest in the required infrastructure. In this context, political will plays a vital role in making a transition possible, which is different from historical patterns. The

energy transition is not solely a technological and economic endeavor, it also encompasses political, social, and cultural aspects that are essential for expediting a low-carbon transition. In this new era, the focus on reducing energy demand and improving energy efficiency can become the "new normal" [18].

There are also opposing opinions claiming that energy production based on all existing sources will continue to increase regardless, and the belief that renewable sources can solve global problems is viewed as harmful and unrealistic [19].

Nevertheless, it needs to be stressed that it is a race against time, and a transition needs to be established to avoid the overexploitation of the limited energy potential of the earth. This shift towards cleaner and more efficient energy practices will have far-reaching implications for society and the environment. The integration of renewable energy sources alone is not the sole solution to fighting climate change. Furthermore, the complete substitution of fossil fuels without changes in consumer behavior and involvement is not feasible. The introduction of a smart grid, as introduced earlier, is a necessary step in achieving an energy transition. With its four key characteristics, it offers a solution that spans technological, economic, political, social, and cultural aspects. However, each of the four key characteristics brings challenges with them.

2.2 Renewable Energy Production & Hybrid Systems

Examining the key characteristic of "Distributed renewable energy sources", it is essential to install distributed renewable energy sources. They are the key energy source in a decentralized energy grid and are the supply of the system.

Renewable energy sources (RES) are widely regarded as environmentally friendly due to their role in reducing carbon emissions in the energy sector. These sources include solar, wind, biomass, hydro, tidal, and ocean power generation, each with distinct advantages and environmental impacts that make them suitable for different situations. The current share of these generation types can be observed in Figure 2.1.
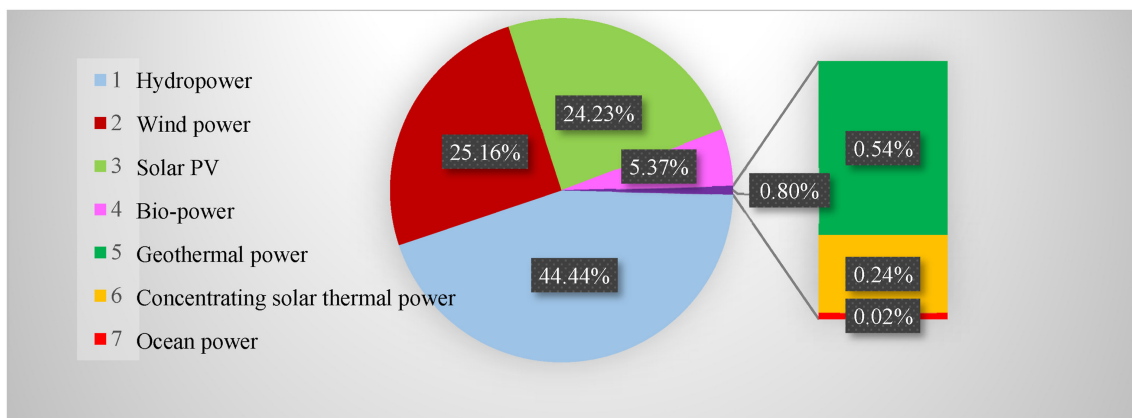
FIGURE 2.1: Electrical Power Generation Share by Renewable Energy Source [20]

It can be seen that hydro, wind, and solar power generation hold the three largest shares, with each having varying environmental impacts based on factors like source type, scale, usage method, location, and additional considerations.

Hydroelectric power has a promising environmental potential but generates only a fraction of the total power compared to other sources. Wind turbines have relatively lower environmental impacts compared to other sources but require significant space for installation and

may not be suitable for densely populated areas. Solar power generation involves the use of materials with detrimental environmental effects. However, the abundance of existing solar power sites and the potential to utilize rooftops and densely populated areas offer significant advantages, minimizing the impact on open land [20].

In short, all renewable energy sources have a substantial environmental impact. The suitability of each source depends on the specific situation and installation settings.

In general, a mix of different energy sources is desired for resilience and reduced weather dependencies. Solar energy production, with its widespread availability and unaffectedness from installation size, serves as a reliable option. Less accessible wind energy can be employed to augment and support energy production on cloudy days or nights, for example [21]. Therefore, the intended purpose of the chosen technology needs to be a key consideration in the decision-making process for larger environmental plans by policymakers, stakeholders, and decision-makers in the energy sector [20].

In urban areas, the selection of renewable technologies is based on their availability and safety. These technologies typically include solar heater collectors, photovoltaic panels, and (ground source) heat pumps, which can be combined into different hybrid systems. Solar panels are a popular choice for electricity generation but require substantial installation space, seasonal tilting, and regular cleaning. Geothermal systems, on the other hand, are reliable with low maintenance needs but involve specialized initial installation [22].

To determine the sizing and installation of renewable systems for different building types (residential, commercial, or industrial), specific energy demand information is essential. The distribution of energy usage varies for each building type, making the demand profile for electricity and heating a crucial factor in selecting the appropriate energy production system. In this context, photovoltaic panels are well-suited for electricity production, while heat pumps provide a reliable and cost-effective source of energy. Combining solar panels and heat pumps creates a relatively self-sufficient system. To ensure maximum efficiency, it is vital to use the produced energy effectively and prioritize energy-saving measures to protect the environment by reducing the energy demand [22].

To achieve an energy-efficient and cost-optimal on-site renewable energy supply not only the implementation of renewable sources is important but also the maximization of their utilization. Here, incorporating energy-saving measures, such as insulation, is essential. This demands significant changes to existing buildings and the renovation process needs to consider factors like financial and legal constraints as well as socio-economic and technical limitations. Financially, it is often a challenge for building owners to turn a profit from these investments. Organizational aspects as well as social acceptance of the architectural changes play a vital role as well, resulting in a positive perception of incorporating renewable energy production into existing buildings [21].

For renewable energy production, combining solar panels with heat pumps in a grid-assisted setting is a practical choice. The size of the system is determined by the relative cooling and heating load. To design a cost-effective system, an understanding of the annual power consumption profile is important for the heat pump. Here, a practical orientation point is to size the solar panel installation at least large enough to independently power the heat pumps during summer and be situated on the building. A reference point can be the weekly peak of electricity demand required [23].

In summary, these hybrid systems offer the best solution to reduce CO_2 emissions and promote renewable energy production. The main parameters influencing the choice include costs, environmental considerations, reliability, installation, maintenance, and usability. Solar electricity production can be the easiest implemented, and heat pumps offer attractive efficiency and environmental benefits [22]. However, this configuration does have two

notable disadvantages. First, during the winter, solar panels can only meet a fraction of the electricity demand. Second, during the spring and fall, the panels produce more energy than required. But these disadvantages can be effectively addressed by integrating seasonal thermal storage and including batteries in the system, ensuring that all the energy produced is put to good use, maximizing the utilization of renewable energy throughout the year [23].

Cost expectations for solar panels, heat pump systems, and external wall insulation can be found by comparing procurement costs and costs for electrical installation and montage. For 420 wattpeak solar panels a price of 84.46€ on average per solar panel was found by comparing prices of different seller websites with a standard deviation of 9.11€. The installation costs for solar power can be expected to be 550€ ± 150€ per kWp, depending on the amount of electrical installation and the montage of the system [24]. Further, the cost of a heat pump can be found using the formula $C_{HP} = 2282 \cdot q^{0.652} \cdot COP^{0.032}$ with a deviation of 15% in CA\$, where q is the heating capacity in [kW] and COP the cooling COP of the heat pump [25]. The cost expectations for simple external wall insulation depend on the material used. Here, on average the costs are expected to be 96.67€ ± 20.66€ per m^2 including installation costs. Energy demand reduction up to 30%-40% are possible to be achieved [26].

In the end, the final design decision depends on the vision of the implementing party and the overall budget. Regardless, prioritization of energy efficiency and minimizing energy waste should be promoted. Measures therefore are improved insulation, energy-efficient lighting and appliances. The implementation of a smart control system is further desirable, in combination with energy storage solutions. Different configurations are possible, considering varying climate conditions and building types. The appropriate configuration is determined based on local conditions and limitations. A universal decision-making framework is required to guide the management and design of self-sufficient buildings that incorporate renewable energy solutions [21].

2.3   Energy Storage

Examining the key characteristic of "Distributed fixed & mobile energy storage", it is essential to install energy storage systems to maximize the utilization of time-dependent renewable energy production. Therefore, in a decentralized setting, the combination of RES and energy storage systems is crucial to ensure a reliable and consistently available energy supply for the end user.

The selection of an energy storage system is influenced by various criteria, including energy/power density, overall efficiency, lifespan, cycle life, self-discharge rates, costs, scalability, application, technical maturity, and environmental impact [27]. Therefore, it is essential to design storage according to each specific case, considering the type of storage (short-term or seasonal), storage medium, acceptable losses, and input/output system. Different types of energy storage are illustrated in Figure 2.2 together with applied technologies for each type. It is possible to install chemical, mechanical, electromagnetic, or thermal energy storage. Depending on the energy production and the release time of the storage, different technologies are suitable for case-dependent decision-making.
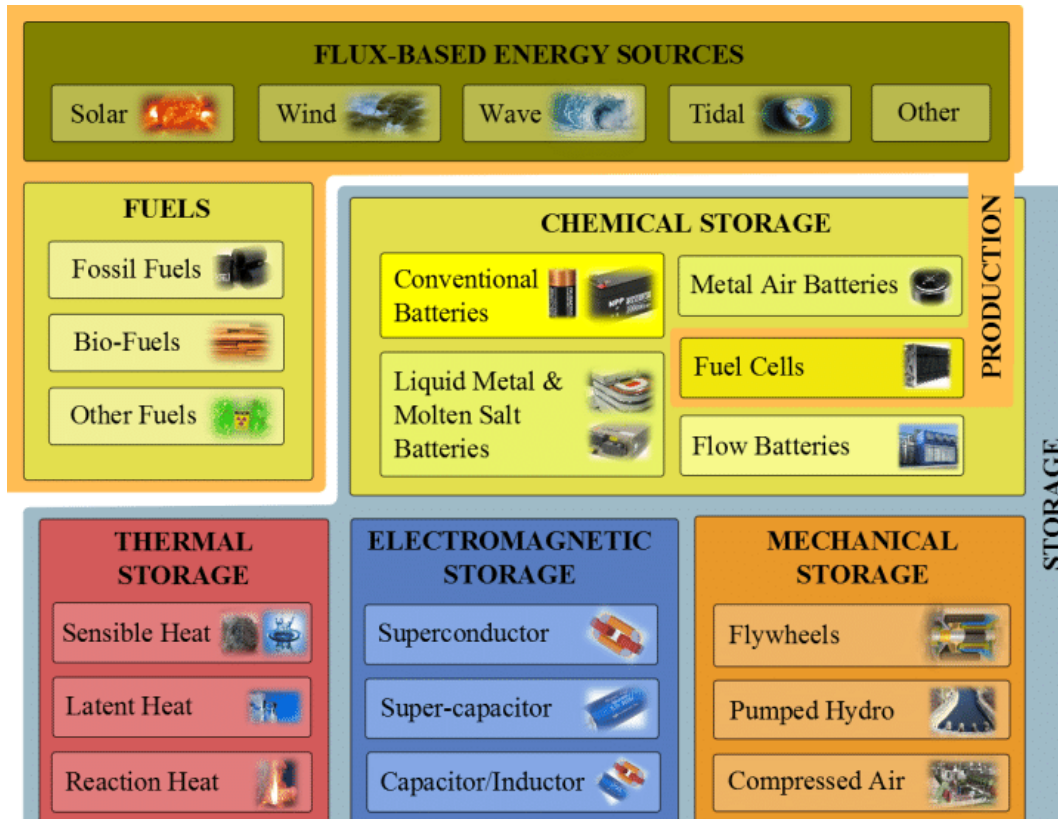
FIGURE 2.2: Different Energy Storage Technologies [27]

Here, storage systems are categorized into small-scale, medium-scale, and large-scale, with corresponding power ratings of smaller than 1 MW, 10-100 MW, and greater than 300 MW, respectively. Applications range from mobile devices, electric vehicles, and satellites for small scale, to office buildings and remote communities for medium scale, and power plants for large scale. Here, more applications are possible for each category [27].

Based on the storage duration, energy storage systems can be used for Power Quality and Regulation ($\leq$ 1 min), Bridging Power (1 min - 1 h), and Energy Management ($\geq$ 1 h). Energy management applications include seasonal storage and annual smoothing ($\geq$ 4 months), renewable integration and backup (hours-days), and peak shaving/generation/time shifting (1-10h) [28].

As stated before, the focus of this thesis is on the integration of solar energy production and heat pumps and the utilization of this system combination can be maximized through thermal and battery storage [23]. Typically, battery storage is used to store electric energy to supply the heat pump system with energy during low solar radiation times, while thermal energy storage is installed between the heat pump and the receiving building as a buffer system [29],[30].

For batteries, different chemical compositions can be used, such as Nickel–Cadmium (NiCd), Lead-Acid (Pb-Acid) and Zinc-Manganese (ZnMn). The most established battery is the Lithium-Ion (Li-Ion) battery. All the compositions are mature technologies ready to be implemented [27]. Cost-effective solutions can be systems like the INTILION scalebloc, scalecube, and scalestac, allowing a scalable indoor or outdoor installation with battery racks of 154 kWh steps [31]. With a Li-Ion battery pack price of 152$/kWh [32] and an assumed installation cost of 225$/kWh [33] the battery size can be scaled with an ap-

proximate price of 377\$/kWh $\pm$ 10\$/kWh. The designed life duration is 15 years with an efficiency of 90% and a C-Rate of 0.9688 [31]. The storage period can last from days to months [27].

For thermal energy, sensible heat, latent heat, geothermal, and thermochemical storage types can be applied. Sensible heat storage is suitable for district heating with a variety of capacities, charge/discharge rates, high heat capacity, and low costs. Geothermal systems are useful for seasonal thermal storage in combination with solar energy systems [34]. For sensible heat storage solutions materials ranging from water to soil, clay, sand, granite, marble, limestone, sandstone, slag and graphite can be used, each having different specific heat coefficients, densities, and conductivities. Here, for long-term thermal storage, hot water tanks can be used, often made from steel or concrete with stainless steel or plastic liner inside and advanced heat insulation minimizing heat losses [35]. The life duration of these tanks is from 20 to 40 years, have an efficiency range from 70% to 95%, and costs averaging 15€/kWh [36] $\pm$ 10€/kWh [34], the storage period can last from days to months, and power outputs from 0.001 - 10 MW are possible [37].

2.4 Data Availability

Examining the key characteristic of "Distributed data sources and vast information size" reveals the critical role of data availability.

In a decentralized energy grid, achieving demand-side management and bottom-up control is essential to align consumption and production, efficiently use storage, curtail energy production, and enhance flexibility. Data plays a vital role in predicting flexibility and uncontrollable loads, such as renewables, on a local level. It is needed for planning the use of devices in future periods and for enabling real-time control of energy systems [38].

Real-time control relies on reliable networks with low latency and high security levels to safeguard distributed energy information and communication. The control and management applications include smart metering, automated demand response, inter-substation response, distribution automation, synchrophasors, SCADA systems, electric vehicles, and microgrid connectivity. With a decentralized, data-oriented, flexible, and efficient information infrastructure, demand responses for various consumer demand parameters can be achieved. These responses can be correlated with weather data to predict and control energy consumption in residential, commercial, and manufacturing sectors. All of this must be conducted while ensuring the quality of service to meet the demand [5]. For instance, the information infrastructure of the Jeju Island test bed recorded data at a rate of 60 samples per second [6].

Demand responses can be fine-tuned toward specific objectives thanks to their inherent flexibility. These objectives can encompass profit, grid load, self-sufficiency, self-consumption, or a combination of these factors represented in a single performance metric and others. However, the data required for implementing these demand responses is essential, necessitating the installation of smart energy metering systems and the availability of historical and current energy consumption data. With this data in hand, algorithms can be applied to align energy production and consumption more effectively in line with the established objective.

Efficiently sizing storage and local energy production systems is essential. To accomplish this, data regarding the expected power output from sources like wind and solar energy, as well as the expected demand, are crucial. This information is used to simulate storage scenarios in both off-grid and on-grid situations [39].

For hybrid renewable energy systems that combine production and storage, along with standalone renewable production systems, the accuracy of data related to connected loads is a key factor in allocating system capacity. In particular, having data with smaller time steps for peak characteristics of solar irradiation and wind speeds is preferred to ensure more reliable results when compared to optimization processes that rely on hourly, daily, or monthly data [40].

However, it is worth noting that this data might not always be readily available, and in some cases, prediction or data imputation may be necessary. For example, energy monitoring in all University of Twente buildings is set to be completed in 2023 [12], as depicted in Figure 1.2. Consequently, the availability of data may still be limited. Next, it is crucial to examine the data's structure and resolution and make assumptions to compensate for any lack of detail or insufficient data, considering factors like location, size, and resource availability.

In cases where data imputation is required to construct an appropriate demand profile using available data, various methods can be considered for this purpose. These methods include Mean/Median, Most frequent, Zero/Constant, K-nearest neighbor, Multivariate Imputation by Chained Equation (MICE), Deep Learning, Stochastic Regression Imputation, Extrapolation, Interpolation, and Hot-Deck Imputation, as outlined in [41].

Ultimately, with an accurate demand profile in place, the integration of renewable energy production and storage technologies can be assessed and implemented, and the resulting system can be sized accordingly.

2.5   Active Surface Selection for Solar Energy Production

For sizing on-site solar energy production, active surfaces on the building of implementation need to be determined. Typically, the selection of active surface areas for solar production is based on an irradiation threshold, ranging from 600 to 800 kWh/m^2 per year, especially for high-rise buildings characterized by a substantial facade-to-roof ratio, such as skyscrapers and commercial office buildings [42].

Hereby, there is a notable gap in methods tailored for selecting active surfaces specifically suited for renovation projects. Many existing methods [43],[44] for sizing solar energy production are both time-consuming and reliant on complex optimization algorithms, making them less user-friendly. While these methods deliver high levels of accuracy, they are less adapted for applications on existing facades where orientation and context are fixed. This limitation can result in unrealistic distributions of active surfaces from an operational perspective.

The roof of the building can provide some extra freedom in terms of the orientation of the solar panels. However, the available roof area is smaller than the facade area of high-rise buildings and can be preoccupied.

In any case, when sizing renewable energy production, there is a trade-off between the self-consumption (SC) and the self-sufficiency (SS) of a building [42]. Here, the degree of self-consumption is defined as shown in Equation (2.1) and the degree of self-sufficiency as shown in Equation (2.2). The self-consumption indicates how much of the produced energy is self-consumed in relation to the total production. The self-sufficiency indicates how much of the total energy demand is fulfilled. It is the total energy supplied to the building from renewable energy sources in relation to the total demand of the building.

Therefore, for the definition of SC and SS follows:

- $TESC$ = Total Energy Self-Consumed

- TEP = Total Energy Production

- TES = Total Energy Supplied

- TED = Total Energy Demand

The definitions of SC and SS are:

$$SC = \frac{TESC}{TEP} \tag{2.1}$$

$$SS = \frac{TES}{TED} \tag{2.2}$$

SC and SS follow opposing trends, as illustrated by a simple example: When a small solar panel installation is implemented, the SC tends to be high because most of the generated energy is consumed in real time by the building. This reflects an efficient use of the installation. However, the SS tends to be low in such cases because the total energy supplied is relatively small compared to the overall energy demands of the building. Therefore, it is crucial to choose the active surfaces with respect to the consumption profile of the building and obtain grouped surfaces for the installation of solar panels. Here, the incorporation of batteries can offer significant advantages, increasing both SC and SS, while simultaneously reducing the reliance of the building on grid-supplied energy [42].

The overall goal is to determine the active surface areas in alignment with the requirements of decentralized energy production, focusing on maximizing energy utilization while maintaining energy efficiency and reducing the reliance on fossil fuels. In this context, the objective can be framed as a maximization challenge. Renovation projects for buildings have limited areas for on-site production and fixed orientations as constraints. To determine the optimal sizing, it is necessary to match the potential energy production from different directions with the energy consumption profile. The initial focus is on facades, given their significance in the facade-to-roof ratio often seen in skyscrapers and commercial office buildings. The energy production profile is based on the installed solar panel areas with their corresponding energy output. Therefore, the total energy production can be formulated as a linear system. This linear system can be solved towards specific objectives. It is wanted to match the energy production profile with the energy consumption profile to achieve high self-sufficiency while maintaining energy efficiency, taking self-consumption as a second parameter into account. The matching of production and demand profiles can be formulated into an optimization problem, minimizing the difference between the two with objective functions. Solving the objective functions gives an optimal result for the linear system with regard to the optimization problem and constraints defined. Here, multiple steps can be made, and the optimization problem is split into sub-problems.

Procedural programming with various solvers for linear systems utilizing objective functions with given equality and inequality constraints can be employed. These solvers are commonly used in engineering design and are also applicable to power grid optimization problems, effectively solving the linear system while adhering to the specified constraints and conditions. Additionally, iterative refinement can be implemented [45]. One solver, utilizing a minimization objective function and implemented in MATLAB, is the linear

least-squares solver [46]. With this solver, the linear system is solved in a least-squares sense subject to set bounds and constraints. The minimization penalizes differences between desired outcomes and the linear system quadratically.

Therefore, it is possible to maximize SS by aligning the energy production profile with the energy consumption profile using the linear least-squares solver and adjusting the optimization problem (objective function) iteratively based on the obtained results thus far.

2.6   Background Summary

In summary, the background of this case study presents a focus on establishing on-site solar energy production within a hybrid system incorporating heat pumps. To maximize energy utilization, the integration of battery or thermal energy storage is proposed. Sizing the overall system requires accurate and preferred high-sample-rate data on energy production and demand. In cases of missing or inaccurate data, data imputation methods must be applied. The selection of active surfaces for sizing the solar energy production system involves procedural programming using a linear least-squares solver iteratively. The primary objective is to achieve a maximization of self-sufficiency (SS) while ensuring efficient energy usage by considering self-consumption (SC). To do so, objective functions are defined minimizing the difference between the energy production profile and the demand profile. Additionally, cost considerations for the hybrid system and energy storage, including installation costs and procurement costs per kWp/kWh, are crucial factors in the decision-making process. The approach aims for universality within a limited design space, not considering the influence of energy management control, such as smart control systems for operating heat pumps and energy storage.

Chapter 3

Methodology

The methodology outlined in this thesis is structured as follows. It commences with an evaluation of the architecture of the building that is being studied, focusing on the orientation and dimensions of its facades and roofs as well as the energy demands of the building. Furthermore, an assessment of the immediate surroundings of the building is conducted. With this data in place, decisions concerning on-site renewable energy production and storage solutions can be made. Hereby, the proposed method is designed as a systematic, step-by-step process, allowing for flexibility to halt at any point when the desired outcomes are achieved. The method utilizes a linear least-squares solver. For the impact assessment and comparison, including cost considerations, Pareto plots showing the degree of self-sufficiency (SS) and the degree of self-consumption (SC) against investment costs are used. A flowchart of the applied method is outlined in Figure 3.1 and an overview of the considered system is shown in Figure 3.2. Within the system overview in Figure 3.2, the system parts for three phases are marked accordingly. First, only the on-site solar panel installation (1.) is considered. In the following phase, the heat pump system (2.) is added. In the last phase, battery storage (3a.) or heat storage (3b.) is considered additionally.

From the assessment of the building follow solar irradiation data, available areas on the facade and roof of the building with corresponding orientations, the electricity demand, and the heating demand. Using a simulation tool, in the case of this thesis DEMkit [47], a solar production profile is generated for each considered oriented area with associated solar energy densities.

The initial phase of the method (1.) involves simulating renewable energy production with PV sizing methods to match the current electricity demand of the building. Objective functions solved with a linear least-squares solver [46] are used to maximize the utilization of the facades of the building first and, subsequently, the roof to fulfill the remaining energy demand as good as possible. This results in solar panel distributions and energy production profiles.

Here, three PV sizing methods are applied, a method comprising four distinct weather days, a method based on a dataset of one year, and a method with more freedom in the solving approach. The first PV sizing method utilizes four distinct weather days: sunny, rainy, cloudy, and mixed. These representative days are weighted based on their prevalence throughout the year to obtain a distribution for solar panels. In contrast, the other two PV sizing methods, based on a dataset of one year and a method with more freedom in the solving approach, do not require weighting, as the solar panel distribution and energy production profile are already directly obtained for the length of a year, without relying on assumed representative days. For the last one, the constraints are altered and the dis-

tribution of solar panels is solved in a single input step, rather than in two input steps. It attempts to match the energy demand of the building directly with the utilization of the facade and roof area simultaneously.

The resulting energy production profiles are combined with the current electricity demand data, leading to a self-sufficiency and self-consumption rate for the building. Summarizing, the outputs of this step are the self-sufficiency and self-consumption of the building, and the investment costs involved.

In the following phase (2.), the focus shifts to the heating system, assessing insulation impact and introducing heat pump systems. An insulation function is fed with the heating demand data and returns modified heating demand data incorporating the influence of insulation and the associated costs for insulation. The original or altered heating demand data is fed to a heat pump function, adjusting the electricity demand. For this new electricity demand profile a solar panel distribution and energy production profile is generated, which is again used to calculate the outputs of the self-sufficiency function.

In the last phase (3.), attention is directed to the impact of energy storage solutions, including batteries and thermal storage. Here, an energy storage function is fed with the already achieved energy production profile leading to a modified profile according to the sizing of the storage options.

It is crucial to acknowledge that the outcomes depend on the data availability and resolution of the input data. Achieving, for example, a simulation output for a full year, with a sample rate of 1h, might require data imputation for missing data or making assumptions as part of the process.
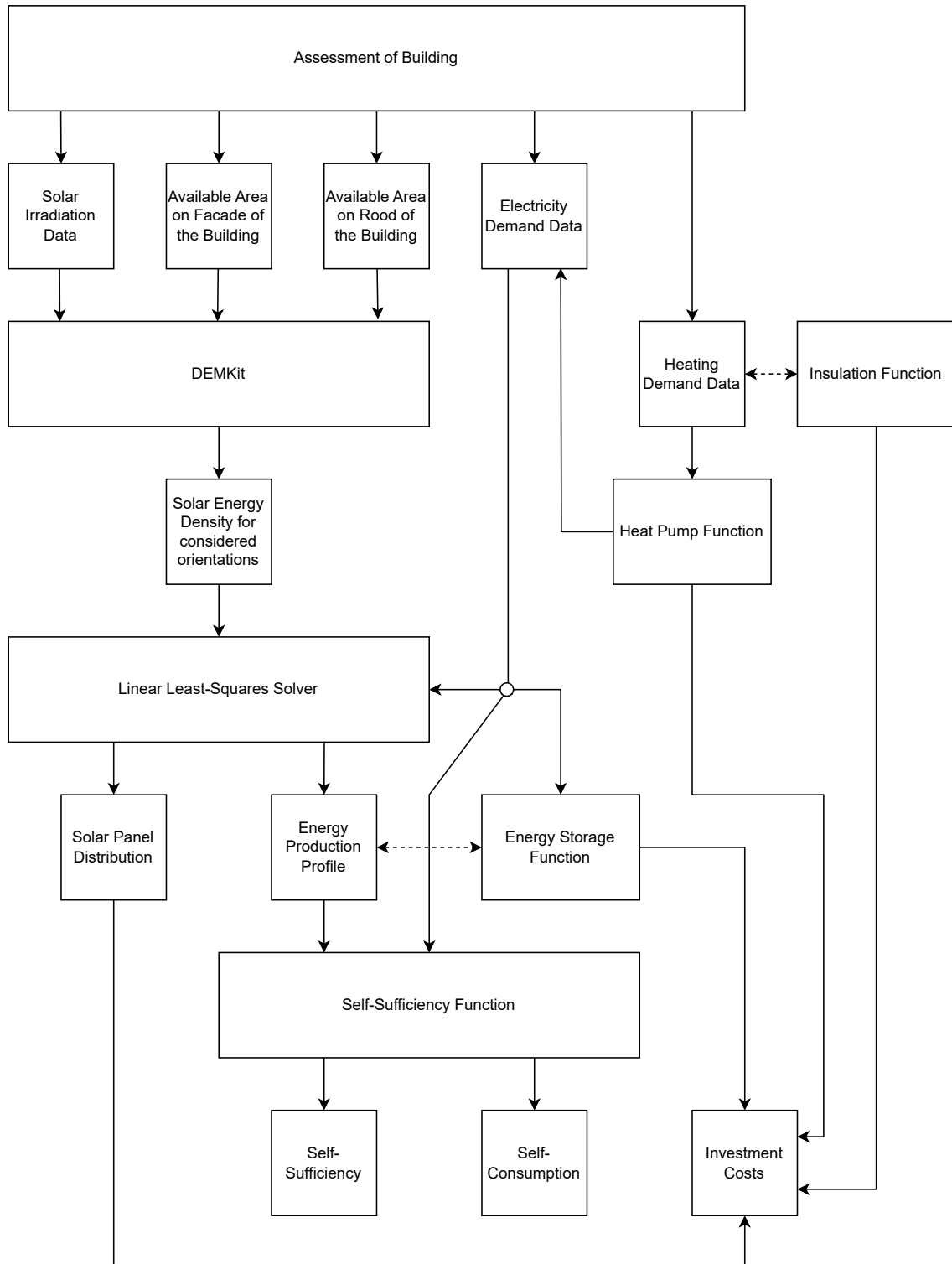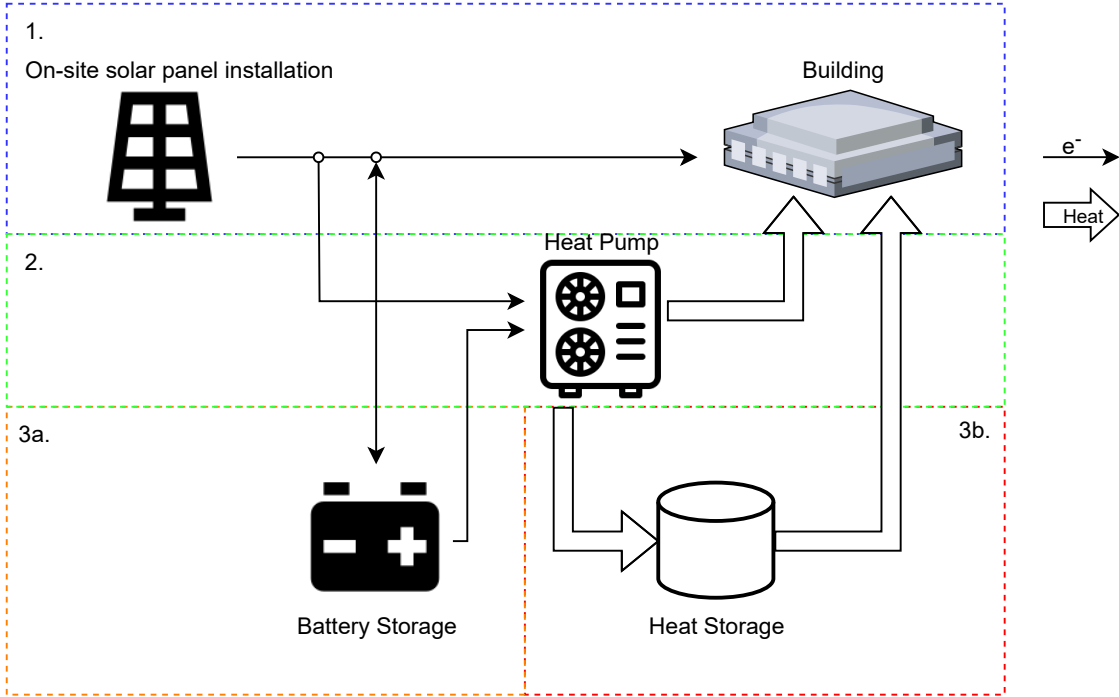
FIGURE 3.1: Method Flowchart

FIGURE 3.2: System Overview

In the following sections, the phases of the previously described method are further explained. Here, the assessment of the building and demand data, the definition of the linear least-squares problem for the solver in different PV sizing methods to obtain the solar panel distributions, the integration of insulation and heat pumps in the heating model, the modeling of energy storage, and the goal of the usage of Pareto plots are presented and detailed further.

3.1 Assessment of Building & Demand Data

In this section, the assessment of the building and the steps involved in obtaining the required demand data are further explained.

The initial step involves an examination of the architecture of the building, considering its orientation and the dimensions of its facades and roof, along with an evaluation of its immediate surroundings. For this, the azimuth angles and available area for each facade of the building must be determined. Hereby, the most relevant orientations for solar production are the East, West, and South facades of buildings in the Northern Hemisphere, as well as the flat roof area commonly found in commercial office buildings. For the facades, an inclination of 90° is considered. In the case of roof areas, inclinations ranging from 0° to 90° and azimuth angles from 0 to 360° are taken into account. For the determination of the optimal inclination and azimuth angles on the flat roof the PVGIS Tool 5.2 [48] is employed. PVGIS allows obtaining data on solar radiation and the energy production of photovoltaic systems based on historical data. It provides a tool to optimize the azimuth and inclination of solar panels for maximizing power output.

Determining available areas can be based on existing building plans when available. In cases where plans are not available, measurements and photographic surveys can be employed. Additionally, the immediate surroundings must be considered to assess whether

the building is freestanding, whether its facades are obstructed by other structures, or if it is part of a complex where solar production areas can be shared. For storage solutions, unoccupied areas in the surrounding vicinity can be of interest for the installation of larger storage technologies. Hereby, employing a drone for a comprehensive overview can be advantageous.

In the second step, the collection of solar irradiation data for the given location and energy data of the building needs to be executed, with a specific emphasis on electricity and heating needs. It is important to evaluate the availability, accuracy, and resolution of the available data sets to ensure that a representative energy profile can be obtained, as the quality of the output is based on the quality of the input. In cases where data is lacking or has low resolution, data imputation or assumptions may be necessary. In Chapter 4 an examination of the Zilverling building based on the stated approach is presented.

3.2 PV Sizing

In this section, the problem formulation for determining the on-site distribution of solar panels on a building is presented. To investigate the influence of data availability and flexibility in the solving approach by splitting the optimization problem into sub-problems and defining different constraints, three distinct PV sizing methods are considered: one based on four distinct weather days, another based on a dataset spanning a year, and a third allowing more flexibility in the solving approach. These are further defined in Subsection 3.2.3.

The energy production of the building depends on the distribution of solar panels with specified orientations. Solar energy production per square meter for each considered orientation is calculated using solar irradiation data. By multiplying this value by the area of installed panels in that orientation, energy production can be determined. Therefore, a linear system can be formulated where:

- x is a variable vector specifying the size of the areas chosen for solar panel installation.

- C is a time series matrix that specifies the energy densities per square meter for the different orientations of the solar panels.

- E is a time series vector specifying the energy produced.

The resulting equation of this linear system is:

$$C \cdot x = E \tag{3.1}$$

As outlined in Section 2.4, the demand response of a system can be fine-tuned towards specific objectives. To achieve high self-sufficiency, it is desired to match the electricity production with the electricity demand of the building. Therefore, the difference between the apparent energy produced and the demand must be minimized. As energy production is linearly related to the distribution of solar panels, it is required to find a distribution optimized towards the demand profile of the building to minimize the difference between production and demand. To find an optimal distribution of solar panels x, an optimization problem with bounds and linear constraints is formulated. A linear least-squares solver, implemented in MATLAB [46], is utilized to solve this problem, where:

- x is a variable vector specifying the size of the areas chosen for solar panel installation.

- C is a time series matrix that specifies the energy densities per square meter for the different orientations of the solar panels.

23

- d is a time series vector containing the given electricity demand.

- lb is a vector containing the minimum available area values of the areas chosen for solar panel installation.

- ub is a vector containing the maximum available area values of the areas chosen for solar panel installation.

The objective function is:

$$\min_x \frac{1}{2}||C \cdot x - d||_2^2 \text{ such that } lb \leq x \leq ub \tag{3.2}$$

With this, the linear system is solved in a least-squares sense, subject to set bounds and constraints. An optimal solution according to the objective function can be obtained and the minimization penalizes differences between energy production and demand quadratically.

To solve the linear least-squares problem for a building, the information gathered with the method described in Section 3.1 is used as input to simulate the energy production of the considered PV sizing methods. For this, weather data is required, including global radiation (measured in $[J/cm^2]$) for the region where the building is located, preferably with an hourly sample rate or higher. The energy production sample rate is matched with the rate of the electricity demand data of the building. To obtain the energy production for the building, electricity densities per square meter of solar energy production for the available areas in each orientation over the course of a year with the aforementioned type of weather data are calculated, using DEMKit [47]. The resulting energy densities, measured in $[kWh/m^2]$, provide information for each orientation with the sample rate of the input data. When multiplied by the utilized area for that orientation, azimuth, and inclination, this data yields the corresponding energy production profile. To find the active surfaces and solve for the utilized areas, the energy densities resulting from DEMKit [47] are fed into the problem as matrix C together with the electricity demand of the building as vector d. Depending on the data availability, resolution, and other goals, as the prioritization of utilizing specific areas on a building, bounds and constraints can be added and adjusted as well as the problem split into sub-problems with different input steps. Therefore, two different problem formulations are presented in Subsection 3.2.1 and 3.2.2. The first formulation splits the optimization problem into two sub-problems to first utilize the facades of a building and subsequently the roof. The second formulation solves the optimization problem for the solar panel distribution on the facades and roof simultaneously with one objective function instead.

3.2.1 Two Objective Functions Problem Formulation

As outlined in Section 2.5, the initial focus is on the utilization of the facades in commercial office buildings and skyscrapers, due to a substantial face-to-roof ratio. After the utilization of the facades, the roof can be utilized with extra freedom in terms of the orientation of solar panels, as the orientation is fixed for the facades. However, the available roof area is smaller than the facade area of high-rise buildings and can be preoccupied. Therefore, the optimization problem is split into two sub-problems to first focus on the facades with fixed orientations of the building and then to focus on the roof considering multiple solar panel orientations and taking advantage of the extra freedom present. Thus, two objective functions are utilized to find a solar panel distribution solution. In the first, the objective function is adjusted to solve just for the areas on the facades of the building, matching the

electricity demand of the building as good as possible. This maximizes the utilization of the facade areas. In the second, the total available area on the roof is objective to minimize the difference between the energy production on the roof and the remaining electricity demand. The aim of utilizing the area fully is to capitalize on the larger energy production densities for the majority of the day, due to the optimized inclination angle and azimuth with regard to power output, consequently enhancing the total energy production. To implement this an equality constraint has to be added. Therefore, for the first problem:

- $x_{Facades}$ is a variable vector specifying the size of the areas chosen for solar panel installation on the facades.

- $C_{Facades}$ is a time series matrix that specifies the energy densities per square meter for the different facades.

- d is a time series vector containing the given electricity demand.

- lb is a vector containing the minimum available area values of the areas chosen for solar panel installation and is set to 0.

- ub is a vector containing the maximum allowable area sizes for each facade of the building.

The first objective function is:

$$\min_{x_{Facades}} \frac{1}{2}||C_{Facades} \cdot x_{Facades} - d||_2^2 \text{ such that } lb \leq x_{Facades} \leq ub \tag{3.3}$$

Consequently, for the second problem:

- x_{Roof} is a variable vector specifying the size of the areas chosen for solar panel installation on the roof.

- C_{Roof} is a time series matrix that specifies the energy densities per square meter for the different orientations on the roof.

- d_2 is a time series vector containing the remaining electricity demand: $d_2 = d - C_{Facades} \cdot x_{Facades}$.

- Aeq is a vector containing ones.

- beq is the available area of the roof.

The second objective function is:

$$\min_{x_{Roof}} \frac{1}{2}||C_{Roof} \cdot x_{Roof} - d_2||_2^2 \text{ such that } Aeq \cdot x_{Roof} = beq \tag{3.4}$$

In the first step, the facades of the building are considered alone, while in the second step, the roof is examined to optimize and meet the remaining energy demand. From Equation (3.3) the optimal solution x_1 for the first problem follows, containing the installation area sizes for the orientation on the facades of the building.

Equation (3.4) defines the second optimization problem, with an objective to minimize the difference between the energy production on the roof and the remaining electricity demand. Hereby, the equality constraint ensures that the total installed area on the roof must be equal to the available area. The two steps are flexible and can be solved for different time-periods of energy density data and demand data, based on data availability and resolution.

3.2.2 One Objective Function Problem Formulation

To determine the utilized areas for solar panel installation required to match the energy demand with the energy production of a building, an alternative approach with more freedom is also considered. This approach does not prioritize the facades of the building first but includes the equality constraint from the two objective functions approach above. Therefore, for this problem:

- x is a variable vector specifying the size of the areas chosen for solar panel installation.

- C is a time series matrix that specifies the energy densities per square meter for the different orientations of the solar panels.

- d is a time series vector containing the given electricity demand.

- lb is a vector containing the minimum available area values of the areas chosen for solar panel installation.

- ub is a vector containing the maximum available area values of the areas chosen for solar panel installation.

- Aeq is a vector containing zeros for the facades and ones for the roof.

- beq is the available area of the roof.

In this approach, the problem is solved with one objective function and is defined as the linear least-squares problem:

$$\min_{x} \frac{1}{2}||C \cdot x - d||_2^2 \text{ such that } lb \leq x \leq ub \text{ and } Aeq \cdot x = beq \tag{3.5}$$

Solving this for different periods of energy density and demand data, based on data availability and resolution, results in a distribution of solar panel installation.

3.2.3 PV Sizing Method Definition

In this thesis, three PV sizing methods are considered to investigate the influence of data availability and flexibility in the solving approach:

- A method comprising four distinct weather days.

- A method based on a dataset of one year.

- A method with more freedom in the solving approach.

The first two methods utilize the Two Objective Functions Problem Formulation shown in Subsection 3.2.1 and the last method utilizes the One Objective Function Problem Formulation shown in Subsection 3.2.2. The results from each method can be compared. In the first method, four distinct weather days are used as input to obtain a solar panel distribution: sunny, rainy, cloudy, and mixed days. Each of these days leads to different solar panel distributions based on the specific weather conditions for that day. The selection process for these day scenarios is explained in more detail in Subsection 3.2.4. To calculate the final distribution for solar panel installation, these day scenarios are weighted based on prevalence throughout the year.

For comparison reasons, in the second method, the two steps outlined in Equations (3.3) and (3.4) are applied to data of an entire year, eliminating the need for scenario weighting to derive the final solar panel distribution.

In the third method, Equation (3.5) is applied to data of an entire year, delivering a final solar panel distribution comparable to the second method.

With these three methods, differences in the solutions based on data input and problem definition in the objective function can be compared and discussed.

3.2.4 Selection of Weather Days

For the first PV sizing method, four distinct weather days are required. In this subsection, it is described how these days are selected.

The selection of the days depends on various weather data parameters. In addition to global radiation, these parameters may include indicators for sunshine duration and rainfall occurrence on an hourly basis. These parameters are chosen within this thesis as data is available from the KNMI [49]. Since solar production is a crucial factor, the chosen scenario days should not be in the winter due to the low global radiation levels in winter. Therefore, the four selected days represent the most common weather scenarios during the other three seasons of the year at the location of the building, hereby excluding factors like snowfall. For the classification of a day, all hours with daylight, when global radiation exceeds 0, are considered. Within these hours:

- For a day to be classified as sunny, there has to be uninterrupted sunshine duration with an indicator score of ≥ 8 for all hours, excluding sunrise and dawn when no direct sunshine is expected. Therefore, at least 80% sunshine duration of an hour is required in most daylight hours for a day to be classified as a sunny day.

- A rainy hour is characterized by a rain indicator for the occurrence of rain during daylight hours, indicating 1 for the occurrence of rain in these hours or 0 for no occurrence. Therefore, if a day has a rain indicator of 1 for all daylight hours, it is classified as a rainy day.

- In contrast, a cloudy day is identified when the rain indicator remains at zero, and the sunshine duration is consistently below 10% for the entire hourly division. Therefore, if these conditions apply for all daylight hours, it is classified as a cloudy day.

- For days when these conditions transition and switch between sunny, rainy, and cloudy conditions, a mixed day is assumed.

The weights used to calculate the final solar panel distribution are based on the conditions and indicators for sunny, rainy, cloudy, and mixed days. To determine these weights, the number of hours that meet each day's conditions is determined. Then, this count is divided by the total number of hours with global radiation greater than zero.

3.3 Heating System

This section outlines the methodology for considering insulation and heat pumps. It encompasses a general approach to estimate the current state of insulation in a building, potential improvements, and the sizing of heat pumps based on the given heating demand. The implementation of insulation affects the heat demand data and, consequently, influences the additional electricity demand required for heating the building with heat pumps.

Following the Trias Energetica principle [1], the initial focus is on reducing energy demand through enhanced insulation. The second step considers using renewable energy sources for energy production, achieved in this case for heating with a hybrid system of solar panels powering heat pumps, maximizing the utilization of the produced electricity by the solar panels.

To explore the effects of these elements, two cases for the heating system are formulated for the considered building: one implementing only heat pumps and the other combining heat pumps with insulation. Insulation can influence the sizing of the heat pumps, potentially leading to lower additional electricity demand. This, in turn, can affect the optimal distribution of solar panels and the energy production profile. The evaluation of the heating system should consider periods of high heat demand, especially winter, to ensure proper sizing with regard to comfort.

3.3.1 Evaluation of Insulation

The estimation of the current state of insulation and potential improvements is based on the methodology by Badenes et al. [50]. This standardized approach correlates heating and cooling energy demands for heat pumps with heating and cooling degree days across various climate classes and building types in Europe. To apply this method to a building, the heating degree days (HDD_d) are calculated based on Badenes et al. [50].

One of the main assumptions made, for this thesis, is the use of a Coefficient of Performance (COP) of 3 for heating and cooling energy demands as the paper is tailored to support the design of ground source heat pumps and these commonly have a COP between 3 and 5 [51],[52].

Furthermore, a base temperature of 18°C and a threshold for the external temperature of 14°C are assumed [50]. The formula for the calculation of daily heating degree days is given in this case by:

$$HDD_d = (T_b - T_d) \text{ if } T_d < 14°C \tag{3.6}$$

where:

- $T_b = 18°C$, the base temperature.

- T_d is the daily mean temperature, calculated based on the daily maximum and minimum temperatures.

Summing up the HDD_d values over a year provides the yearly heating degree value HDD_y for the building. This value, combined with the electricity consumption per square meter for heating annually, allows determining the insulation state with three standardized linear regression scenarios: no insulation, low insulation, and good insulation, corresponding to the building type and climate class. The three linear regression scenarios for Building 3 in [50] are shown in Figure 3.3 as an example.
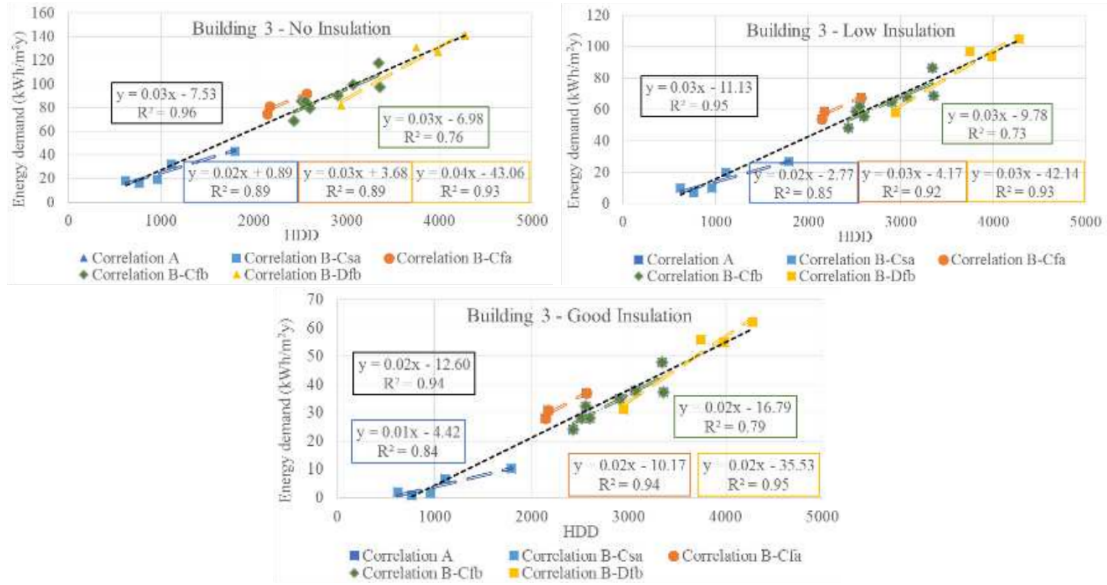
FIGURE 3.3: Linear Regression between Heating Energy Demand and HDD_y for Building 3 [50]

Based on this, a potential reduction in energy demand by improving the insulation of a building to the next regression line can be calculated. This energy reduction, together with the effect of a slower-reacting system on the heating demand, needs to be applied.

To apply this standardized approach, temperature measurements for at least one year at the location of the building are required, along with the total heated area of the building in square meters to determine the annual electricity consumption per square meter for heating. This area excludes staircases and space occupied for elevators in this case.

3.3.2 Heat Pump Sizing

As explained in Section 2.2, the size of the heat pump system is determined by the relative heating load. Based on the annual power consumption profile the heat pump system needs to be sized to cover high-demand periods, especially in winter. A possible approach is to consider the distribution of the largest 25% of heating demand values for the year, as these occur during the winter [53]. To avoid oversizing the system based on a single maximum demand occurrence, a limit to meet 97.5% of these 25% highest heating demands is the chosen approach. A system sized with this approach covers approximately 99.38% of the year's heating demand fully. For the case of only implementing heat pumps, the applicable heat demand data is used for the determination, and for the case of heat pumps in combination with insulation, modified heat demand data incorporating the effect of insulation is used.

3.4 Energy Storage System

This section outlines the implemented energy storage system considerations for this thesis. In general, multiple combinations of different energy storage systems are possible, depending on the considered case. In this thesis, two independent storage systems are assumed. First, a Li-Ion battery operating with no smart control, including the C-Rate and overall

efficiency for different scaled capacity sizes, based on a real-life example, neglecting self-discharge rates. Second, a thermal heat buffer system using water operated on the thermal output side of the heat pump system is considered, implementing a wide span of overall efficiency and neglecting self-discharge rates again. The self-discharge rates are neglected to have a simplified energy storage model that takes an overall efficiency range into account, to not require a temperature- and time-dependent heating model for the thermal buffer storage that determines possible losses in long-term storage during operation.

3.4.1 Battery Energy Storage

For the energy storage simulation incorporating the Li-Ion battery, the example of INTIL-ION scale racks with steps of 154 kWh capacity is assumed, with an efficiency of 90% and a C-Rate of 0.9688 [31]. The battery charges with the surplus energy production of the solar panels and discharges prioritized to the heat pump system. Here, the battery discharges to the heat pump system when the possible supplied heat to the building is larger than the electrical demand of the building. Therefore, if the initial electricity demand of the building is larger than the heating demand divided by the COP of the heat pump system, the battery discharges to fulfill the initial electricity demand.

With this prioritization, the COP of the heat pump system is used effectively, as significantly more energy can be pumped into the building with the electricity supplied by the battery than using this electricity directly for the electricity demand of the building. The total energy supplied to the building is maximized here. This prioritization also resembles the connections from the battery in the system overview in Figure 3.2 and is oriented on the system shown in Appendix Figure 8.1. The decision-making for this choice is further supported by an example of the difference in prioritization of electricity supply for an intermediate solution of this thesis, shown in Appendix Figure 8.2, and the principle of a heat pump, shown in Appendix Figure 8.3. The prioritization is described by the following algorithm:

if Heating Demand/COP < Electricity Demand **then**
    Discharge to building
else
    Discharge to heat pump system
end if

With the assumed battery storage case, the influence on self-sufficiency and self-consumption per installed battery capacity size can be analyzed. Based on the results, an installation size can be picked and a viable option for the building decided on, which is commercially available. Additionally, as a simple control is assumed and this thesis is design-oriented, it can be said that this simplified case resembles a basis that can be even further improved once an installation size is decided on with the implementation of smart control algorithms as shown in [54].

3.4.2 Thermal Buffer Storage

For thermal energy storage, a heat buffer system operated on the thermal output side of the heat pump system using water as the storage medium is assumed. The efficiency range assumed is 70% to 95%, with a standard efficiency assumed to be 82.5% [36],[37]. To have a fair comparison to the battery case, the buffer storage capacity is scaled by the assumed COP for the heat pump system times 154 kWh.

This considered buffer system is an independent case not operating with a battery. The scaling including the COP is chosen to have a direct comparison between the two cases for

the improvement of self-sufficiency and self-consumption per storage medium.

For the decision-making of a viable option for the building with an installation size picked, the volume of water needed to store the heat can be calculated with the rearranged formula of specific heat [55], where:

- Q is the to-be-stored heat amount in [kJ]

- m_{Water} is the mass of water in [kg]

- c_p is the specific heat capacity of water in [kJ/kg°C]

- ΔT is the supply temperature range considered in [°C]

- T_{HP} is the maximum output temperature of the heat pump system in [°C]

- T_R is the minimum temperature required in the heating system of the building (e.g. radiator) in [°C]

The rearranged formula is:

$$m_{Water} = \frac{Q}{c_p \cdot \Delta T} = \frac{Q}{c_p \cdot (T_{HP} - T_R)} \tag{3.7}$$

With the density of water at the considered supply temperature range (ρ_{Water}) [56], this mass can be converted to the required volume:

$$V_{Water} = \frac{m_{Water}}{\rho_{Water}} \tag{3.8}$$

With the required volume of water for the heat buffer system the dimensions of the required tank can be determined and considerations for placing be made.

3.5   Pareto Plots

For the evaluation of the cost considerations for the hybrid system and energy storage, mentioned in Section 2.6, Pareto plots are used. This section outlines the goal of the use of Pareto plots showing the degree of self-sufficiency (SS) and the degree of self-consumption (SC) against investment costs. The primary objective is to achieve a maximization of self-sufficiency while ensuring efficient energy usage by considering self-consumption. The economic feasibility is maintained by assessing the gain in self-sufficiency per additional investment. Therefore, two objectives to optimize are present: SS and SC. In multi-objective optimization, the Pareto front indicates the Pareto optimal solutions and is widely used in the field of engineering [57]. Focusing on the Pareto front enables one to focus on the set of efficient choices, facilitating the navigation of trade-offs within this set, rather than considering the full range of parameters present [58],[59].

Therefore, the use of Pareto plots helps prioritize choices for implementation, analyze their impact, and helps in prioritizing to increase the considered gain. However, additional data to the set of points on the Pareto front is required to provide a solution, as different points on the Pareto front can have different system setups. The Pareto plots assist in finding a fitting solution based on the preferences of stakeholders and the goals to be achieved. Additional information such as the payback time of the investment costs and energy demand reduction can be considered.

In the case of this thesis, the payback time is calculated by dividing the total investment

costs by the total costs saved yearly for electricity and heat with the installation of the considered system. For the calculation of the saved costs for electricity and heat, the energy amounts self-supplied and self-consumed by the building and energy amounts reduced are multiplied by an assumed energy price per kWh of electricity and per GJ of heat. The payback time is calculated with the formula shown in Equation (3.9), where:

- PBT = Payback Time in [years]

- IC = Investment Costs in [€]

- TCS_E = Total Costs Saved for Electricity in [€/year]

- TCS_H = Total Costs Saved for Heat in [€/year]

- ESC = Electricity Self-Consumed by Building in [kWh/year]

- THS = Total Heating Self-Supplied to the Building in [GJ/year]

- TER = Total Energy Reduction in [GJ/year]

- C_{kWh} = Price per kWh of Electricity in [€/kWh]

- C_{GJ} = Price per GJ of Heat in [€/GJ]

$$PBT = \frac{IC}{TCS_E + TCS_H} = \frac{IC}{ESC \cdot C_{kWh} + (THS + TER) \cdot C_{GJ}} \tag{3.9}$$

Chapter 4

Use-Case Zilverling

For this thesis, the proposed method is applied to the Zilverling building situated at the University of Twente campus. The primary emphasis here lies in the domain of on-site renewable energy production, involving the utilization of solar panels, as well as heating solutions that incorporate heat pumps and external wall insulation. Furthermore, the consideration extends to the potential integration of batteries and thermal heat storage systems. In this chapter, the assessment of the building is done, and the available demand data is presented alongside the solar irradiation and outside temperature profile for the region where the building is located.

In the following, the available information about the Zilverling building is presented. For this, a thorough examination of the building is required. To initiate the examination of the Zilverling building, it is essential to explore all relevant areas available on the building. These areas include the East, West, and South facades of the building, as well as the roof. Pictures of these areas can be observed in Figure 4.1. Figure 4.1a shows that the roof of the building is flat. It has an entire unobstructed area of 879.81 m^2 available, allowing for solar panel installations with various orientations. The orientations, azimuths, inclinations, and available areas are detailed in Table 4.1. This information has been acquired through measurements and photographic surveys, which included the use of a drone to provide a comprehensive overview.

Figures 4.1b, 4.1c, and 4.1d illustrate the East, West, and South facades. The building encompasses five floors with an area of approximately 1548 m^2 per floor. It holds an energy label of C.

TABLE 4.1: Available Areas on Zilverling for Solar Production Installation

Orientation	Azimuth	Inclination	Available Area [m^2]
East	127°	90°	201.10
South	219°	90°	923.06
West	288°	90°	163.55
Roof	0 - 360°	0 - 90°	879.81

On the roof, all azimuth angles from 0° to 360° and inclination angles from 0° to 90° are theoretically possible. To determine the optimal angles on the flat roof, the already mentioned PVGIS Tool 5.2 [48] is employed. The evaluation of the roof is restricted to the same orientations as the facades: East, South, and West, and additionally, an orientation leading to the highest overall production for the roof is considered. Using the PVGIS Tool 5.2 [48] results in the following configurations:

1. Three azimuth angles for the East, South, and West facades, all with an inclination of 35°.

2. A production-optimal roof configuration with an azimuth of 178° and an inclination of 39°.

Thus, seven installation configurations for the Zilverling building are obtained, as shown in Table 4.2.

TABLE 4.2: Installation Configurations on Zilverling for Solar Production

Orientation	Azimuth	Inclination
East	127°	90°
South	219°	90°
West	288°	90°
Roof East	127°	35°
Roof South	219°	35°
Roof West	288°	35°
Roof Optimal	178°	39°

Furthermore, the surroundings of the building are depicted in Figure 4.2. This becomes relevant when considering the incorporation of energy storage and management solutions. Notably, there is a nearby free parking lot area, along with other substantial buildings such as Carre (marked with red) on the West side of the Zilverling and Ravelijn (marked with blue) on the East side of the Zilverling building. The Zilverling building is marked with yellow.
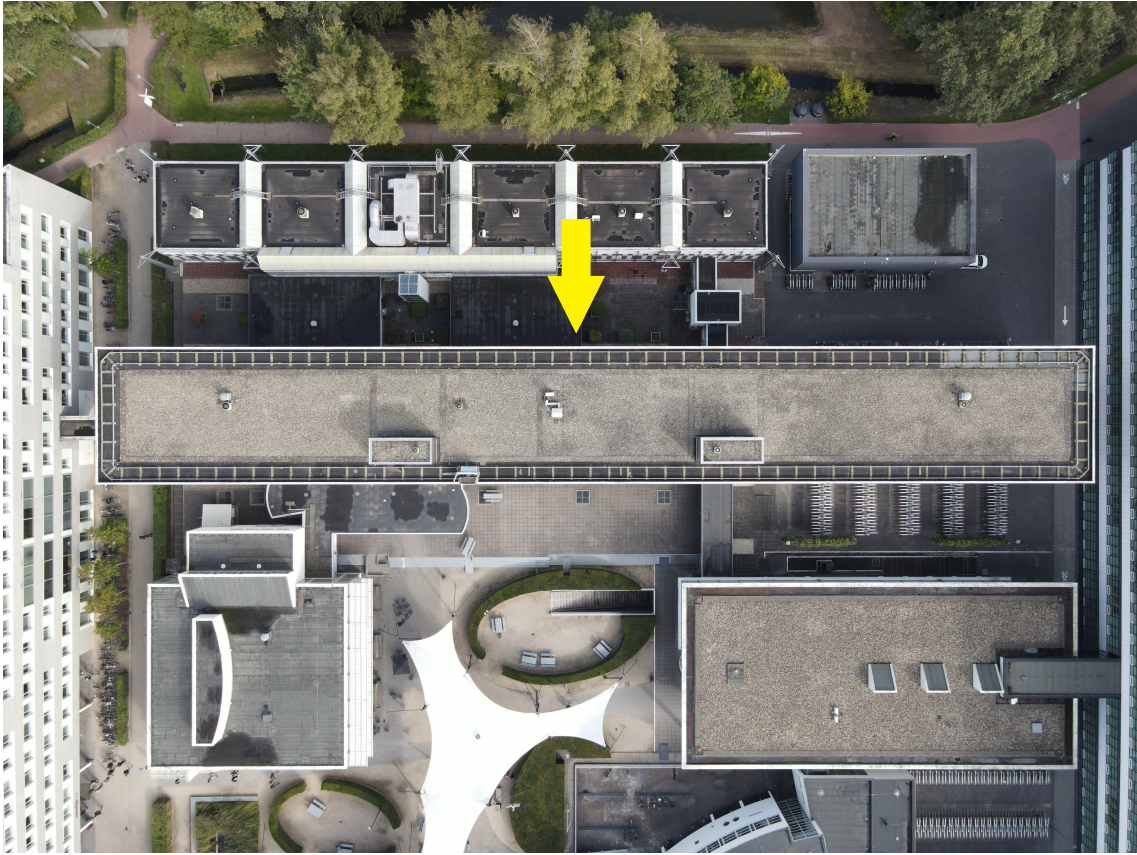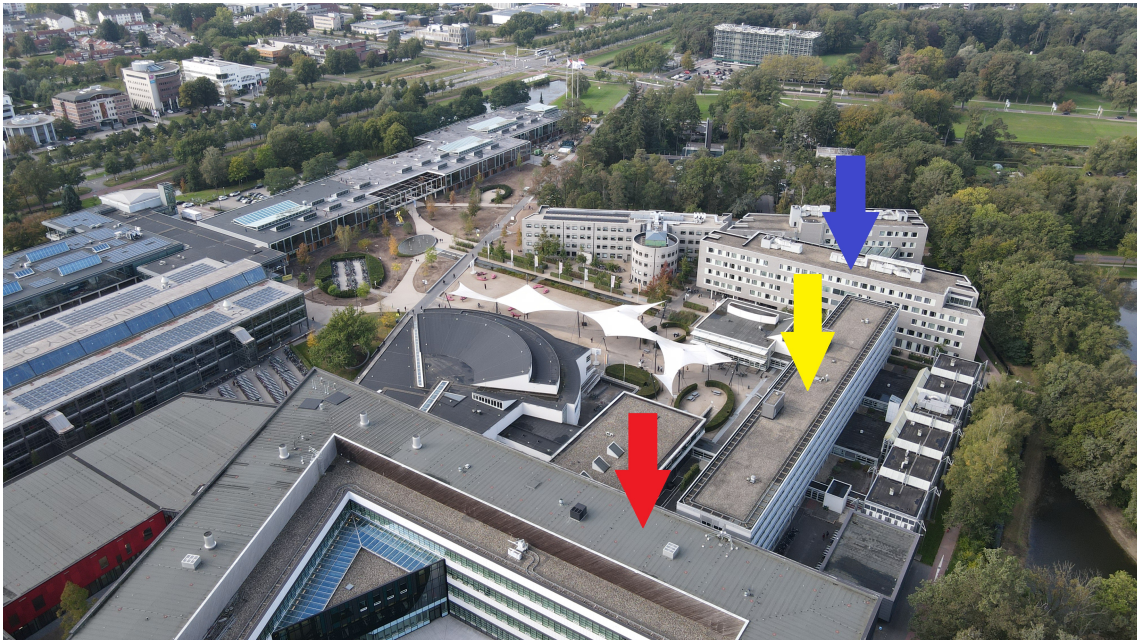
(A) Roof

(B) East

(C) West

(D) South

FIGURE 4.1: Roof, East, West & South View of the Zilverling Building (marked with yellow arrow)

(A) Parking Lot located close to Zilverling

(B) Buildings surrounding Zilverling

FIGURE 4.2: Surroundings of the Zilverling Building

Next to the assessment of the architecture of the building and its surroundings, also the available energy data needs to be examined. In this context, data about the electricity and heating demands of the Zilverling building can be accessed through the University of

Twente's energy data [60]. To get a representative dataset unaffected by external factors, one year from the 13th of July 2022 to the 13th of July 2023 has been chosen. This period was selected due to the previous years being influenced by the Covid-19 pandemic, and the aim to work with recent data. The electricity and heating demand for this period can be seen in Figure 4.3. In both instances, the data is collected on an hourly basis. The heating demand data has a resolution of 1 GJ and, therefore, is not accurate with regard to hourly values. The total electricity demand is 531,198 kWh and the total heating demand is 3,222 GJ for the year.

Further, weather data from Twente Airport, being the closest weather station to the Zilverling building, is used. The data is obtained from the KNMI [49] and is collected for the time period from the 13th of July 2022 to the 13th of July 2023. The global radiation is measured in $[\mathrm{J/cm^2}]$ and the outside temperature is measured in [°C]. The global radiation and outside temperature over the year can be seen in Figure 4.4.

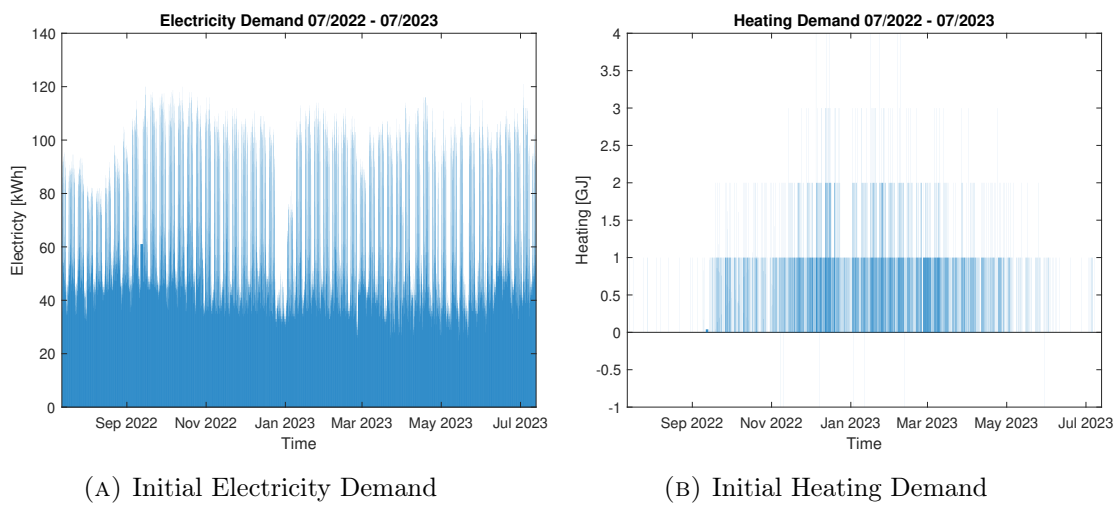(A) Initial Electricity Demand

(B) Initial Heating Demand

FIGURE 4.3: Electricity and Heating Demand of the Zilverling Building from the 13th of July 2022 to the 13th of July 2023

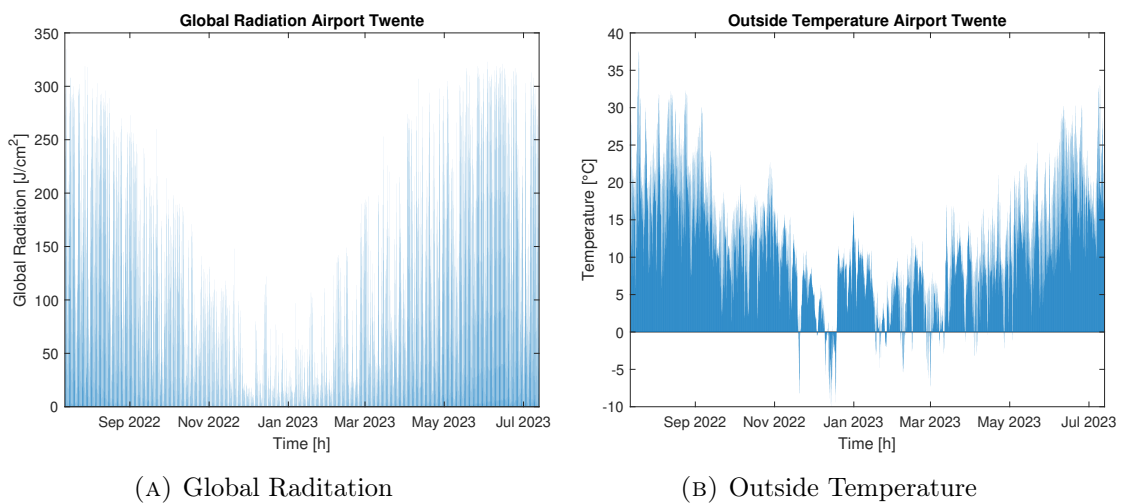(A) Global Radiation

(B) Outside Temperature

FIGURE 4.4: Global Radiation and Outside Temperature from the 13th of July 2022 to the 13th of July 2023

Chapter 5

Results

In this chapter, the results of applying the presented method to the Zilverling building are given. It begins with renewable energy production, considering the three PV sizing methods including a method comprising four distinct weather days, a method based on a dataset of one year and a method with more freedom in the solving approach, as outlined in Subsection 3.2.3. Next, two cases for the heating system, are presented: one with only implementing a heat pump system and another incorporating a heat pump system and external wall insulation. Subsequently, the integration of energy storage technologies, Li-Ion Battery and Thermal Buffer Storage, is demonstrated. Finally, the resulting Pareto plots are displayed to illustrate the achievable degree of self-sufficiency in relation to investment costs and a universal impact indication is provided. Additionally, the payback time of considered system combinations is calculated, and the results are compared to the current energy plan for the Zilverling building by the University of Twente.

5.1 Zilverling: Renewable Energy Production

In this section, the results from solving the linear least-squares problem as formulated in Section 3.2 are presented. The seven installation configurations obtained for the building, along with the weather data, are used for simulating solar energy densities utilizing DEMKit [47]. The Zilverling building is assumed to be freestanding and therefore, shadow from the surrounding buildings is neglected. First, the resulting solar panel distributions for the PV sizing methods are given. Then, the resulting energy production profiles for four distinct weather days and the specifications for the objective functions in each PV sizing method are shown for the case of the Zilverling building.

TABLE 5.1: Energy Densities for each Orientation on Zilverling

Orientation	Energy Density [kWh/m^2]	Azimuth	Inclination
East	$\rho_E(t)$	127°	90°
South	$\rho_S(t)$	219°	90°
West	$\rho_W(t)$	288°	90°
Roof East	$\rho_{RE}(t)$	127°	35°
Roof South	$\rho_{RW}(t)$	219°	35°
Roof West	$\rho_{RS}(t)$	288°	35°
Roof Optimal	$\rho_{RO}(t)$	178°	39°

For the selected period, 8,760 data points representing a year follow for each orientation representing energy production per square meter for every hour in a year. To calculate the

energy produced within one hour for each orientation, Equations (5.1), (5.2), and (5.3) are used, where x_E, x_S, x_W, x_{RE}, x_{RS}, x_{RW}, and x_{RO} represent the installed areas of solar panels on the building for the East, South, West, Roof East, Roof South, Roof West, and the Roof Optimal orientation.

$$E_{Facades}(t) = \rho_E(t) \cdot x_E + \rho_S(t) \cdot x_S + \rho_W(t) \cdot x_W \tag{5.1}$$

$$E_{roof}(t) = \rho_{RE}(t) \cdot x_{RE} + \rho_{RS}(t) \cdot x_{RS} + \rho_{RW}(t) \cdot x_{RW} + \rho_{RO}(t) \cdot x_{RO} \tag{5.2}$$

$$E_{Total}(t) = E_{Facades}(t) + E_{roof}(t) \tag{5.3}$$

5.1.1 Solar Panel Distribution

The final distributions of solar panels on the Zilverling for each PV sizing method can be seen in Table 5.2. x_1 is the distribution for the method comprising four distinct weather days, x_2 for the method based on a dataset of one year, and x_3 for the method with more freedom in the solving approach.

TABLE 5.2: Installed Solar Panel Areas in m^2 per PV Sizing Method and # Amount of Panels needed [1.65m^2]

$[m^2]$	x_1	x_2	x_3
x_E	201.10	201.10	201.10
x_S	837.72	863.24	0
x_W	163.55	163.55	162.85
x_{RE}	427.42	0	133.99
x_{RS}	0	0	0
x_{RW}	452.39	879.81	363.95
x_{RO}	0	0	0
Facades	1202.37	1227.89	363.95
#	728	744	220
Total	2082.18	2107.7	1243.76
#	1261	1277	753

The distribution of x_1 for the installed solar panel areas includes the complete available area on the East and West facades of the Zilverling building. Additionally, the South facade of the building is nearly fully utilized, and the roof is divided between solar panels oriented to the East and West. With this distribution, the total energy production over one year is 378.01 MWh of electricity, in relation to the total electricity demand of 531.20 MWh. The self-sufficiency in this case is 15.5% and the self-consumption is 58.48%.

With the distribution of x_2 the East and West facades of the building are again fully utilized, slightly more panels are needed on the South facade, and the roof has a fully west-oriented solar panel installation. The total energy production over one year is lower with 305.53 MWh of electricity than the 378.10 MWh produced with x_1. The self-sufficiency in this case is 13.93% and the self-consumption is 65.02%.

The distribution of x_3 combines the use of the East and West facades of the building, as

well as the available roof area with solar panel orientations in both East and West directions. No solar panels are installed on the South facade of the Zilverling. The total energy production over one year is 218.51 MWh of electricity. The self-sufficiency in this case is 12.36% and the self-consumption is 80.64%.

5.1.2 Energy Production Profiles

The selection of the four distinct weather days, with the classification as described in Subsection 3.2.4, results in the following days:

- Sunny day: 09-08-2022

- Cloudy day: 26-08-2022

- Rainy day: 26-09-2022

- Mixed day: 30-05-2023

For these days, the energy production profiles for the installation of x_1 are shown in Figure 5.1, for the installation of x_2 in Figure 5.2, and for the installation of x_3 in Figure 5.3.

(A) Sunny Day: 09-08-2022

(B) Cloudy Day: 26-08-2022

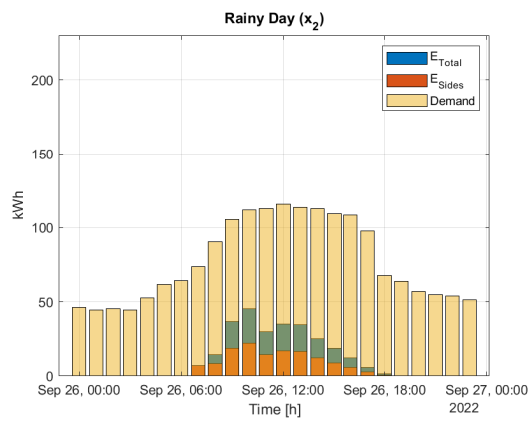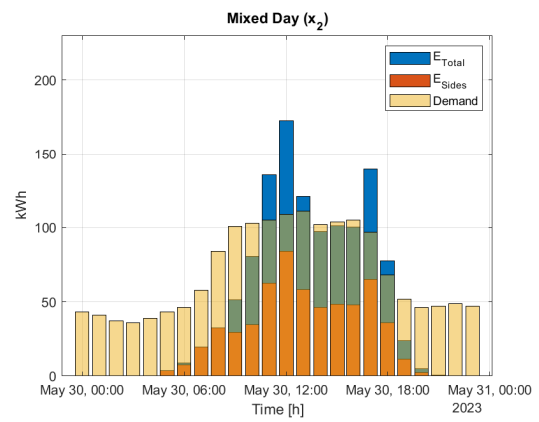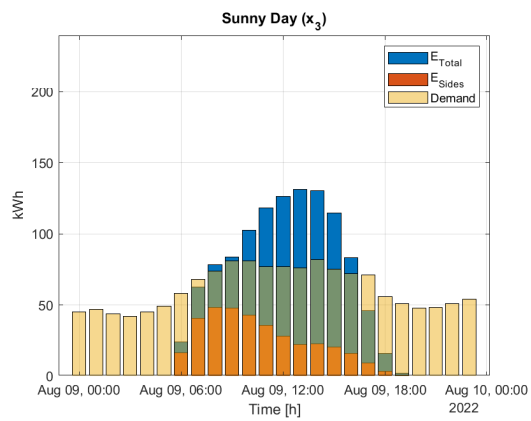(C) Rainy Day: 26-09-2022

(D) Mixed Day: 30-05-2023
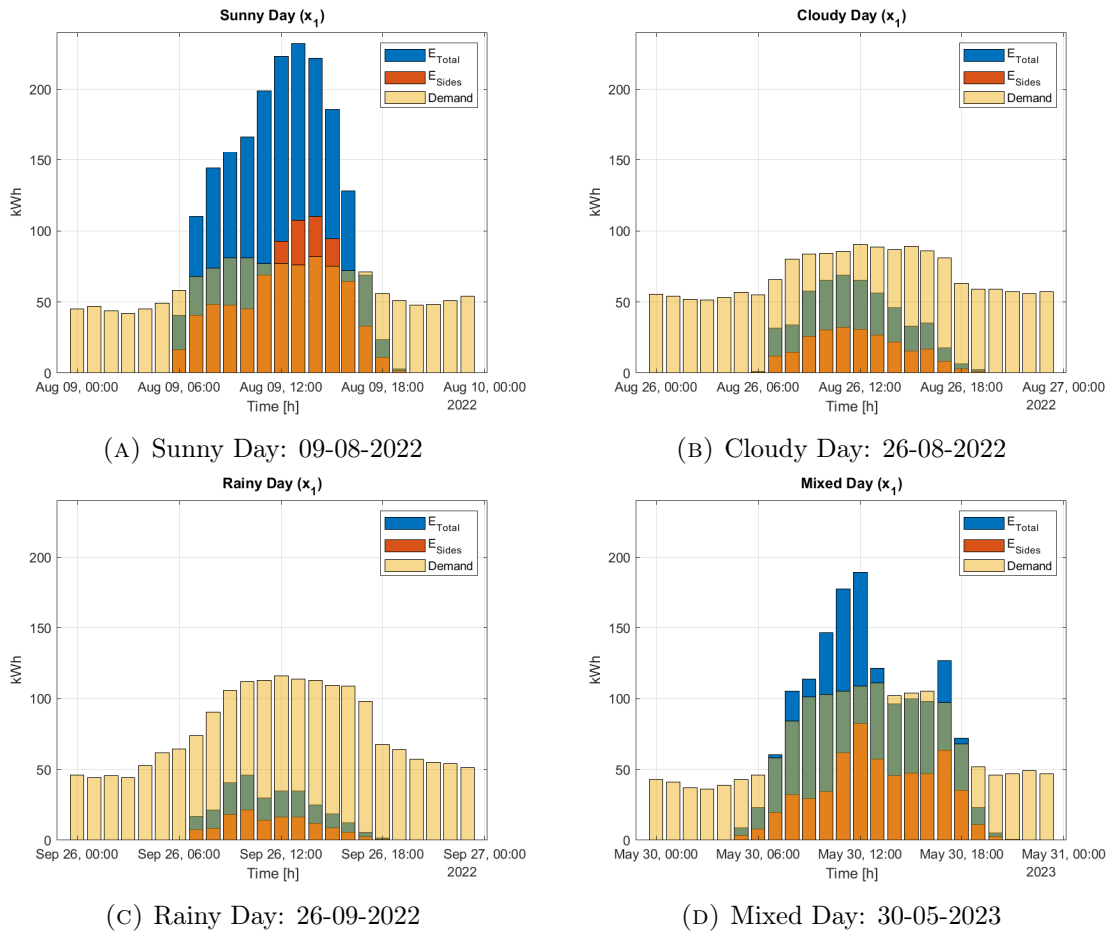
FIGURE 5.1: Energy Profiles of Four Distinct Weather Days with x_1 installed
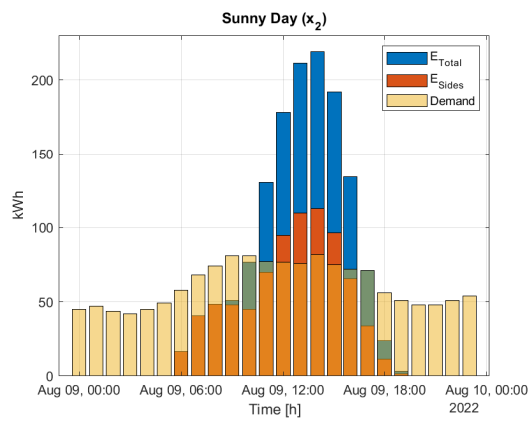
(A) Sunny Day: 09-08-2022
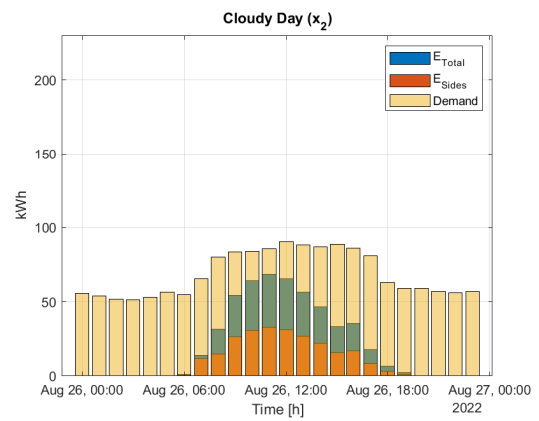
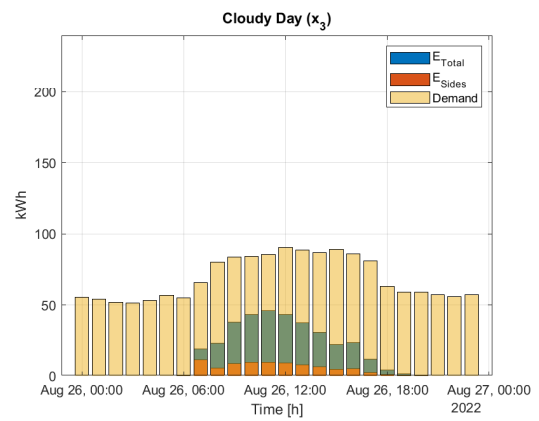
(B) Cloudy Day: 26-08-2022

(C) Rainy Day: 26-09-2022

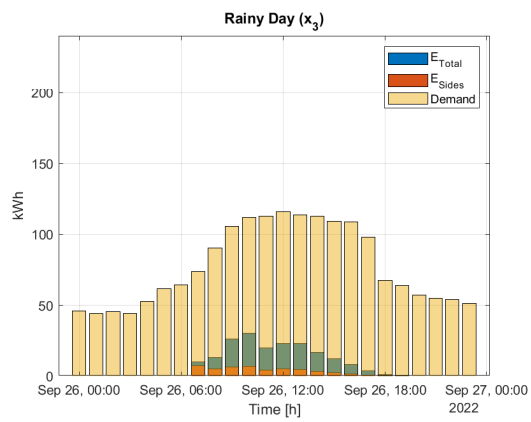(D) Mixed Day: 30-05-2023

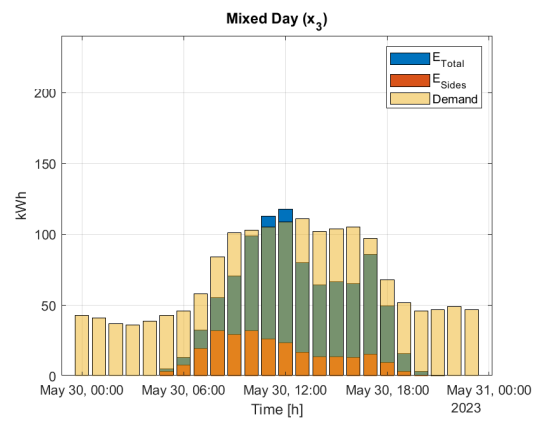FIGURE 5.2: Energy Profiles of Four Distinct Weather Days with x_2 installed

(A) Sunny Day: 09-08-2022

(B) Cloudy Day: 26-08-2022

(C) Rainy Day: 26-09-2022

(D) Mixed Day: 30-05-2023

FIGURE 5.3: Energy Profiles of Four Distinct Weather Days with x_3 installed

It is evident that, compared to the installation of x_1 and x_2, the overall energy overshoot during midday is reduced in the case of x_3. However, the total energy production is also significantly lower. This outcome is logical since the solver has more flexibility and thus penalizes overshoots more severely. On the roof, due to the optimized inclination angles, the energy densities are higher. Therefore, fewer panels can be used to fulfill a similar energy demand than with solar panels on the facades. In the case of x_3, the South facade of the Zilverling building remains unused. Consequently, this potentially active surface goes to waste. As the objective is to meet the demand, no panels are added on the South facade. Thus, the overshoot is reduced, but with it, the total energy production decreases. Self-sufficiency also decreases, but self-consumption increases. Therefore, lower amounts of energy are produced but used more efficiently. However, it is important to note that an energy overshoot is not inherently negative. It can be effectively harnessed for various purposes. The surplus energy can be used effectively, whether by selling it back to the grid, distributing it to other buildings, managing it for other energy-related purposes, or storing it for later use.

5.1.3 PV Sizing Method 1 & 2 Specification: Two Objective Functions Problem Formulation

To obtain the before-shown solar panel distributions x_1 and x_2 for the first two PV sizing methods, the gathered data is used in Equations (3.3) and (3.4). The specifications incorporating the available information of the Zilverling building are given here. Therefore, it follows to solve the problem denied in Equation (3.3):

- $x_{Facades} = [x_E, x_S, x_W]$.
- $C_{Facades} = [\rho_E, \rho_S, \rho_W]$.
- d = Initial Electricity Demand of the Zilverling building (Demand).
- $lb = [0,0,0]$.
- $ub = [201.10, 923.06, 163.55]$.

Consequently, for the second problem defined in Equation (3.4) it follows:

- $x_{Roof} = [x_{RE}, x_{RS}, x_{RW}, x_{RO}]$.
- $C_{Roof} = [\rho_{RE}, \rho_{RS}, \rho_{RW}, \rho_{RO}]$.
- d_2 = d - $E_{Facades}$.
- $Aeq = [1, 1, 1, 1]$.
- $beq = [879.81]$.

For the first method, the objective problems are solved with demand and energy density data from the four distinct weather days. In the second method, these are solved with the demand and energy density data of the one-year period. In both PV sizing methods, a linear least-squares solver, implemented in MATLAB [46], is utilized to solve these problems.
In the first method, for each distinct weather day, a distribution of installed solar panels follows x_{Sunny}, x_{Cloudy}, x_{Rainy}, and x_{Mixed}. To obtain the final distribution x_1 from these

four distributions, a weighted average is computed based on the occurrence of the weather day conditions over a year, represented as:

$$W = [W_{sunny}; W_{cloudy}; W_{rainy}; W_{mix}] \tag{5.4}$$

Consequently, the weights for these days, derived from the year-long weather dataset are:

- $W_{sunny} = \dfrac{1612h}{4694h} = 34.34\%$

- $W_{cloudy} = \dfrac{1232h}{4694h} = 26.25\%$

- $W_{rainy} = \dfrac{808h}{4694h} = 17.21\%$

- $W_{mix} = \dfrac{1042h}{4694h} = 22.20\%$

When comparing these values to the average annual sunshine and rainfall amounts in the Netherlands, it becomes evident that the derived values are within the same range and order of magnitude, as indicated in references [61] and [62].

The final distribution x_1 is calculated with the dot product:

$$x_1 = \begin{bmatrix} x_{sunny}, x_{cloudy}, x_{rainy}, x_{mix} \end{bmatrix} \cdot W \tag{5.5}$$

The resulting distributions of installed solar panel areas from the four distinct weather days and the final distribution x_1 are shown in Table 5.3. Figure 5.4 displays the solar production profiles for the four distinct weather days, with each profile corresponding to the distribution of installed solar panel areas for that day, respectively.

TABLE 5.3: Installed Solar Panel Areas in m^2 per Weather Day

$[m^2]$	x_{Sunny}	x_{Cloudy}	x_{Rainy}	x_{Mixed}	x_1
x_E	201.10	201.10	201.10	201.10	**201.10**
x_S	674.57	923.06	923.06	923.06	**837.72**
x_W	163.55	163.55	163.55	163.55	**163.55**
x_{RE}	0	879.81	879.81	202.98	**427.42**
x_{RS}	0	0	0	0	**0**
x_{RW}	879.81	0	0	676.83	**452.39**
x_{RO}	0	0	0	0	**0**

(A) Sunny Day: 09-08-2022

(B) Cloudy Day: 26-08-2022

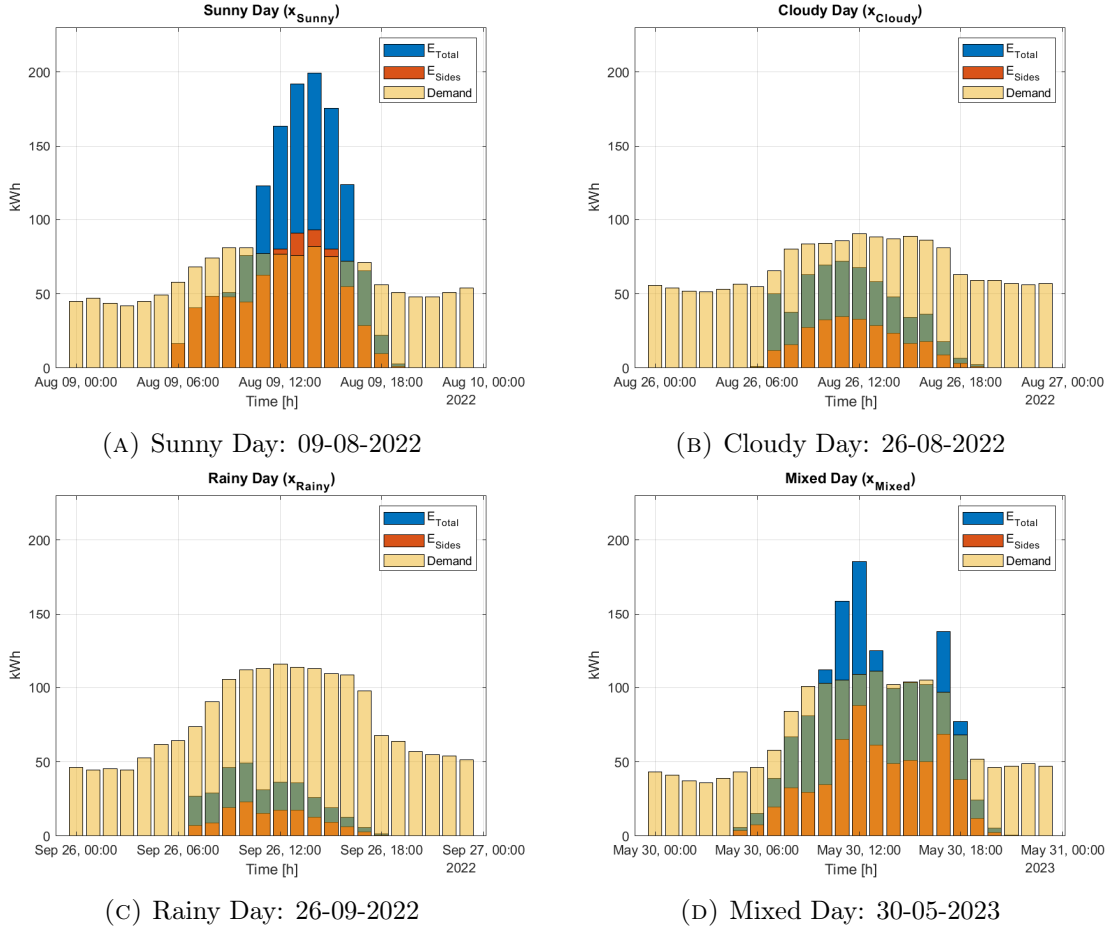(C) Rainy Day: 26-09-2022

(D) Mixed Day: 30-05-2023

FIGURE 5.4: Energy Profiles of Four Distinct Weather Days with the Solar Panel Distribution installed of the Corresponding Day

5.1.4 PV Sizing Method 3 Specification: One Objective Function Problem Formulation

To obtain the before-shown solar panel distribution x_3, for the third PV sizing method, the gathered data is used in Equation (3.5). The specifications incorporating the available information of the Zilverling building in one objective function are given here. Therefore, it follows to solve the problem defined in Equation (3.5):

- $x = x_3 = [x_E,\ x_S,\ x_W, x_{RE},\ x_{RS},\ x_{RW}, x_{RO}]$.

- $C = [\rho_E, \rho_S, \rho_W, \rho_{RE}, \rho_{RS}, \rho_{RW}, \rho_{RO}]$.

- d = Demand

- $lb = [0,0,0,0,0,0,0]$.

- $ub = [201.10, 923.06, 163.55]$.

- $Aeq = [0,\ 0,\ 0,\ 1,\ 1,\ 1,\ 1]$.

- $beq = [879.81]$.

46

For this PV sizing method, the objective problem is solved with demand and energy density data for the one-year period. Also in this method, a linear least-squares solver, implemented in MATLAB [46], is utilized to solve the problem.

5.2 Zilverling: Heating System

In this section, the methodology part from Section 3.3 is applied to the heating system of the Zilverling building. First, the heating demand data is assessed. As outlined in Chapter 4, the distribution of the heating demand is unknown and an accurate profile missing. Subsequently, two cases are formulated for the current and insulated Zilverling building, and the heat pump system is sized accordingly.

When initiating the assessment of the heating demand data for the Zilverling, the data structure, as illustrated in Figure 4.3b, reveals some key patterns. Notably, heating demand is most prominent during the colder months of the year, spanning from October to May. The data resolution is set at 1 GJ, with the system recording usage once every 1 GJ is consumed. This level of resolution can be deemed impractical, as the steps are too high and lack the necessary accuracy to establish a meaningful profile. Therefore, in the case of the Zilverling building, data imputation is necessary.

In this case, linear interpolation is employed to derive a new heating demand distribution based on the overall heating consumption of the University of Twente. The heating demand for each day is summed to obtain the total heating consumption for each individual day. This consumption is then redistributed linearly to the heating demand distribution of the entire University of Twente for that day.

Figure 5.5 illustrates the annual heating demand in GJ for both the University and the Zilverling building. Examining the days with the highest heating demand during the weekdays over a one-year period reveals significant patterns, as shown in Figure 5.6. Applying the linear interpolation to the heating data of the Zilverling building and redistributing it according to the heating demand profile of the University results in Figure 5.7.
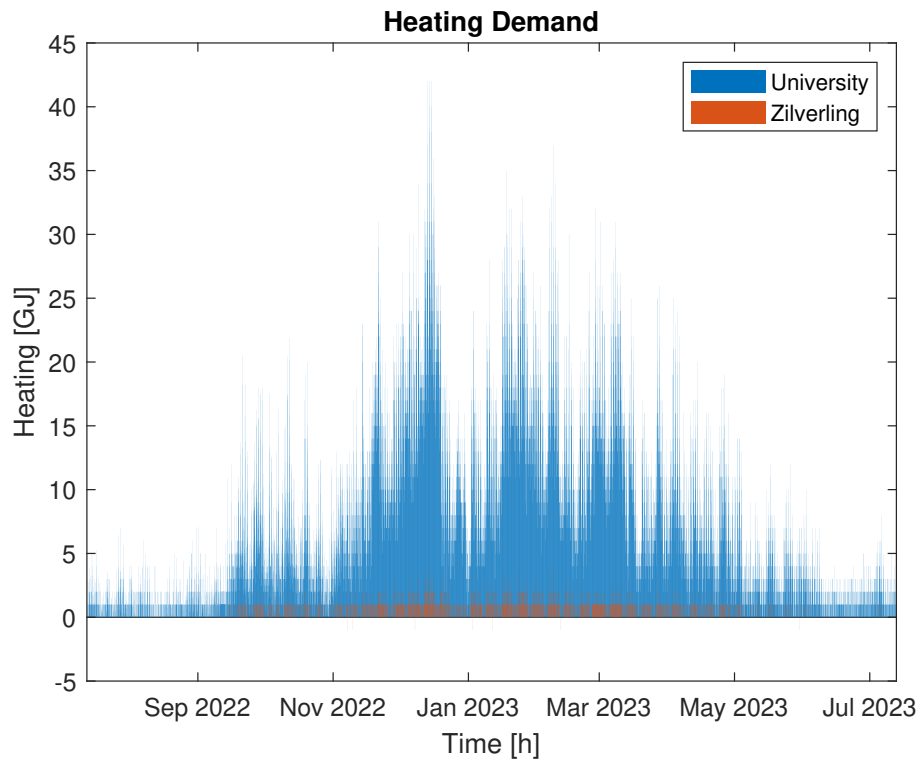
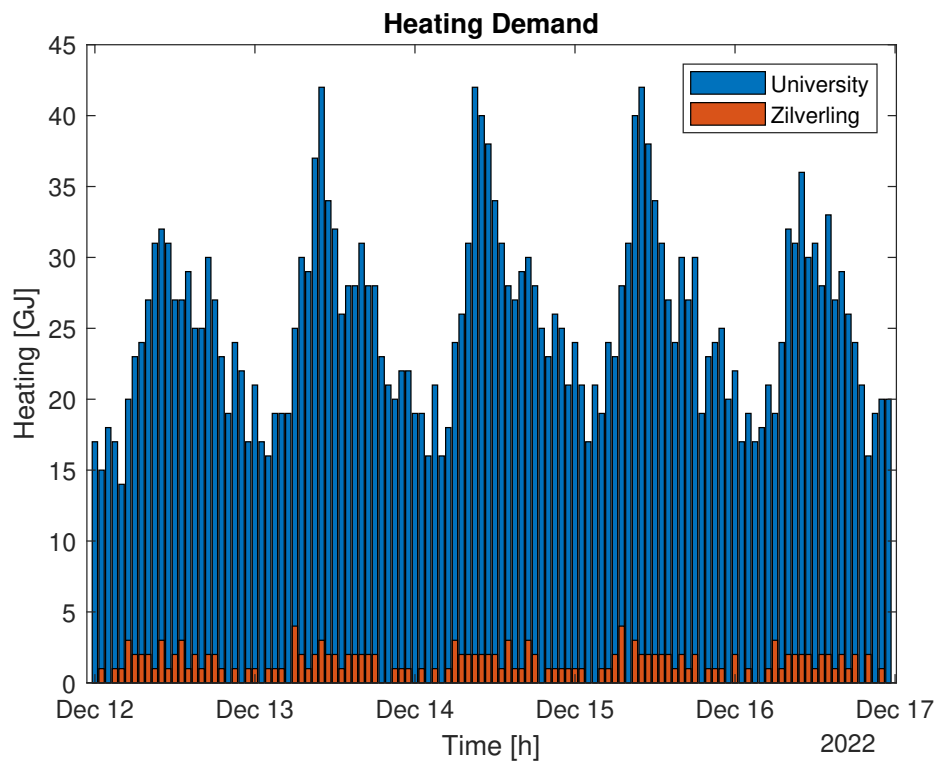FIGURE 5.5: Heating Demand of the University of Twente and the Zilverling Building over a Year

FIGURE 5.6: Heating Demand of the University of Twente and the Zilverling Building in December during the Highest Demand Days
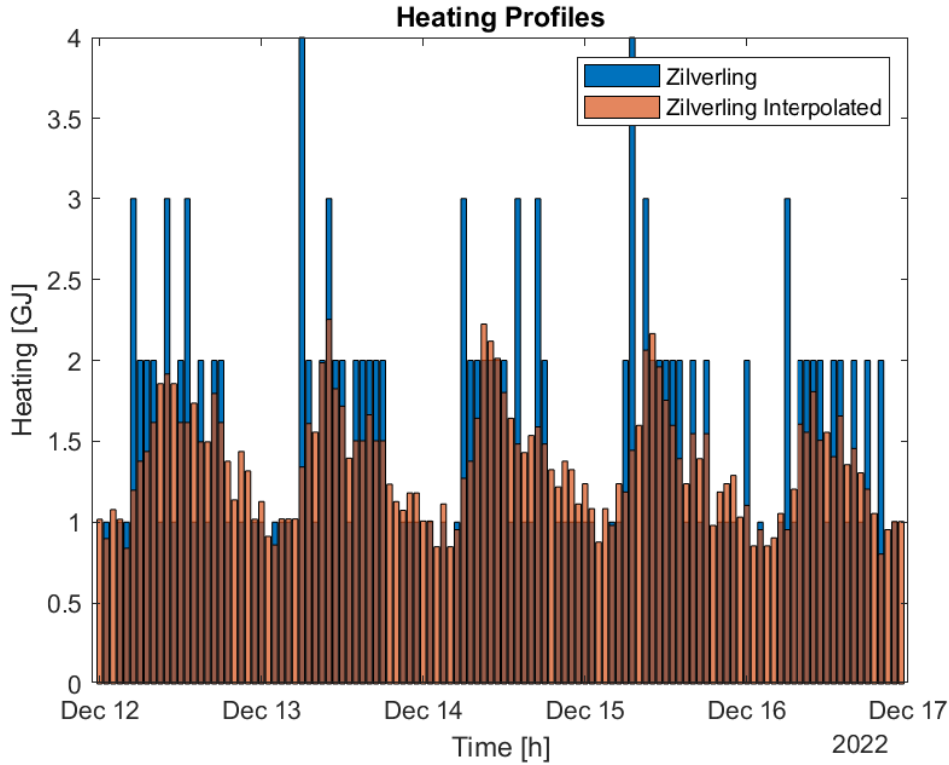
FIGURE 5.7: Interpolated Heating Demand Profile of Zilverling

The interpolated heating profile is considered the applicable heating profile for the Zil-verling building. Based on this profile, the impact of insulation and the introduction of heat pumps is assessed. Two cases are formulated: the first represents the current state of the Zilverling building with an energy label of C, and the second reflects a well-insulated Zilverling building with an energy label of A. To assess the impact of insulation on the Zilverling building, a standardized approach is used due to the absence of a more detailed heating model for the building. This standardized approach is based on the case discussed in [50], outlined in Subsection 3.3.1 before.

5.2.1 Current State Zilverling: Label C

To implement the standardized approach by Badenes et al. [50], it is crucial to determine the climate class and building type of the Zilverling building, according to the study. This information is essential for selecting the corresponding linear regression lines representing a non-insulated, low-insulated, and good-insulated building. By calculating the heating degree days and electricity consumption per square meter for heating annually, following the assumptions made in [50], an evaluation of the insulation of the Zilverling building can be conducted using the standardized approach.

The Zilverling building, with a heated area of approximately 1548 m^2 per floor and span-ning 5 stories, is located in climate class Cfb within [50]. It is comparable to building 3 among the cases presented in [50]. In this approach, three simple linear regressions between heating energy demand and yearly Heating Degree Days (HDD_y) are used to size heat pumps with a Coefficient of Performance (COP) of 3 assumed.

Applying Equation (3.6) with the temperature recorded at the Airport Twente and sum-ming up the resulting HDD_d values over a year gives the HDD_y value for the Zilverling

building. This results in a value of $HDD_y = 2561$. To obtain the corresponding electricity demand in [kWh/m²year] the following calculation needs to be done:

$$E_{HeatPump} = \frac{H_{Yearly} \cdot 277.778}{COP \cdot A}$$ (5.6)

where:

- $E_{HeatPump}$ is the electricity demand needed for the heat pump in kWh/m^2year

- H_{Yearly} is the yearly heating demand in GJ

- 277.778 is the conversion factor from GJ to kWh

- COP is the Coefficient of Performance of the heat pump

- A is the heated area of the building, including all floors, in m^2

Given the COP value of 3, and the heating demand data and information about the Zilverling building results, for the case comparison, in $H_{Yearly} = 3221.7$ GJ, COP = 3 and $A = 5417.5 \ m^2$. This results in a calculated value of 55.06 kWh/m^2year for the Zilverling building.

As described in Subsection 3.3.1, the energy demand for heating for a building like the Zilverling in the climate zone of the Netherlands (Cfb) can be described with three different insulation scenarios as linear regressions, where y represents the electricity demands for heat pumps and x represents the yearly heating degree days (HDD) [50]:

$$\text{No Insulation: } y = 0.03x - 6.98$$ (5.7)

$$\text{Low Insulation: } y = 0.03x - 9.78$$ (5.8)

$$\text{Good Insulation: } y = 0.02x - 16.79$$ (5.9)

These linear regressions, representing different insulation scenarios, along with the positioning of the Zilverling within this case, are depicted in Figure 5.8.
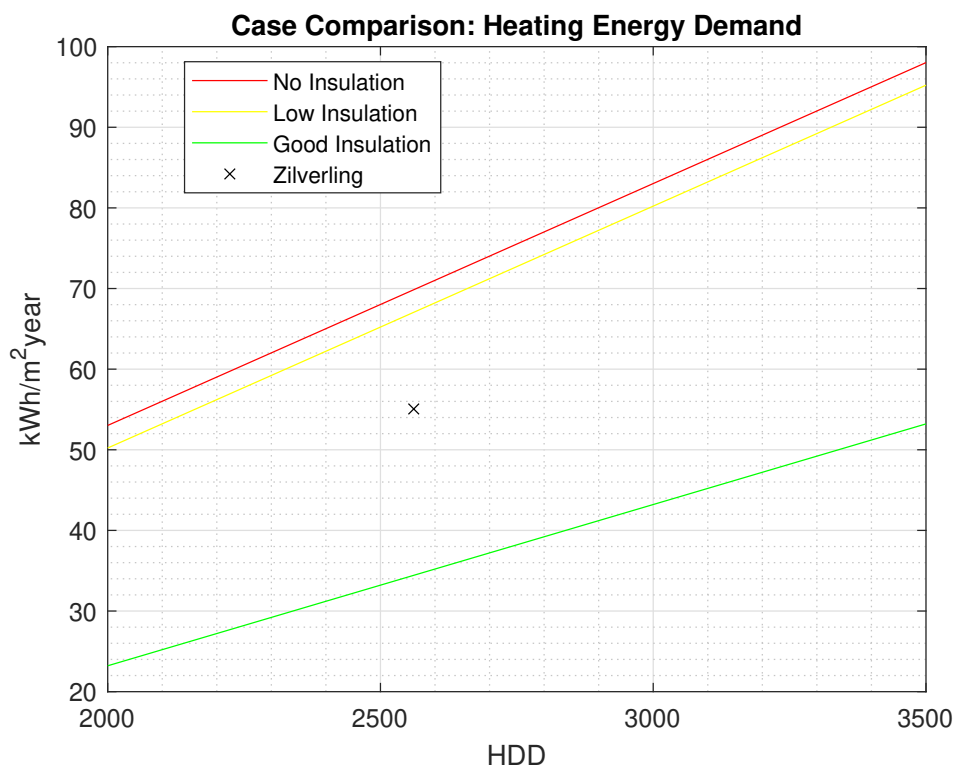
FIGURE 5.8: Electricity Consumption for Heating against Heating Degree Days

Based on Figure 5.8, the Zilverling building falls between a low-insulated and a good-insulated building, with a heating energy demand for heat pumps of 55.06 kWh/m^2year. For the current state Zilverling (Label C), the interpolated heating demand profile shown in Figure 5.7 is considered applicable.

5.2.2 Insulated Zilverling: Label A

In the previously presented case, a good-insulated building with an equivalent HDD_y value would have an electricity demand for heating of 34.43 kWh/m^2year. Therefore, by improving the insulation of the Zilverling to the level of a good-insulated building, it is possible to achieve a 37.47% reduction in heating energy demand, resulting in a yearly energy reduction amount of $TER = 1207.19$ GJ.

Insulation has the potential to decrease the overall net energy demand by reducing energy losses to the surrounding environment. Furthermore, it can change the dynamics of a building's heat demand due to the time lag and decrement factor of the insulation. This means that heat can be retained longer in the building with lower losses and a slower-reacting system is achieved [63] [64]. This can be beneficial for heating by avoiding large demand peaks through preheating. However, it can also be less favorable for cooling during the summer, as additional heat, for example, from solar radiation, is retained, making cooling more challenging.

To implement the energy reduction and the effects of a slower-reacting system on the heating demand of the Zilverling building for the energy label A case, the general assumption is made to first reshape the heating demand by signal smoothing using the moving mean (movmean) function implemented in MATLAB [65]. Subsequently, the new profile is scaled accordingly to the possible energy reduction of 37.47% due to improved insulation.

In the movmean process, a window size of four elements forward and one element backward is chosen. The choice of four elements forward represents half of a workday in the sliding window, further dividing the day into six distinct parts, allowing anticipation of the peak heating demand in the morning hours of the workday and smoothing the demand curve. The window size seems practical for additional considerations, for example, the implementation of preheating the building during the night to flatten the peak in the morning. The inclusion of one element backward provides an influence on whether the building is in a heating or cooling phase. Through using movmean the overall energy amount is preserved. The resulting heating demand profile, compared to the current state's Zilverling heating demand profile, is presented in Figure 5.9. This comparison focuses again on the weekdays with the highest heating demand.
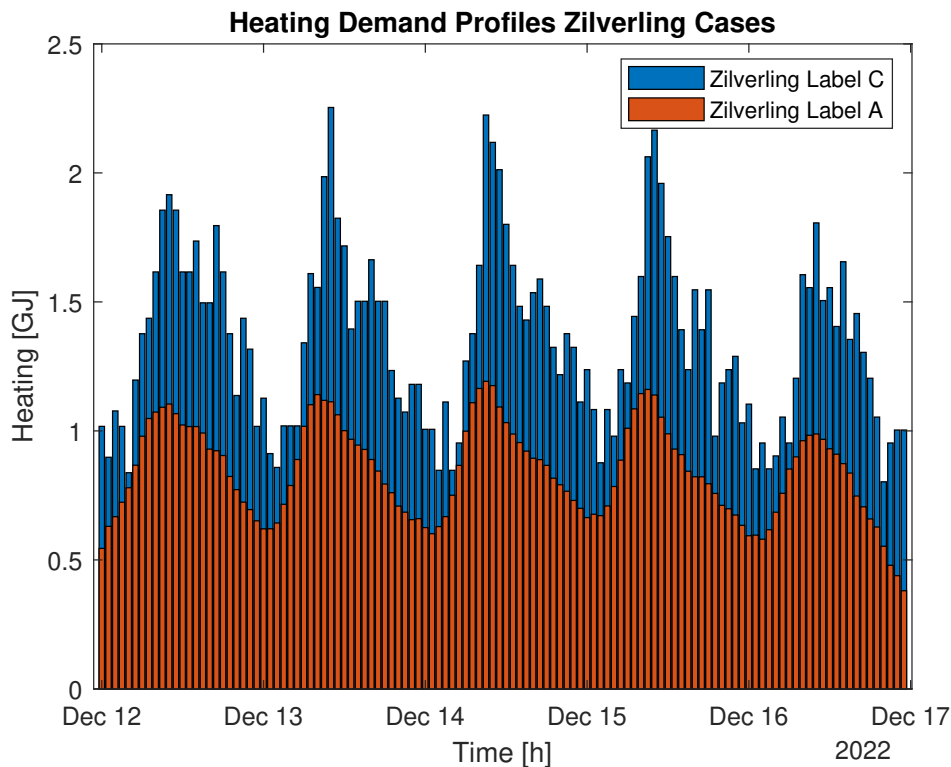

FIGURE 5.9: Heating Demand Profiles for the Zilverling Cases showing the Weekdays with the Highest Heating Demand

5.2.3 Zilverling: Heat Pump Sizing

Based on the heating demand profile of the current and good insulated Zilverling building, the heat pump system can be sized as outlined in Subsection 3.3.2. For sizing, the distribution of the heating demand needs to be known to ensure it adequately meets individual demands, especially larger ones. This prevents oversizing the heat pump based on a single occurrence of maximum demand. The distribution for both cases is shown in Figure 5.10.

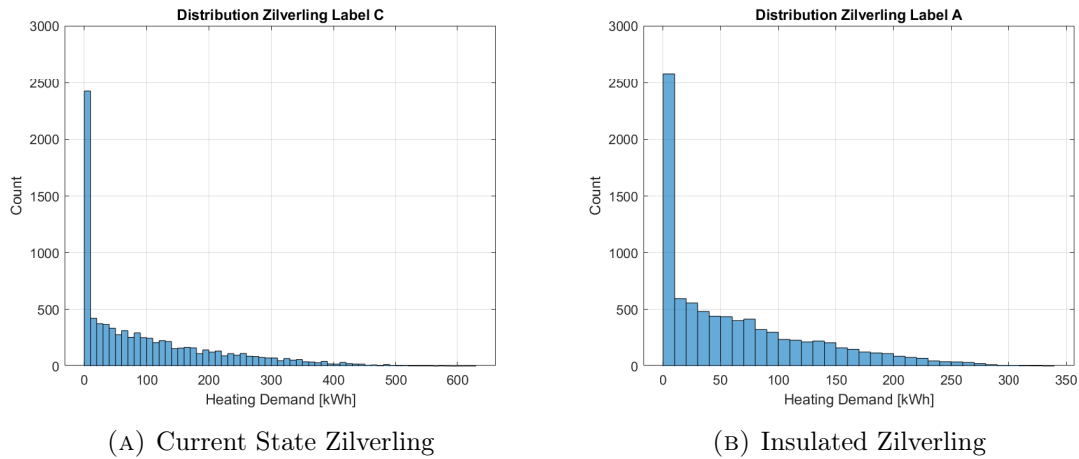(A) Current State Zilverling (B) Insulated Zilverling

FIGURE 5.10: Histograms of Heating Demand in kWh for the Two Cases

The histograms clearly show that the majority of heating demands fall within the lower range. However, when sizing the heat pumps, it is crucial to focus on the larger demand amounts, especially to ensure sufficient heating during the winter. To do this, it is practical to examine the distribution of the largest 25% of heating demand values for the year, as these occur during the winter in this case and others in the same climate zone [53]. Setting a limit to meet 97.5% of the 25% highest heating demand intervals is a reasonable approach to avoid oversizing the system based on a single maximum demand occurrence. The histograms for this and 97.5% coverage are shown in Figure 5.11.

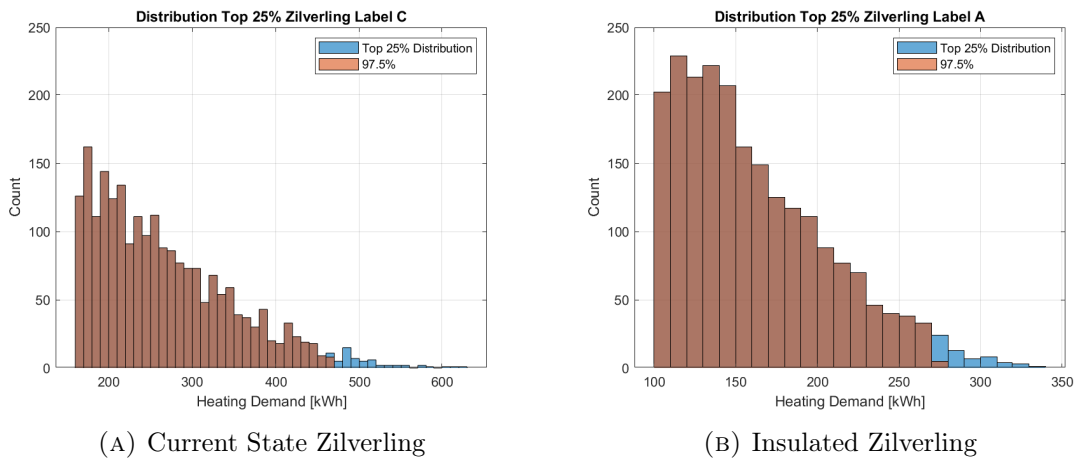(A) Current State Zilverling (B) Insulated Zilverling

FIGURE 5.11: Histograms of Top 25% Heating Demand in kWh for the Two Cases

For the current state of the Zilverling building, a heat pump with a heating capacity of 465 kW is required, while for the insulated Zilverling case, a heat pump with a heating capacity of 272 kW is needed. In both cases, these heat pump sizes are sufficient to cover 99.38% of the yearly heating demand fully. When implementing the heat pump systems, it is advisable to set up systems with capacities equal to or, if a system equal to the number is not available, slightly above these values to ensure coverage of the heating demands in practice.

The distribution in time of the leftover heating demand with the installed heat pump systems is shown in Figure 5.12. In 55 hours distributed over the winter months, in both

cases, the heat pump system cannot provide all necessary heating. For the Zilverling Label C, this means a total heating not provided of 8.84 GJ in the year, and for the Zilverling Label A, a total heating not provided of 3.74 GJ in the year. Compared to the total annual heating demand of the Zilverling building Label C with 3,222 GJ and of the Zilverling Label A with 2,015 GJ, these amounts are small and only occur during short intervals in peak hours of high-demand days but not for entire days and longer periods.
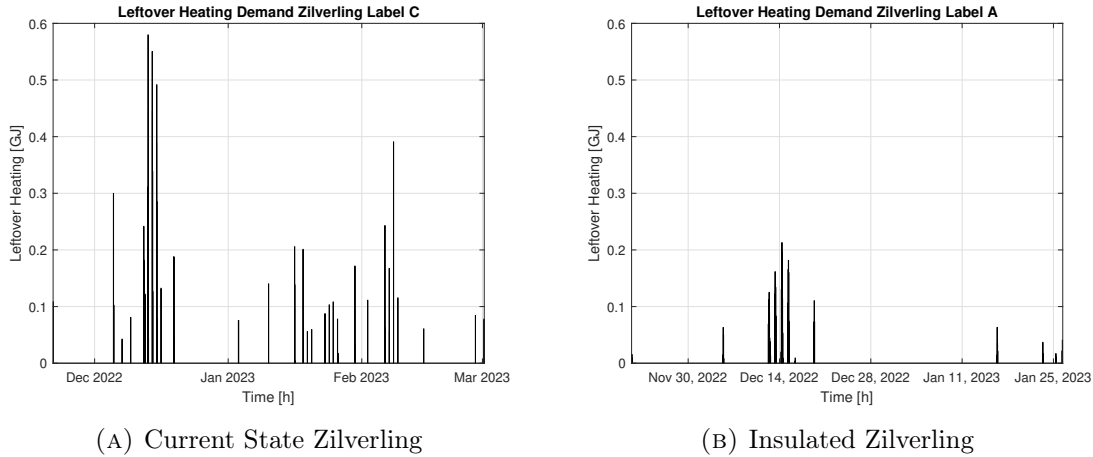

(A) Current State Zilverling

(B) Insulated Zilverling

FIGURE 5.12: Distribution in Time of Leftover Heating Demand for the Two Cases

5.2.4 Implemented System

For each of the possible proposed Zilverling cases, it is assumed that the heating capacity from the heat pump sizing is installed with a COP of 4.3 referring to systems produced by Viessmann [66]. Due to the heat pumps, the initial electricity demand will increase to provide the energy for heating the building. Accordingly, the influence of heat pumps on the electricity demand can be seen in Figure 5.13 and 5.14. The total electricity demand increases over the year from 531.20 MWh to 738.74 MWh in the case of Zilverling Label C and 661.09 MWh in the case of Zilverling Label A. This resembles an increase of 39.07% and 24.45%, respectively. It is obvious that the well-insulated case requires less energy as less energy is lost to the environment reducing the heating demand and therefore, the total demand and the additional electricity required to supply the heating. The different total electricity demands for both cases results also in different self-sufficiency and self-consumption rates. Therefore, the inclusion of a 465 kW heat pump system achieves a self-sufficiency of 31.16% and a self-consumption of 64.44% for the Zilverling Label C with solar panel distribution x_1 installed. For the Zilverling Label A, the installation of a 272 kW heat pump system results in a self-sufficiency of 33.68% and a self-consumption of 62.33% with solar panel distribution x_1 installed. It can be seen that the self-sufficiency is higher and the self-consumption is lower for the Label A case than for the Label C case. This is logical as the total demand is lower in the case of Label A influencing the self-sufficiency, as well as the energy consumed is lower in the case of Label A, while the energy production stays the same.
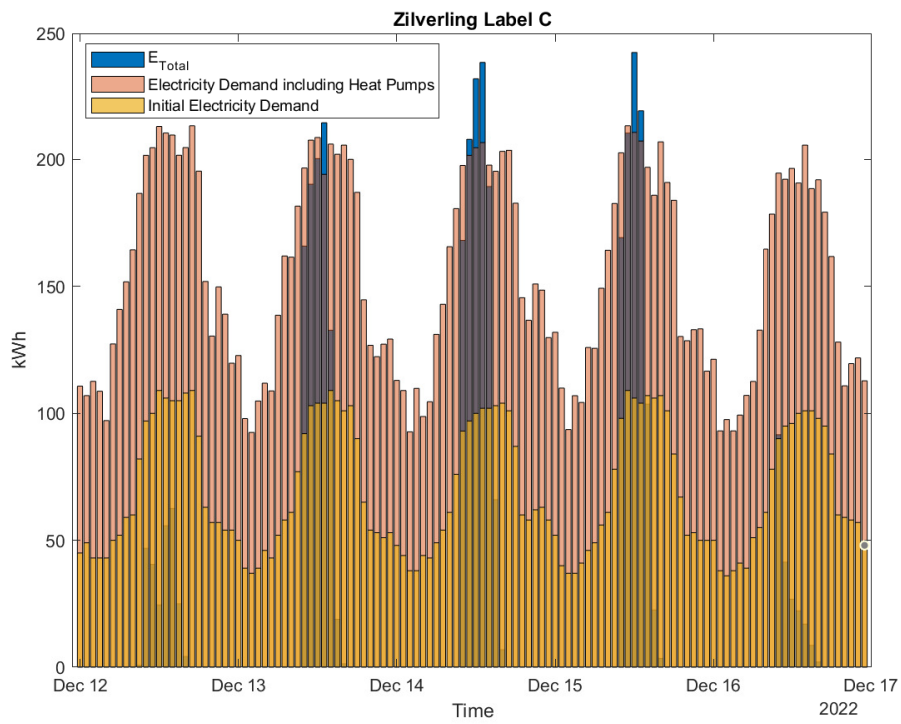
FIGURE 5.13: Influence of Heat Pump System on Electricity Demand - Zilverling Label C
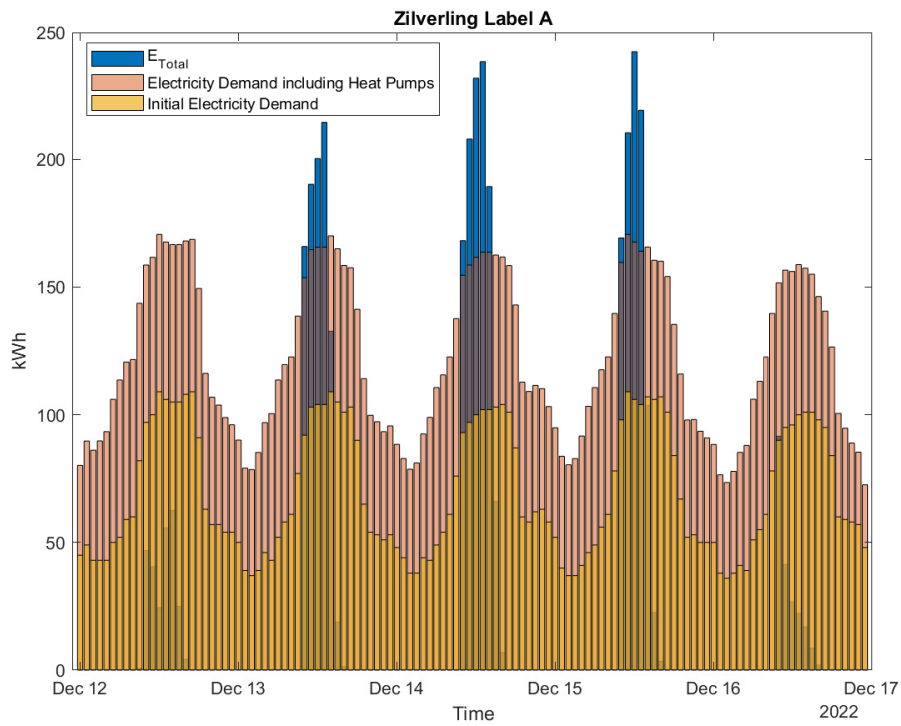

FIGURE 5.14: Influence of Heat Pump System on Electricity Demand - Zilverling Label A

5.2.5 Redistribution of Solar Panel Installation

Including the electricity demand for the respective installed heat pump systems in the linear least-squares problem formulations results in new redistributed solar panel distributions. These are shown in Table 5.4 with the initial distributions. To obtain these, the energy demand data for the entire year needs to be considered. As the heating demand occurs mainly in winter and the main energy production, due to high solar irradiation, is in summer, the production and additional demand need to overlap to influence the distribution of solar panels following the formulation of the linear least-squares problems. This overlap mainly occurs during spring and fall times. Therefore, the PV sizing method based on four distinct weather days can not be included here as a dataset length of at least a year is required in this case.

TABLE 5.4: Redistributed Installed Solar Panel Areas (rd) in m^2 for Zilverling Energy Label C and A and # Amount of Panels needed [1.65m^2]

$[m^2]$	x_2	x_{2-rd-C}	x_{2-rd-A}	x_3	x_{3-rd-C}	x_{3-rd-A}
x_E	201.10	201.10	201.10	201.10	201.10	201.10
x_S	863.24	923.06	923.06	0	85.93	13.36
x_W	163.55	163.55	163.55	162.85	163.55	163.55
x_{RE}	0	130.94	57.78	133.99	272.75	211.89
x_{RS}	0	0	0	0	0	0
x_{RW}	879.81	748.87	822.03	745.82	607.05	667.92
x_{RO}	0	0	0	0	0	0
Facades	1227.89	1287.71	1287.71	363.95	450.58	378.01
#	744	780	780	220	273	229
Total	2107.7	2167.52	2167.52	1243.76	1330.38	1257.82
#	1277	1313	1313	753	806	762

5.3 Zilverling: Energy Storage System

In this section, the implementation of a battery storage system and thermal buffer storage are applied to the Zilverling building. The methodology of Section 3.4 is applied here. First, a Li-Ion battery operating with no smart control, including C-Rate and overall efficiency for different scaled capacity sizes, based on the INTILION scale racks [31], neglecting self-discharge rates, is implemented. Second, a thermal heat buffer system using water operated on the thermal output side of the heat pump system is considered, implementing an overall efficiency of 70% to 90% and neglecting self-discharge rates again. For each of the two storage types, a sizing suggestion is given as a viable option for the case of the Zilverling building.

5.3.1 Li-Ion Battery

For the first energy storage case, the methodology of Subsection 3.4.1 is applied. The example of INTILION scale racks with steps of 154 kWh capacity is assumed, with an efficiency of 90% and a C-Rate of 0.9688 [31]. With this assumed battery storage, the influence on self-sufficiency and self-consumption is analyzed per installed capacity size with no smart control operation considered. For the Zilverling cases of Label C and Label A with the installed solar panel areas resulting from the four distinct weather days x_1, the

self-sufficiency and self-consumption against the installed battery capacity size can be seen in Figure 5.15. This solar panel installation was chosen as it has the largest overall energy production.
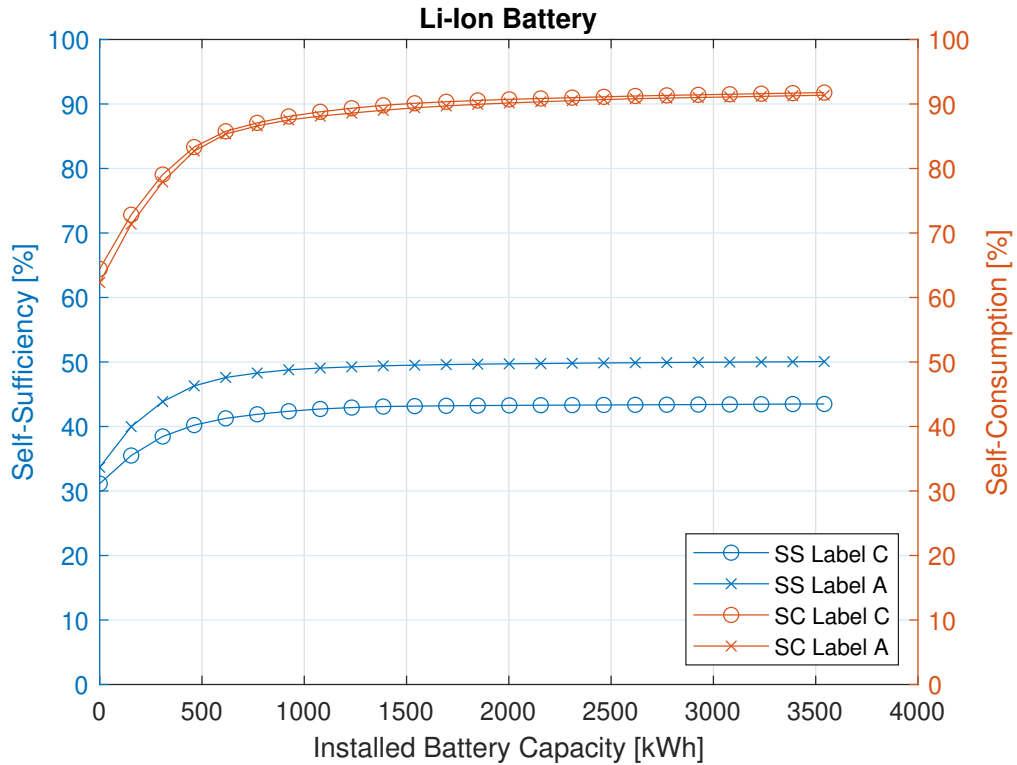

FIGURE 5.15: SS and SC shown against installed Battery Capacity for Zilverling Label C and Label A

The relationship between installed capacity and self-sufficiency, as well as self-consumption, exhibits saturation. For smaller capacities, the storage system is almost linearly scalable. After reaching a point of 308 kWh installed capacity, the system becomes partially saturated, and after 1000 kWh, it reaches saturation. The curve begins to flatten as more capacity is required to utilize smaller amounts of produced surplus energy for later demand. The areas of interest for implementing a storage system are the first two regions, linearly scalable and partially saturated. Here, an increase in capacity significantly influences self-sufficiency and self-consumption. In the saturated area, the gained benefit is marginal compared to the extra installed capacity.

For the Zilverling building, the installation of an indoor storage system such as the INTILION scalestac, with capacity sizes up to 1200 kWh [31], could be a viable option for commercial use. This system offers the advantage of occupying a relatively small but necessarily secure area within the building.

5.3.2 Thermal Buffer System

For the second energy storage case, the methodology of Subsection 3.4.2 is applied. A thermal heat buffer system operated on the thermal output side of the heat pump system using water as the storage medium is assumed. An efficiency of 82.5% is assumed as the standard, within an efficiency range of 70% to 90%. To have a direct comparison to the previous battery case, this independent buffer case is scaled by the assumed COP of 4.3 of

the heat pumps system times 154 kWh, so, in steps of 662.2 kWh of installed heat capacity. With this assumed water heat storage, the influence on self-sufficiency and self-consumption is analyzed per installed heat capacity size. For the Zilverling cases of Label C and Label A with the installed solar panel areas resulting from the four distinct weather days x_1, the self-sufficiency and self-consumption against the installed buffer capacity size can be seen in Figure 5.16.
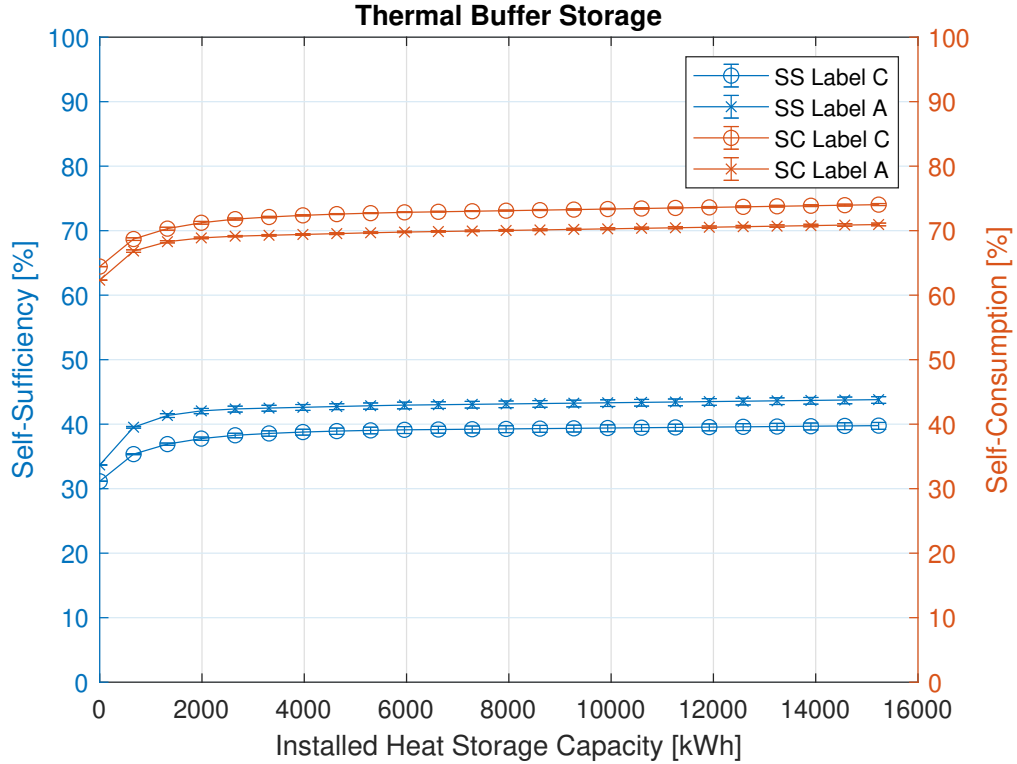

FIGURE 5.16: SS and SC shown against installed Heat Storage Capacity for Zilverling Label C and Label A

Similar to the saturated relationship observed with the battery case, a similar pattern emerges with the thermal buffer storage. However, since the thermal buffer storage responds only to heating demands and not electricity demands of the building, the saturated self-sufficiency and self-consumption levels are lower. This is because less total surplus energy can be utilized. Consequently, the curve saturates more quickly and is saturated after 2000 kWh of installed heat storage capacity. Therefore, the interesting area for implementing the thermal buffer system is below 2000 kWh of installed capacity. Considering the following:

- Q = 2,000 kWh = 7,200,000 kJ

- T_{HP} = 65°C for the assumed heat pump system by Viessmann [66]

- T_R = 50°C for the radiators in the Zilverling building

- c_p = 4.19 kJ/kg°C (for 57.5°C) [55]

- ρ_{Water} = 984.46 kg/m³ (for 57.5°C) [56]

Solving with these inputs Equations (3.7) and (3.8) results in a mass of water required $m_{Water} = \textbf{114,558.47 kg}$, corresponding to a volume of $V_{Water} = \textbf{116.37 m}^3$. Comparing this volume to other tank sizes [35],[36],[37], it is reasonably large. Indoor and Outdoor solutions can be considered dependent on the preferences of the stakeholder. An outdoor installation of such a tank in the surrounding area of the Zilverling would be possible underground or overground. The span of possibilities is large as the tank required does not have a size of 20,000 m^3 like for example the above-ground water reservoir for district heating in Dessau-Rosslau, Germany, and has approximately twice the size of a basement installation for long-term heat storage in the same location [35]. Both systems can be seen in Appendix Figure 8.4.

5.4   Zilverling: Pareto Plots

In this section, the Pareto Plots, introduced in Section 3.5, for the case of the Zilverling building are presented, together with all possible solutions based on the cases assumed in this thesis. The possible solutions encompass five different solar panel distributions in two case scenarios for the heating system of the Zilverling Label C and Label A. Here, the solutions show the impact on the self-sufficiency and self-consumption of the Zilverling building through the implementation using only the facades of the Zilverling building to the inclusion of the roof and the addition of a heat pump system, also considering the redistribution of solar panels based on the inclusion of the heating demand in the linear least-squares problem formulation. Therefore, 10 possible solar panel distribution solutions are presented with three different installation setups.

Based on these solutions, two Pareto fronts follow, one for the Pareto optimal self-sufficiency points and one for the Pareto optimal self-consumption points. The primary objective is to achieve a maximization of self-sufficiency while ensuring energy-efficient energy usage by considering self-consumption as the second prioritized parameter. Therefore, with the Pareto front for self-sufficiency, the trade-off between self-sufficiency and additional investment costs can be investigated on a smaller set of Pareto optimal points. All installation possibilities, represented in the points, are reduced to a set of efficient choices. Within this set of efficient choices, points for further investigation are picked, and additional considerations can be made based on those. Further, additional information is required to find a fitting solution as points on the Pareto front can have different system setups, so, the self-consumed energy, total energy supplied to the building, total energy demand of the building, and payback time can differ. The assumed costs for each system part for the Zilverling building are summarized in Table 5.5.

The 10 resulting solutions are depicted in Figure 5.17. The first point on each line represents the SS and SC for the energy produced at the facades of the Zilverling building. The second point includes the roof and denotes the SS and SC values for the total installed solar panel distribution. The third point shows the SS and SC for the inclusion of the heat pump system. Additional information for each point, including the total electricity produced, total electricity self-consumed, total electricity demand, electricity self-consumed by the building, electricity self-consumed for heating, total heating self-supplied, and total energy supplied, can be found in Table 5.6 and 5.7 for the Zilverling Label C and in Table 5.8 and 5.9 for the Zilverling Label A. The total heating demand and total energy demand are also presented. Within these Tables, the electricity production differs due to the different installed solar panel distributions and the heating supplied differs due to the different-sized heat pumps. Also, as the third point of each solution includes the heating system, the electricity self-consumed, the total heating self-supplied and the total energy

supplied differ.

The resulting Pareto plot, based on the presented solutions, is shown in Figure 5.18. It displays the Pareto Front for self-sufficiency and for self-consumption with the corresponding self-consumption and self-sufficiency points associated with the other front respectively. The points picked for further investigation are marked with a black circle.

TABLE 5.5: Investment Costs per System Part for the Zilverling Building based on Costs shown in Chapter 2

System Part	Investment Costs	Deviation
Solar Panel [420wp/1.65m^2]	315.46 € per Panel	72.11 € per Panel
Heat Pump System [Label C]	87,129 €	13,069 €
Heat Pump System [Label A]	61,422 €	9,213 €
External Wall Insulation	213,707 €	45,665 €
Battery	346.84 €/kWh	9.2 €/kWh
Heat Storage	15 €/kWh	10 €/kWh

TABLE 5.6: Total Electricity Demand and Electricity Supply for each Case Zilverling Label C

Solar Panel Distribution	# Point	Total Electricity Produced (TEP) [MWh]	Total Electricity Self-Consumed (TESC) [MWh]	Zilverling Label C Total Electricity Demand [MWh]
x_1	1	172.98	149.55	531.20
	2	378	221.07	531.20
	3	378	243.58	738.51
x_2	1	176.26	151.22	531.20
	2	305.53	198.67	531.20
	3	305.53	209.88	738.51
x_{2-rd-C}	1	183.93	154.97	531.20
	2	336.41	211.86	531.20
	3	336.41	226.51	738.51
x_3	1	65.49	65.15	531.20
	2	218.51	176.22	531.20
	3	218.51	180.37	738.51
x_{3-rd-C}	1	76.56	76.07	531.20
	2	254.17	191.25	531.20
	3	254.17	198.84	738.51

TABLE 5.7: Electricity and Heating Consumption Zilverling Label C with a COP of 4.3

Solar Panel Distribution	# Point	Electricity Self-Consumed by building (ESC) [MWh]	Electricity Self-Consumed for Heating [MWh]	Total Heating Self-Supplied (THS) [MWh]	Zilverling Label C Total Energy Supplied (TES) [MWh]
x_1	1	149.55	-	-	149.55
	2	221.07	-	-	221.07
	3	182.75	60.83	261.57	444.32
x_2	1	151.22	-	-	151.22
	2	198.67	-	-	198.67
	3	154.20	55.68	239.42	393.62
x_{2-rd-C}	1	154.97	-	-	154.97
	2	211.86	-	-	211.86
	3	167.83	58.68	252.31	420.14
x_3	1	65.15	-	-	65.15
	2	176.22	-	-	176.22
	3	130.37	50.00	215.01	345.38
x_{3-rd-C}	1	76.07	-	-	76.07
	2	191.25	-	-	191.25
	3	144.95	53.89	231.71	376.67
Total Heating Demand: 894.90 MWh					
Total Energy Demand (TED): 1.4261 GWh					

TABLE 5.8: Total Electricity Demand and Electricity Supply for each Case Zilverling Label A

Solar Panel Distribution	# Point	Total Electricity Produced (TEP) [MWh]	Total Electricity Self-Consumed (TESC) [MWh]	Zilverling Label A Total Electricity Demand [MWh]
x_1	1	172.98	149.55	531.20
	2	378	221.07	531.20
	3	378	235.60	660.98
x_2	1	176.26	151.22	531.20
	2	305.53	198.67	531.20
	3	305.53	206.31	660.98
x_{2-rd-A}	1	183.93	154.97	531.20
	2	323.44	205.95	531.20
	3	323.44	214.85	660.98
x_3	1	65.49	65.15	531.20
	2	218.51	176.22	531.20
	3	218.51	178.98	660.98
x_{3-rd-A}	1	67.25	66.90	531.20
	2	234.08	183.61	531.20
	3	234.08	187.32	660.98

TABLE 5.9: Electricity and Heating Consumption Zilverling Label A with a COP of 4.3

| Solar Panel Distribution	# Point	Electricity Self-Consumed by building (ESC) [MWh]	Electricity Self-Consumed for Heating [MWh]	Total Heating Self-Supplied (THS) [MWh]	Zilverling Label A Total Energy Supplied (TES) [MWh]
x_1	1	149.55	-	-	149.55
	2	221.07	-	-	221.07
	3	195.67	39.93	171.70	367.38
x_2	1	151.22	-	-	151.22
	2	198.67	-	-	198.67
	3	167.91	38.40	165.13	333.04
x_{2-rd-A}	1	154.97	-	-	154.97
	2	205.95	-	-	205.95
	3	175.87	38.98	167.62	343.49
x_3	1	65.15	-	-	65.15
	2	176.22	-	-	176.22
	3	143.97	35.01	150.55	294.52
x_{3-rd-A}	1	66.90	-	-	76.07
	2	183.61	-	-	191.25
	3	151.73	35.59	153.02	304.75
Total Heating Demand: 559.57 MWh					
Total Energy Demand (TED): 1.0908 GWh					
Total Energy Reduction (TER): 1207.19 GJ = 335.33 MWh					
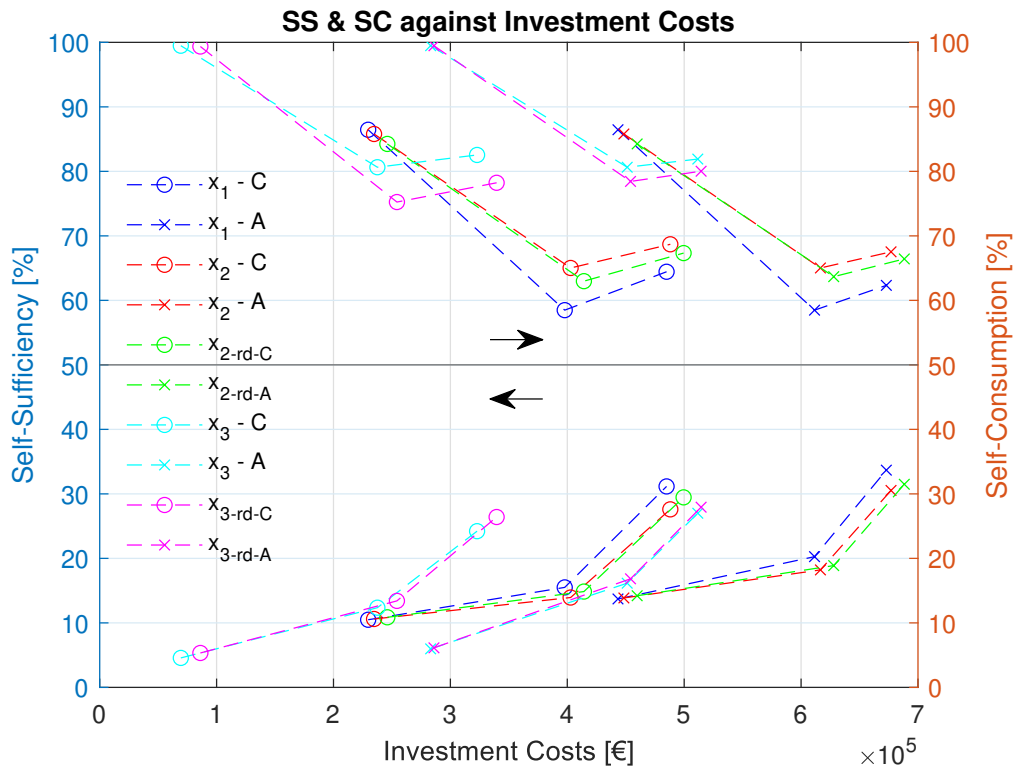
FIGURE 5.17: SS & SC of all 10 Solutions, Arrows indicate association of lines to y-axis, under the black y-line to SS over it to SC
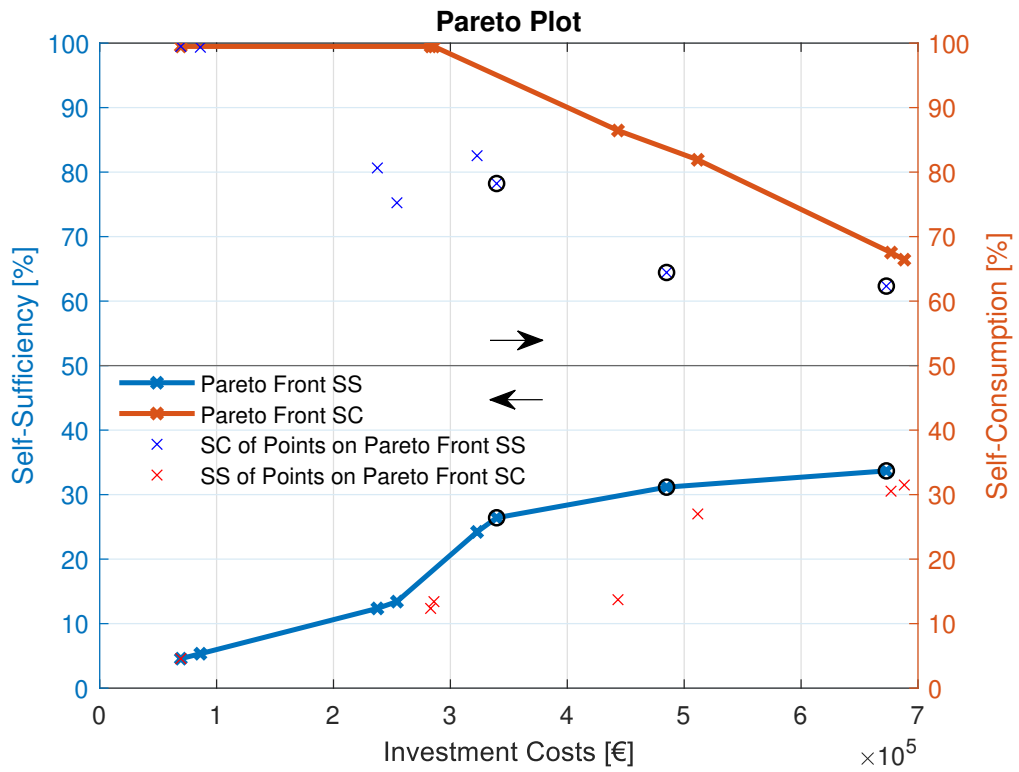

FIGURE 5.18: Pareto Front of Pareto Optimal Solutions, Arrows indicate association of lines to y-axis, under the black y-line to SS over it to SC

In Figure 5.17 it can be observed that the self-sufficiency of the utilization of only the facades of the Zilverling building is in every solution the lowest but has the highest self-consumption. This is to be expected because the overall energy production is lower and therefore more energy produced can be directly consumed. Therefore, with further increasing installation size by utilizing the roof with solar panels, the self-sufficiency increases while the self-consumption decreases from points 1 to 2. The overall energy production increases here in every solution.

Further, it can be observed that the solar panel distribution of x_3 in the case of Zilverling Label C and A has the lowest investment costs per heating system case. They also have a lower self-sufficiency and a higher self-consumption through the overall lower energy production. The lower investment costs follow from the additional freedom in the solving approach. The roof is utilized first due to higher energy densities obtained due to the higher received irradiation through optimal inclination compared to the installation at the facades of the building. Therefore, fewer panels are required, and thus the investment costs are lower.

The difference in costs for the same installation of solar panels between Zilverling Label C and Label A is the installation costs of the external wall insulation of €213,707. Through the insulation, the heating demand and therefore the overall energy demand is also reduced. Thus, it follows that self-sufficiency is increased in Zilverling Label A solutions compared to Zilverling Label C solutions.

In all solutions, the integration of the heat pump system shows the largest gain in self-sufficiency and also increases self-consumption. The energy production stays the same but due to the inclusion of the heat pump based on the COP, more heat is pumped into the building with a smaller increase in electricity consumption. The advantages of a hybrid system of solar energy production and heat pumps and the prioritization of the supply of heat demand can be seen here.

In Figure 5.18 the Pareto plot of the before-presented solutions is shown. From the Pareto optimal points for self-sufficiency, the three points with the largest self-sufficiency are picked for further investigation. These points are the third point of the solar panel installation x_{3-rd-C}, and x_1 for Zilverling Label C and Label A. They are Pareto optimal points for self-sufficiency. However, it can be seen that their self-consumption is not Pareto optimal. The point associated with x_{3-rd-C} has the highest self-sufficiency for the lowest investment costs relative to the other Pareto optimal points on the front, as it is located in the region of the largest gain per additional investment costs. For the points associated with x_1 for Zilverling Label C and Label A, more additional investment costs are required for a smaller gain in self-sufficiency, but these points have the two largest self-sufficiency values of the Pareto optimal points. For further investigation, the inclusion of the battery and thermal storage is demonstrated on the three picked Pareto optimal points. For the three picked points, it is expected that the inclusion of storage solutions has the largest benefit for the solar panel installation of x_1 for Zilverling Label C and Label A as these points have the largest total energy production and the lowest self-consumption. Therefore, more energy is still available for consumption compared to x_{3-rd-C}.

The impact of the inclusion of storage solutions with the Pareto fronts is shown in Figure 5.19 and 5.20.
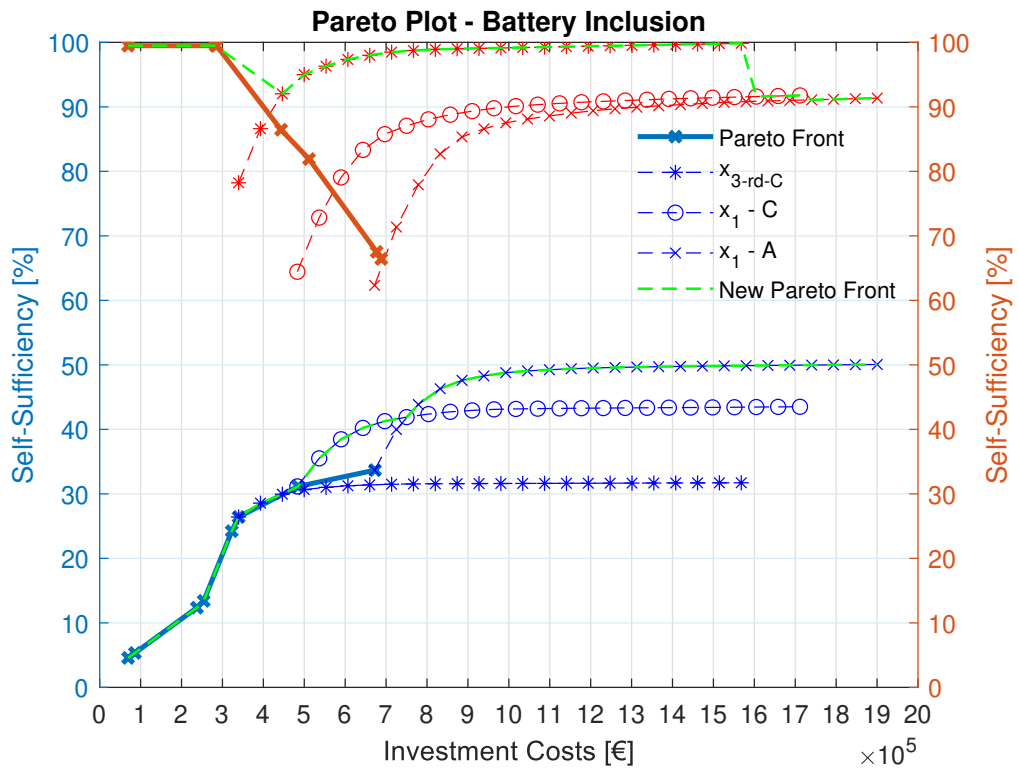
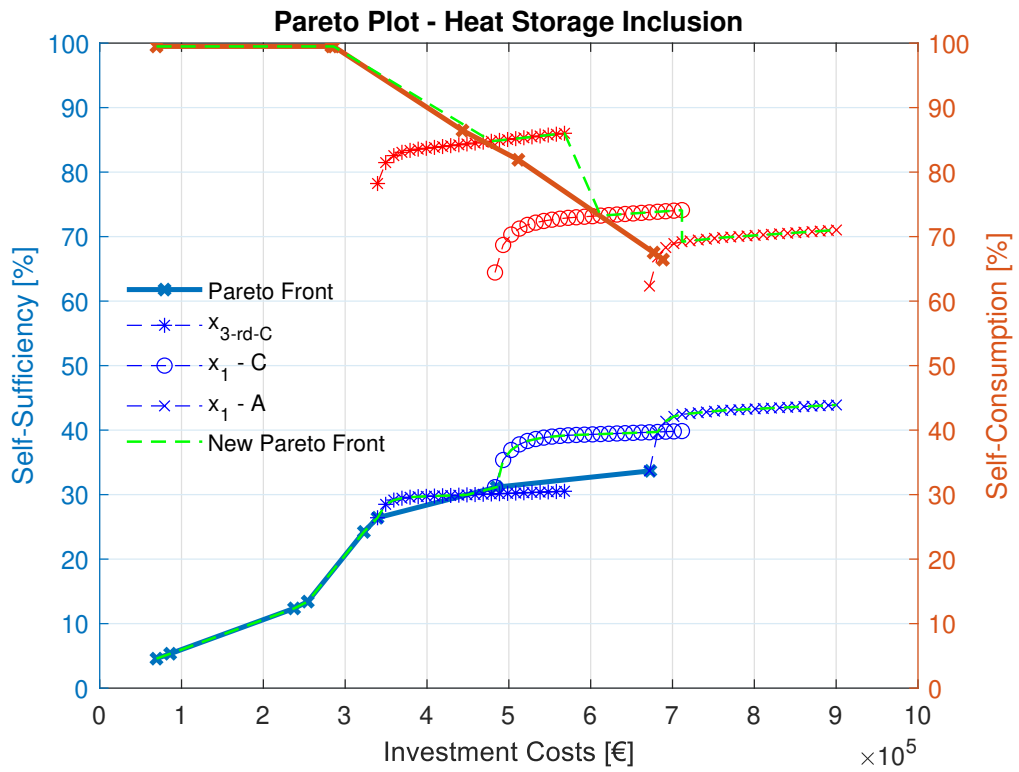FIGURE 5.19: Pareto Plot with Impact on Self-Sufficiency and Self-Consumption of Battery Inclusion

FIGURE 5.20: Pareto Plot with Impact on Self-Sufficiency and Self-Consumption of Heat Storage Inclusion

Based on the impact of the storage technologies in both cases, a new Pareto front could be defined for self-sufficiency and self-consumption. It can be seen that the Pareto optimal points from the storage inclusion lay in the almost linearly scalable and partially saturated regions of the energy storage curves for self-sufficiency. For self-consumption, the storage system for the solar panel distribution with the lowest overall energy production and therefore, the highest self-consumption determines the new Pareto front for self-consumption. Due to the overall highest energy production and lowest self-consumption without energy storage installation, and from the new Pareto fronts, it follows that the solar panel distribution x_1 for the Zilverling Label C and Label A is the most interesting for the inclusion of a battery and thermal storage. Therefore, the self-sufficiency and self-consumption against investment costs for the installation of x_1 in the Zilverling Label C and Label A with all points considered from the three points considered in Figure 5.17 to the installation sizes of energy storage, shown in Figure 5.15 and Figure 5.16, can be seen in Figure 5.21 and Figure 5.22, for the inclusion of a battery, and Figure 5.23 and Figure 5.24, for the inclusion of a thermal buffer storage. These plots include in more detail the possible deviation of the investment costs. For this solar panel distribution x_1, then the bar plots showcasing the energy demand, electricity production, electricity consumption, and energy supply, as well as the costs and payback time for different system combinations (points), are presented. Particularly the impact of insulation between the two Zilverling Label C and Label A is shown as this is the prominent difference. The points presented are marked in Figure 5.21, Figure 5.22, Figure 5.23 and Figure 5.24.
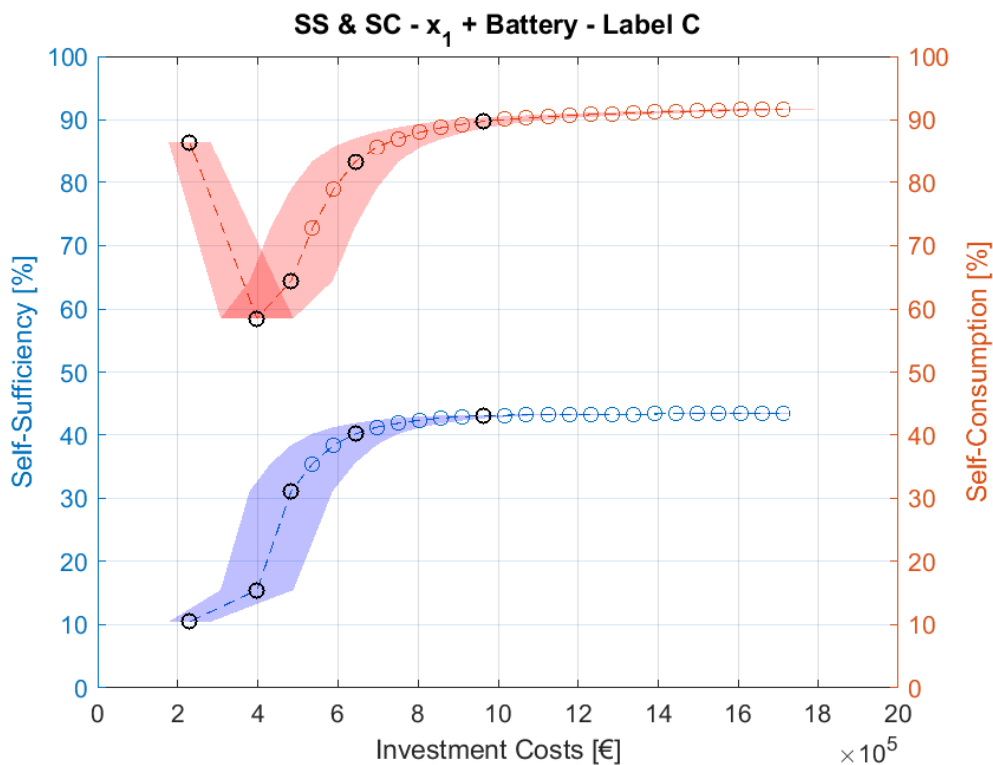

FIGURE 5.21: Self-Sufficiency & Self-Consumption of x_1 in Battery Case for Zilverling Label C
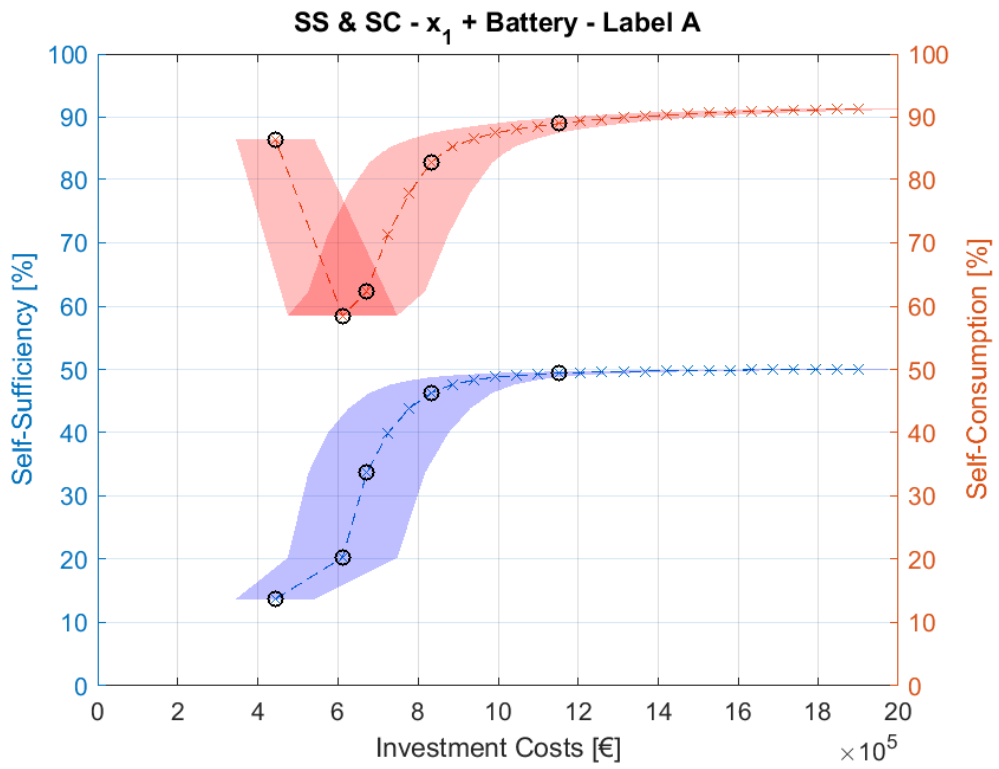
FIGURE 5.22: Self-Sufficiency & Self-Consumption of x_1 in Battery Case for Zilverling Label A
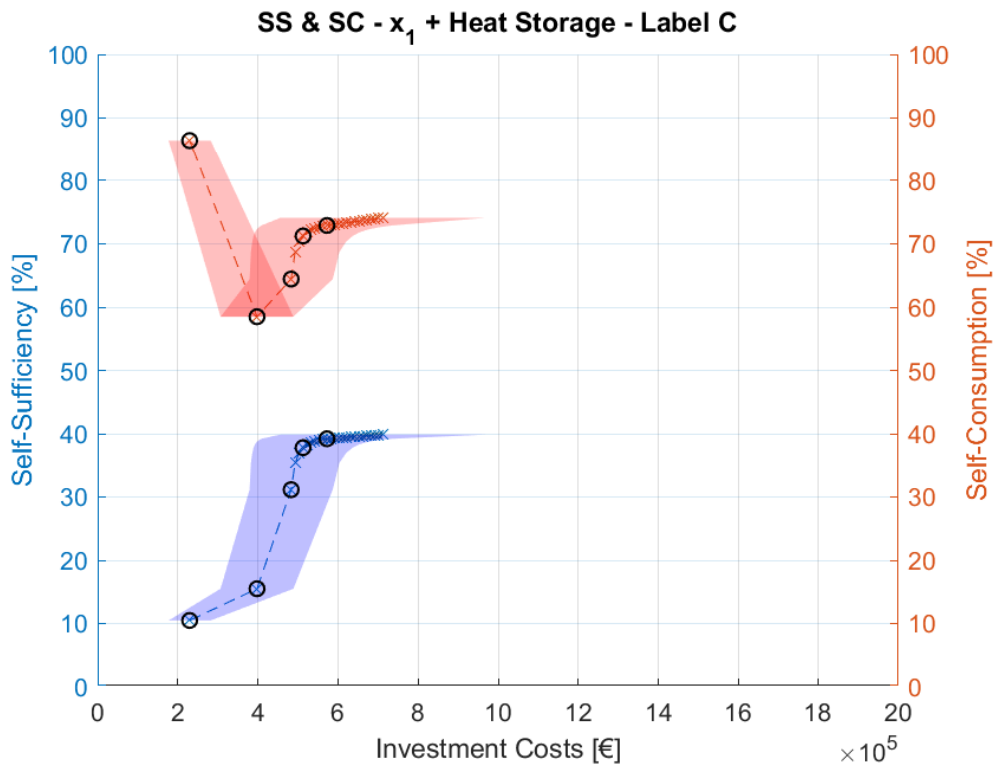

FIGURE 5.23: Self-Sufficiency & Self-Consumption of x_1 in Thermal Buffer Case for Zilverling Label C
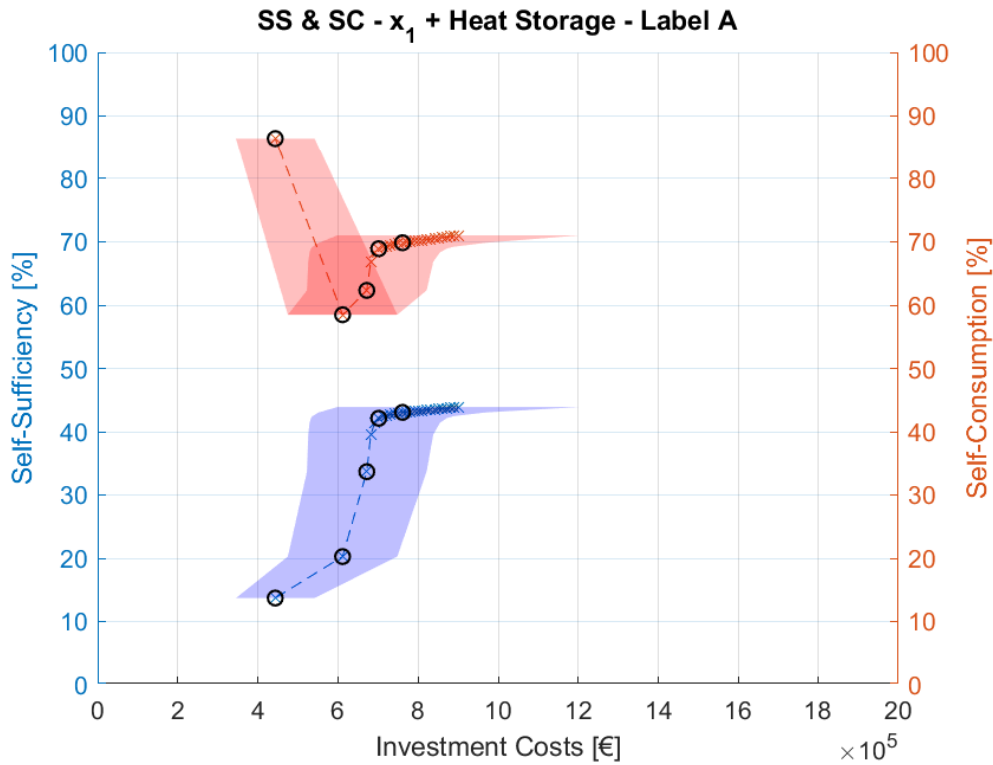
FIGURE 5.24: Self-Sufficiency & Self-Consumption of x_1 in Thermal Buffer Case for Zilverling Label A

In all four Figures can be observed that the inclusion of a storage system increases self-sufficiency as well as self-consumption. The saturated relation as observed before with installation size can also seen here with the investment costs as they are linear related. It can be observed that the increase is sharper for the thermal buffer storage than for the battery due to the lower associated cost per installed kWh of storage. However, with the battery electrical and heat demands can be supplied in combination with the heat pump system. Therefore, the overall achievable self-sufficiency and self-consumption is higher for the battery cases compared to the thermal buffer cases. Between Zilverling Label C and Label A can be seen that self-sufficiency is higher for Label A because the overall energy demand is lower for the building. The self-consumption is lower for Label A due to the lower energy consumption for the smaller-sized heat pump system. Therefore, more surplus energy is available.

Finally, the bar plots showcasing the energy demand, electricity production, electricity self-consumption, and energy self-supply, as well as the costs and payback time for different system combinations of the solar panel distribution x_1 following from the four distinct weather days are presented. In Figure 5.25 the total electricity production (TEP) and electricity consumption are shown for the Zilverling Label C. In Figure 5.26 the total energy demand (TED) and the supplied energy to the building are shown. The investment costs and payback time are shown in Figure 5.27 and 5.28 for the Zilverling Label C. Similarly, the total energy production and electricity consumption, the total energy demand and supplied energy, as well as the investment costs and payback time for the Zilverling Label A are shown in Figure 5.29, Figure 5.30, Figure 5.31 and Figure 5.32. Within these plots, x_{1F} indicates the installation of the solar panels on the facades of the Zilverling, x_1 the installation of the total solar panel distribution, HP the installation of the heat pump

system, B the installation of a battery size in the Pareto optimal area, B_S the installation of a battery size in the saturated area, TB the installation of a thermal buffer system sized in the Pareto optimal area and TB_S the installation of thermal buffer system sized in the saturated area.

With the information visualized in Figure 5.25 and Figure 5.29 the self-consumption for different system combinations can be calculated. With the information visualized in Figure 5.26 and Figure 5.30 the self-sufficiency for different system combinations can be calculated. The corresponding self-consumption and self-sufficiency is shown on top of the associated bar.

The considered sizes are for B = 462 kWh and B_S = 1386 kWh. Similarly, the considered sizes are for TB = 1987 kWh and TB_S = 5960. These correspond to the third and ninth installation sizes greater than 0 in Figure 5.15 and Figure 5.16 for both Zilverling Label C and Label A. Correspondingly in Figure 5.21, Figure 5.22, Figure 5.23 and Figure 5.24 these are the sixth and twelfth point and are marked.

For the calculation of the total investment costs with error bars, the costs summarized in Table 5.5 are used in Equation (3.9). For the calculation of the Payback time with error bars of the system combinations for the Zilverling building, an electricity price of C_{kWh} = 0.1762 €/kWh [67] is assumed and a heating price of C_{GJ} = 45.73 €/GJ [68] from the heating provider of the University of Twente.
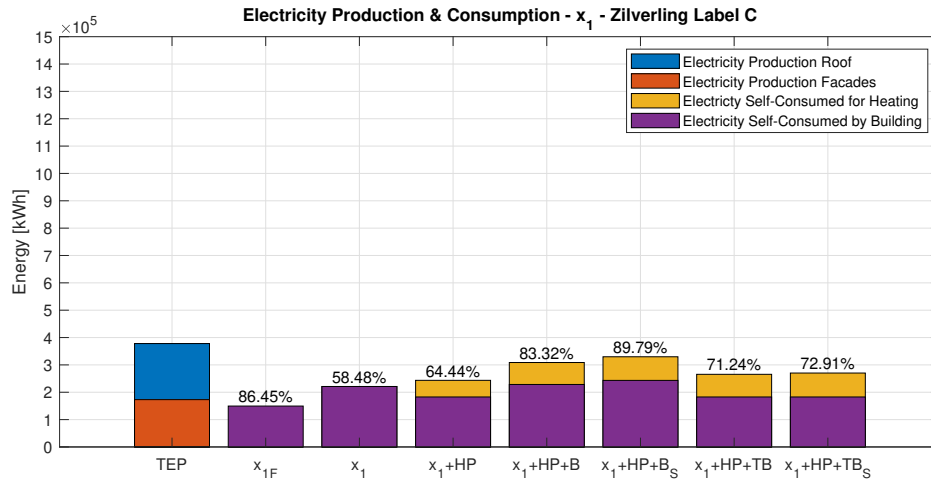

FIGURE 5.25: Total Electricity Produced and Consumed with Different System Combinations installed for Zilverling Label C. Corresponding SC is presented on Top of Bar
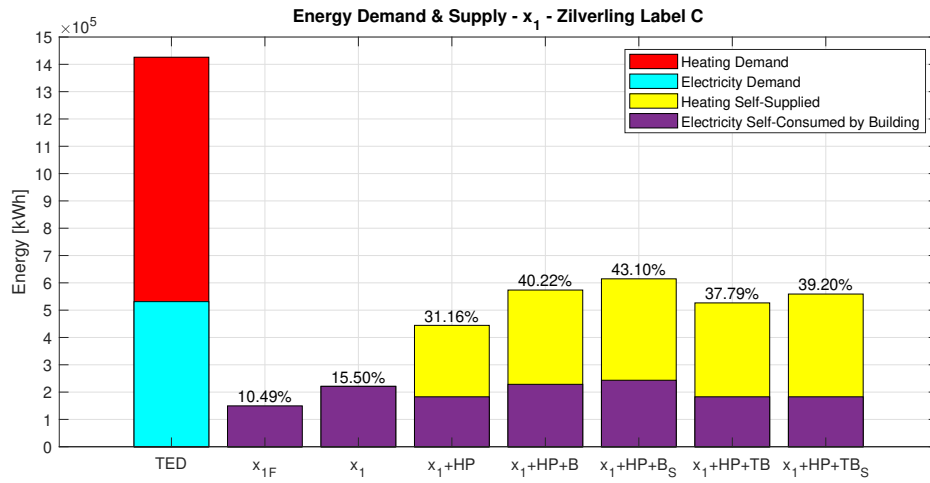
FIGURE 5.26: Total Energy Demand and Supplied with Different System Combinations installed for Zilverling Label C. Corresponding SS is presented on Top of Bar

FIGURE 5.27: Investment Costs of Different System Combinations installed for Zilverling Label C

FIGURE 5.28: Payback Time of Different System Combinations installed for Zilverling Label C

FIGURE 5.29: Total Electricity Produced and Consumed with Different System Combinations installed for Zilverling Label A. Corresponding SC is presented on Top of Bar

FIGURE 5.30: Total Energy Demand and Supplied with Different System Combinations installed for Zilverling Label A. Corresponding SS is presented on Top of Bar
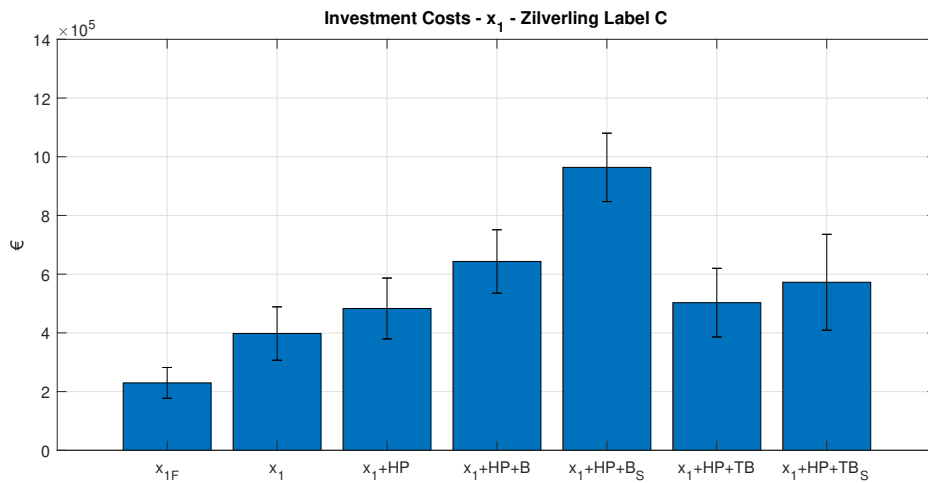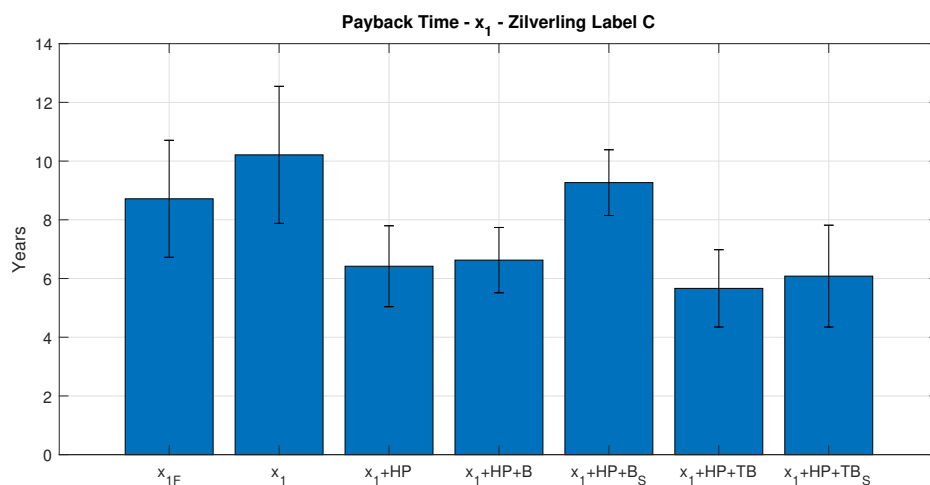

FIGURE 5.31: Investment Costs of Different System Combinations installed for Zilverling Label A

FIGURE 5.32: Payback Time of Different System Combinations installed for Zilverling Label A
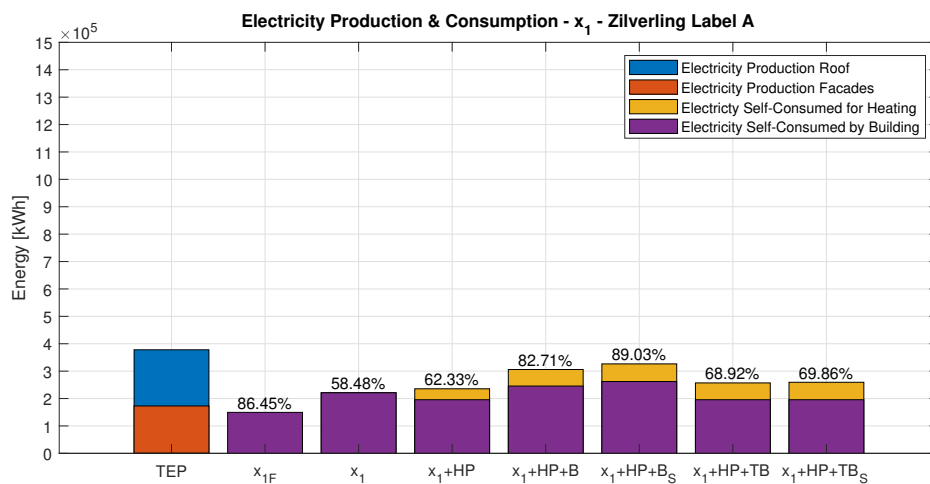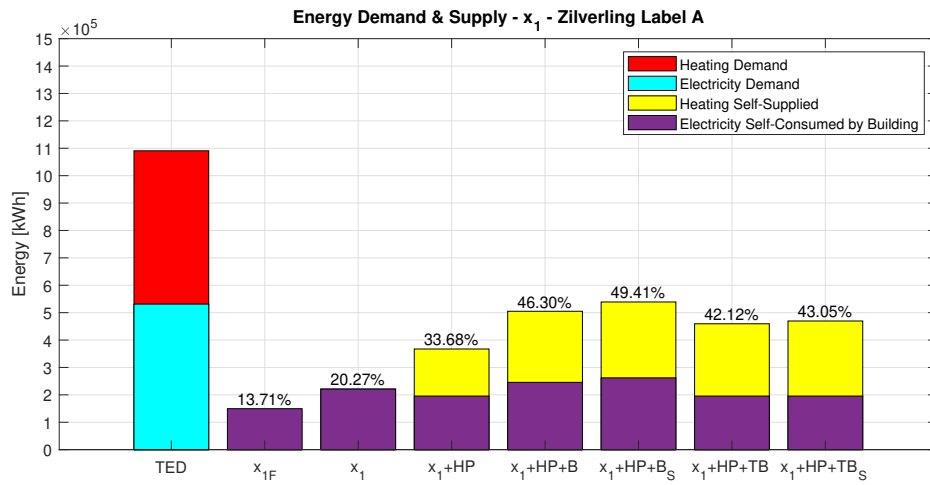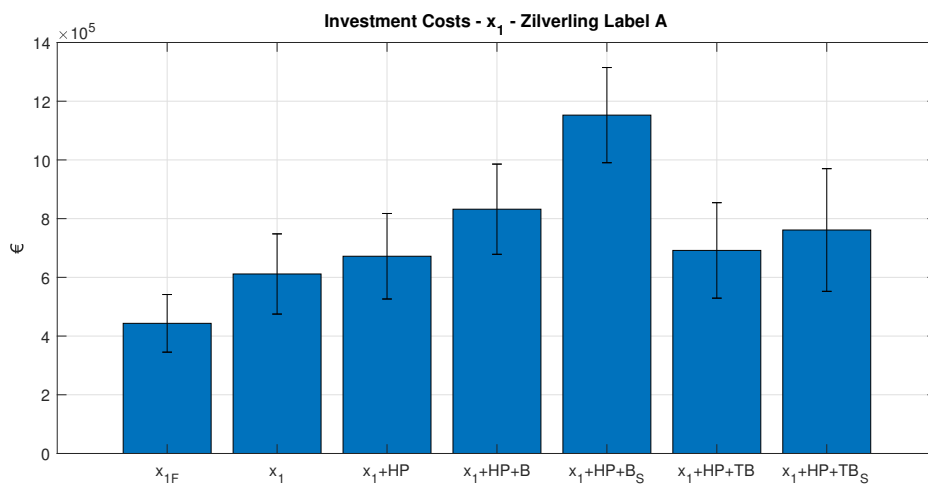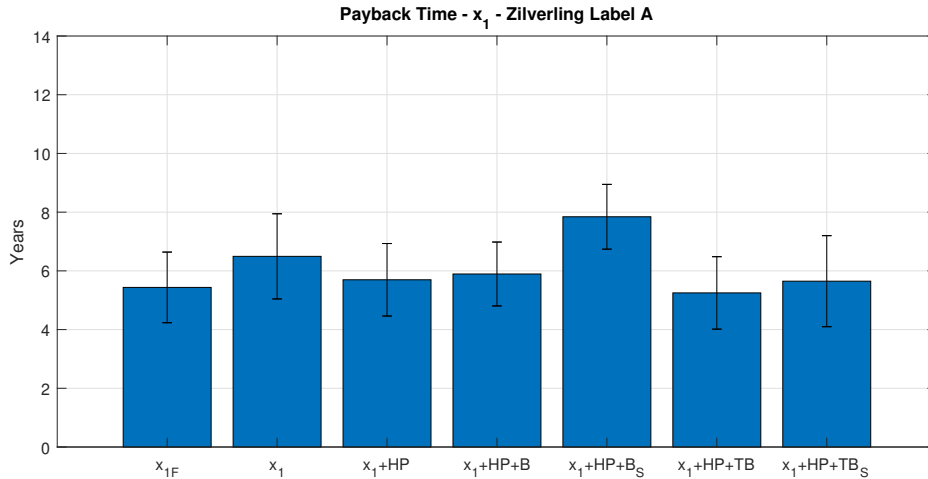
Comparing Figure 5.25 and Figure 5.26 with Figure 5.29 and Figure 5.30, it can be observed that the total energy demand (TED) is lowered by 334 MWh for the Zilverling Label A through the inclusion of insulation. The total electricity production (TEP) by the solar panels is equal in both cases, but the self-consumption differs due to the different installed heat pump sizes. In the case of the Zilverling Label A, more electricity is self-consumed by the building than used for heating compared to Zilverling Label C. However, due to the demand reduction, the self-sufficiency of Zilverling Label A is higher. Further, it can be seen that the gain in self-consumed electricity and supplied energy is small from the installation of B to B_S and TB to TB_S in both cases of Zilverling Label C and Label A.

Including a comparison of Figure 5.27 and Figure 5.28 with Figure 5.31 and Figure 5.32, it can be observed that before the inclusion of the heat pump system the investment costs differ by 213,700€, the costs for insulating the Zilverling externally, and after the inclusion of the heat pump system they differ by 188,800€. The difference is reduced due to the different costs for the installed heat pump system sizes. In all considered system combinations, the investment costs of the Zilverling Label C are lower than the investment costs of the Zilverling Label A. However, it can be observed that the payback time is in the case of Zilverling Label A for all system combinations lower. Due to the energy reduction for heating through the insulation, a significant amount of money is saved through no need to provide this heating demand. The difference in payback time, therefore, also becomes smaller with larger investment costs including more technologies in the system combination, as can be seen for the heat pump, battery, and thermal buffer inclusions, as more energy is self-supplied in total to the building.

Based on the presented information and the Pareto plots a fitting solution can be generally advised for the Zilverling building by comparing the results to the energy plan for the building. In the customized advice for the Zilverling building [15], the installation of a 500 m^2 solar panel area, improved insulation, an improved ventilation system, and a heat pump system are included. Here, the investment costs for 500 m^2 of solar panels are estimated at 112,500€ and the investment costs for a heat pump system are at 75,000€. The investment costs for improved insulation are at 113,715€ and additional considerations like better-insulated windows for the building and the improved ventilation system are set to a combined cost of 1,124,150€. Therefore, a maximal investment of 1,311,650€ is considered in [15].

Taking this maximal investment as an economically feasible and considerable upper limit indicates that, in the case of the Zilverling, the inclusion of a solar panel installation in combination with a heat pump system is advised in any consideration based on the achieved self-sufficiency, moderate investment costs and the payback time. Following from the Pareto fronts in Figure 5.19 and Figure 5.20 the next consideration should be a thermal buffer storage or for higher self-sufficiency and self-consumption a battery storage system. After these, to obtain the highest self-sufficiency, following the Pareto fronts, external wall insulation should be considered. However, when considering additional information, due to the overall positive impact on the payback time and the application of the Trias Energetica [1], insulation should be prioritized if economical funding is available.

Therefore, with the upper limit of 1,311,650€, first, the insulation of the Zilverling building should be improved, followed by a solar panel distribution with an accordingly, due to insulation smaller sized, heat pump system installed. For additional self-sufficiency and self-consumption, a thermal buffer storage can be considered next. If higher self-sufficiency than with the thermal buffer storage is wanted, a battery should be installed instead, following the Pareto fronts. In the end, it is the decision of a stakeholder which system is prioritized and which investment is willing to be made. Considering alone, the investment costs against the gained self-sufficiency leads to the solution including the installation of insulation last. Considering payback time and sustainability additionally leads to the prioritization of insulation and the inclusion of the other system parts, as described before, accordingly after.

Following the results of this thesis, an economically feasible and fitting solution for the Zilverling building is the integration of external wall insulation, solar panel distribution x_1 with a heat pump system with a heating capacity of 272 kW, and a battery with a capacity of 462 kWh to achieve a self-sufficiency of 46.29% and a self-consumption of 81.67% for the considered time period. The total investment costs of this system combination are 832,100€ ± 153,600€, with an expected payback time of 5.89 years ± 1.09 years.

Chapter 6

Discussion

The energy transition necessitates innovative solutions to enable decentralized renewable energy production in a desired smart grid. Ensuring resource security and enhancing self-sufficiency at a local level requires effective energy consumption of locally produced energy. In the broader context, the Trias Energetica principles need to be applied, and key characteristics of a smart grid must be incorporated to transform buildings from passive energy consumers to active energy participants. Ongoing initiatives and policies by multiple stakeholders aim to facilitate this transition. Different renewable energy production and storage solutions are best suited for buildings based on local circumstances. However, challenges such as limited data availability, poor data resolution, and information gaps can arise during implementation. The integration of these technologies needs to be steered to ensure resource security at a local level. Ensuring this while avoiding centralized loads possibly causing grid congestion requires solutions that are not necessarily set for maximum power output, but rather adjusted to an apparent demand. This thesis presented a method that adapts to this new type of energy production. The design-oriented approach is extendable and includes additional technologies and considerations iteratively. Based on assumptions and standardizations, an impact estimation for the implementation of renewable energy and storage technologies into commercial office buildings on self-sufficiency against investment costs with the associated self-consumption for the case of the Zilverling building could be given.

Nevertheless, in this thesis, the Zilverling building is assumed to be freestanding, no heating model of the Zilverling building and the thermal buffer storage is present, and simplifications of more complex problems are applied. Therefore, when considering implementing the given fitting solution, one needs to take into account these discussable considerations made in this thesis.

Starting with the assessment of building & demand data, it can be seen that the Zilverling building is not freestanding. This assumption was made to neglect the shadow fall of the surrounding buildings. Therefore, taking this into account, the solar panel distributions and correspondingly the energy production profiles would differ as the East and West facades of the building will likely not be utilized. To receive a more realistic outcome, the shadow fall consideration needs to be implemented into the method for the assessment of the building. Further, additional demand data as the cooling demand of a building can be included, affecting the sizing of heat pumps and electricity demand profile in the summer months. In any case, for the implementation of the proposed solutions into a building, the correspondence between the provided demand data and the information of the building needs to be checked. Differences in the heated area of the building and false demand amounts can make a large impact on the accuracy of energy labeling and considerations of

implementable system solutions.

From the PV sizing methods, different results based on different data inputs and constraints in the problem formulation were obtained. The PV sizing, based on four distinct weather days, indicates here what can be achieved with limited data availability. Historical weather data, like solar irradiation, is not a problem to be obtained, the corresponding and accurate demand data in a necessary accurate solution can cause difficulties to be obtained, due to smart metering not being integrated into buildings or undesired resolutions. With PV sizing, based on a dataset of one year, and, based on a method with more freedom in the solving approach, was shown that the energy profile can be better fitted to the demand profile of the building, increasing energy efficiency by reducing overshoots and lack of energy, therefore, enhancing self-consumption but on the cost of self-sufficiency. Here, further investigations need to be made into other methods considering different constraints for the utilization of the roof and facades, and including a different penalization for lack of energy and overshoots, as an overshoot of energy does not have necessarily a negative impact, due to the possibility to store the surplus energy for later use. Further, in the case of the Zilverling building, the electricity production benefited a lot from the flat roof of the building and the associated larger energy densities per square meter due to the power output optimized orientations available. For other buildings, more orientations on the facades as well as on the roof, if the area size is more limited, can be considered. In those cases, the utilization of orientations with larger power output is set to increase.

Taking a look at the heating system considerations made, data imputation was employed on the heating demand data, and the evaluation of insulation is based on a standardized approach rather than an accurate heating model of the Zilverling building. Through this, an estimate of the impact of insulation and the heating needs is made, but more accurate results can be obtained through a heating model determining the actual needs based on more advanced simulations. Further, the heat pump sizing is only based on the year considered in this thesis. If, for example, the winter in that year was mild the system can be in both cases undersized and if the winter was cold it is oversized. A longer period over multiple years can be of advantage here to include in the distribution to find a range of possible heat pump sizes for the considered cases. Further, additional consideration of cooling demand in the summer can influence the sizing as well. The system considered is also based on one assumed COP. The COP can change depending on the source temperature and the temperature output required. Therefore, dynamic analysis can be considered here as well to be implemented instead of one assumed value, resulting in different supplied heating to the building based on the temperature of the air (air-source heat pump) or ground (geothermal heat pump).

For the considered energy storage system, two basis systems are assumed with the Li-Ion battery and thermal buffer storage using water as the storage medium. Other battery systems or thermal storage solutions can be considered and implementation discussed. Within this thesis, a discussable basic control was assumed to ensure the prioritization of the heating needs of the building. It ensures that the heat pump can draw enough electricity in the modeling setup of this thesis on the costs of the electricity self-consumed by the building to fulfill the initial heating demand. This greedy algorithm can be used as a basis case and replaced with smart control algorithms, further enhancing the energy supplied to the building. The discharge rate of the thermal buffer storage is neglected and no heating model is made. Therefore, solutions might differ in the realization of such a system. Additional considerations are the combination of these two types of storage and sizing accordingly. If a setup is chosen, the operation of the storage system can be optimized, extending the limited design space of this design-oriented method.

In general, the accuracy and implementation considerations of this method can be increased, by the inclusion of additional models for the heating, extended period of data, and dynamic values for the simplified assumed values, like the COP of the heat pump or possible energy reduction. Additional considerations can be included like including a storage size and scheduling in the PV sizing after a first installation size was found, the inclusion of other PV systems like PV thermal collectors, applying the method to multiple buildings located closely, exploring energy trading between those by taking the generated overshoot as an additional input for another building, and larger storage solutions to fulfill the demand of multiple buildings or a district with a large water tank system or borehole solution. These additional considerations and expansions of the method lead then to new self-sufficiency and self-consumption values that can be evaluated with Pareto front plots and additional information, like the payback time, can be considered. Here, as well, dynamic pricing instead of assumed values can be integrated and the expected costs and payback time made more accurate.

In the end, in the case of the Zilverling building, the method delivered a possible fitting solution for the Zilverling building under the assumptions made. In the case example presented, an estimation of the impact and associated costs of implementing renewable energy and storage technologies on the self-sufficiency of buildings is provided, aligning with the cost considerations of an externally customized advice for the Zilverling building. Thus, this comprehensive study contributes to the broader energy transition by guiding the transformation of existing buildings from passive consumers to active energy participants. The main contributions of this thesis are:

- A method that analyzes the effect of incorporating solar energy production and storage technologies without relying on high-resolution data.

- A versatile approach to optimize renewable energy consumption with regard to self-sufficiency that is extendable and iterative.

- Highlighting the advantages of hybrid systems and efficient energy usage.

- Emphasizing the importance of energy storage on self-sufficient systems.

- Providing a basic framework to guide the management and design of self-sufficient buildings incorporating renewable energy solutions, aligning with smart grids, and realizing energy plans.

In the end, the method offers a basic framework to guide the management and design of self-sufficient buildings incorporating renewable energy solutions, aligning with smart grids, and the realization of energy plans. It provides a means to evaluate the incorporation of renewable energy solutions, is adaptable to other cases, and is extendable. This can facilitate discussions on innovative solutions for buildings in smart grids, enabling a comparison with existing energy plans. The utilization of the method can contribute to the realization of these plans, such as the University of Twente's energy plan, providing additional incentives for the renovation of existing buildings. This, in turn, supports the broader energy transition and the establishment of smart grids by incorporating the key characteristics at a local level.

6.1 Future Work

The work presented in this thesis establishes a fundamental framework for integrating renewable energy and storage technologies into commercial office buildings. To enhance and

advance the method, future work should address certain limitations.

Firstly, the method was applied to the Zilverling case in this thesis. In the scenario, it is assumed that the Zilverling is freestanding and shadow fall from surrounding buildings is neglected. Further, the heat demand data required data imputation to be applicable to the method. Therefore, future works should implement a selection procedure for solar panel installation areas obstructed timely by other buildings and apply the method to a case with data that does not require data imputation with a sufficient resolution and sample rate. Through this, an actual profile instead of an assumed profile can be used in the method.

Secondly, for the inclusion of insulation in commercial office buildings, an actual heating model of the assessed building can be incorporated. This results in a more accurate and case-specific effect of insulation than the standardized approach used in this thesis.

Thirdly, the implementation of energy storage was covered by two individual examples in a limited design space with simplified assumptions. Future research should explore combinations of different energy storage systems, considering advancements in energy storage technologies and smarter control systems for more effective energy management with smaller sizing and fewer costs.

Next to these, the method is extendable and can be applied iteratively. An extension could involve applying the method to multiple buildings located closely, exploring an energy trading scenario between buildings in a local decentralized setting, where the energy overshoot of one building is an additional input for another. Additionally, if a system setup including energy storage is determined, the effect of the charging and discharging of the storage system on the PV sizing can be studied by including these in the demand profile and applying the PV sizing methods iteratively.

Further extensions could include incorporating cooling demands, and studying the effect of different production sources, like exploring a mix of solar and wind inputs, for resilience and reduced weather dependency. However, it is advisable to limit the extension of the method to a local level, perhaps incorporating a district or university campus.

To increase the accuracy of the method, future work could consider including a predictive energy demand system for real-time control, dynamic costs for energy, a temperature-dependent COP, and prosumer interaction in energy reduction. Different solvers for linear least-squares problems could be explored for comparison, such as nonnegative linear least-squares solvers or alternative problem formulations. The impact of changed constraints and different penalization of negative and positive differences between energy production and energy demand need to be studied, to find an optimal PV sizing method, ensuring high self-sufficiency with efficient energy consumption.

Based on the outcomes of the utilization of other problem formulations to solve for an optimal solution, then the focus can be switched to complete off-grid scenarios to analyze what measures are required to achieve 100% self-sufficiency with efficient energy consumption.

In the end, the points for further consideration that need to be stressed are the need for an accurate heating model of the building and a less simplified inclusion of energy storage solutions. Impact estimations can be given with the current method and the standardized approach, but for the actual effect of the inclusion of different insulation and thermal buffer storage, a heating model needs to be included.

In summary, the method presented provides a basis for predicting the impact of integrating renewable energy production and storage technologies into commercial office buildings. It can provide this with the use of basic means that can be advanced and validated through the inclusion of accurate data sets, longer time periods of data, and comparison to actual system implementation. Taking into account the points that need to be stressed in the method and improving those through further research can lead to an optimal tool to in-

corporate the key characteristics of a smart grid and apply the Trias Energetica. It can be used as a basic framework to facilitate collaboration between different stakeholders and prosumer involvement. Therefore, the method contributes to the broader energy transition and can be extended and improved by incorporating additional information and data. Case-specific simulation results, if available, can enhance the accuracy of the method.

Chapter 7

Conclusion

Based on the obtained results presented in this thesis, the main research question and the sub-questions can be answered. Starting with the main research question, which is as follows:

- **How can the integration of renewable energy and storage technologies in commercial buildings achieve a high level of self-sufficiency while remaining economically feasible?**

The integration of renewable energy and storage technologies demonstrated varying impacts on self-sufficiency depending on the installed system combination and sizing. First, for on-site energy production, a maximization of the utilization of the available areas for solar energy production with orientations associated with the (expected) demand profile is implemented. This ensures effective energy usage while providing sufficient production over the day at high solar irradiation times, including surplus energy that can be stored for later use. However, in the case of the Zilverling building a self-sufficiency of 46.29% was achieved, requiring additional energy source considerations to fulfill its entire demand. The inclusion of a heat pump system to create a hybrid system significantly increases self-sufficiency as well as self-consumption. Economically, the largest absolute gain in self-sufficiency compared to extra investment costs is achieved through the introduction of the hybrid system, supplying heat to the building next to electricity from the solar panels. Following that, self-sufficiency and self-consumption increase with the implementation of energy storage solutions bridging the time dependency of energy produced by renewable energy sources and enabling later usage. To find economically feasible solutions, the Pareto front plots enable it to focus on a set of efficient choices rather than considering the full range of solutions present. Considered solutions can be compared and Pareto optimal solutions further investigated. This makes an extendable comparison possible between different setups to implement the Trias Energetica and key elements of a smart grid. Based on the size of a building, local circumstances, available funding and preferences of stakeholders, a choice with the Pareto front plot and this additional information for the integration of renewable energy and storage technologies in commercial office buildings can be made. For the Zilverling building, an economically feasible and fitting solution was found with the integration of external wall insulation, solar panel distribution x_1 with a heat pump system with a heating capacity of 272 kW, and a battery with a capacity of 462 kWh to achieve a self-sufficiency of 46.29% and a self-consumption of 81.67% for the considered time period. The total investment costs of this system combination are 832,100€ ± 153,600€, with an expected payback time of 5.89 years ± 1.09 years. This investment is in the economically feasible range of the University of Twente with a maximal investment of 1,311,650€ considered.

With these results obtained, the focus switches to answering the sub-questions, giving additional information on the overall obtained solutions. Here, the first sub-question considered is:

- What is the impact on self-sufficiency of a different prioritization of energy usage?

Taking a look at the initial yearly total energy demand of the Zilverling building as an example, it can be seen that 37.35% is the electricity demand and 62.75% is the initial heating demand of the 1.426 GWh in the year. The heat demand constitutes the largest share of total energy demand and can be reduced through the inclusion of insulation. Therefore, prioritizing to reduce and supply the remaining heating demand has a positive impact on self-sufficiency. As both demands, electricity and heating, need to be supplied to the building, the total energy demand is considered for the determination of the degree of self-sufficiency. The supply of heat to the building is first achieved with the inclusion of heat pumps in this system setup, utilizing an additional electricity demand to supply heating to the building by using the electricity to pump energy from an outside source into the building. Here, the heat pump system operates as an open system, allowing significantly more heat to be pumped into the building from a given source (e.g., air or geothermal). The increase of heat supplied is the COP, associated with the heat pump system, times the electricity consumed by the heat pump system. Therefore, to maximize the total energy self-supplied to the building the electricity produced by the solar panels is prioritized to be consumed by the heat pump to supply COP times more the amount of heating than electricity to the building when heating demand is required first and then the remaining electricity produced to fulfill the initial electricity demand of the building. Therefore, the electricity self-consumed by the building is slightly reduced to supply a larger amount of total energy as can also be seen in the bar plots shown in Figure 5.25, Figure 5.26, Figure 5.29 and Figure 5.30. The impact on self-sufficiency from a different prioritization of energy usage can also be found in Appendix Figure 8.2. Therefore, on the cost of less electricity self-supplied to the building, more heat can be supplied to the building, maximizing the total self-sufficiency of the building, as the larger heating demand is fulfilled more. The consumption of overall electricity increases due to the additional load of the heat pump. The second sub-question considered is:

- How does the storage size influence self-sufficiency and investment costs?

The inclusion of a battery or thermal energy storage extends the operation time of the hybrid system, increasing the supply of locally produced electricity and heat by making energy surplus available for later use after storing these amounts. Batteries and thermal energy storage have a positive impact on self-sufficiency and self-consumption, but this impact saturates with increasing installed capacity and, thus, with the associated investment costs. The area of interest lies in the partially saturated region, where, based on criteria chosen by the system operator, cost-effective sizing is possible. In the saturated area, additional installed capacity and investment costs provide minimal gain compared to smaller sizes in the partially saturated region. Systems with a lower self-consumption benefit from the inclusion of an energy storage system the most as the unused surplus energy can be utilized at a later time, enhancing the self-consumption and self-sufficiency even more. It is also evident that while initial investment costs rise, the payback time for the overall system stays in the same range compared to the inclusion of the heat pump system, as more energy is self-consumed and supplied to the building, and lower than the payback time of just the inclusion of the solar panel distribution, as can be seen in Figure 5.28 and Figure 5.32. Therefore, including storage solutions is a logical choice. If costs for

energy storage decrease, the impact can potentially increase even further.

The impact of a combination of battery and thermal energy storage in a hybrid storage system needs to be investigated. Based on the self-sufficiency and self-consumption shown against investment costs for the battery and thermal buffer system in Figure 5.21, Figure 5.22, Figure 5.23 and Figure 5.24 a combination of hybrid storage can potentially reduce investment cost by the heating demand being covered by the cheaper thermal buffer storage and further gain in self-sufficiency and self-consumption achieved by a smaller sized battery for the additional consumption of surplus electricity. To confirm this, further research needs to be done on the operation of a hybrid storage system with chosen installation sizes for a given case.

The last sub-question considered is:

- How do the resulting solutions differ with regard to larger flexibility and data availability?

First of all, the distribution of solar panel orientations differs. With fewer data available, the overshoot of energy not consumed is larger, and, therefore, self-consumption is lower. The self-sufficiency is slightly larger through more overall energy produced. This can be utilized with storage solutions and is not necessarily negative in the first place. With more flexibility, the orientations with higher energy density are preferred, resulting in fewer solar panels installed, needed for energy consumption in the same range as more restricted solution approaches.

The more information is available, the better. The inclusion of additional demands in the solving approach results in higher energy consumption and adjusts the distribution of panels accordingly. To find further improved solutions additional demands, like cooling in the summer or scheduling of a battery for a smart energy management system, can be included. Therefore, the thesis offers a method to analyze the effect of incorporating solar energy production and storage technologies in commercial office buildings and is extendable by the inclusion of additional information. The versatile approach can be repeated iteratively with this additional information available, as shown by the redistribution of solar panels based on the heating demand.

Considering additional PV sizing methods by altering the constraints and penalization of differences, next to the three PV sizing methods used in this thesis, results in new solutions that can be evaluated again with Pareto front plots and result potentially in a new set of Pareto optimal solutions. Through the inclusion of data obtained from a heating model of the building and an improved energy storage model, relying on fewer simplifications, more accurate solutions follow from the additional data available. Further, more applicable demand data for multiple years can give a range of self-sufficiency and self-consumption, and the sizing of the considered systems, validating the method.

In the end, the method provides an engineering-friendly and straightforward approach to estimate the impact on self-sufficiency without relying on high-resolution data. An impact estimation can already be given with the demand data of four distinct weather days. Improvements can be made by including data that does not require data imputation and is following from more advanced models in the heating demand and storage considerations of the method. Therefore, the versatile approach offers a tool to find a high level of self-sufficiency while remaining economically feasible with limited data. For further research, the method should be applied to similar buildings with more accurate demand data available or based on measured values with higher resolution for the Zilverling for validation. Further, different PV sizing methods can be analyzed and compared to the results presented in this thesis, also considering the appliance of the method on multiple buildings

that are located close to each other as discussed before. The accuracy of the resulting impact estimation of the integration of different renewable energy and storage technologies increases with higher data availability. The method is expandable.

In conclusion, this method, as presented on the Zilverling building, can be applied to other cases and buildings, contributing to the transition from centralized to decentralized energy production and the development of smart grids by transforming buildings from passive consumers into active energy participants. The method supports realizing energy plans by examining the integration of renewable energy and storage technologies while ensuring efficient energy usage with high self-sufficiency.

Bibliography

[1] E. H. Lysen, "The trias energica: Solar energy strategies for developing countries," December 1996.

[2] Agora Energiewende, "Energiewende 2030: The big picture. megatrends, targets, strategies and a 10-point agenda for the second phase of germany's energy transition." `https://static.agora-energiewende.de/fileadmin/Projekte/2017/Big_Picture/134_Big-Picture_EN_WEB.pdf`, April 2018. (Accessed on 07/30/2023).

[3] D. Gies, "Lecture: Industrial organization, managerial economics, and finance of interconnected power systems," September 2021. NJIT.

[4] Office of Electricity, "The smart grid: An introduction.." `https://static.agora-energiewende.de/fileadmin/Projekte/2017/Big_Picture/134_Big-Picture_EN_WEB.pdf`, September 2008. (Accessed on 07/30/2023).

[5] K. Budka, J. Deshpande, J. Hobby, Y.-J. Kim, V. Kolesnikov, W. Lee, T. Reddington, M. Thottan, C. White, J.-I. Choi, J. Hong, J. Kim, W. Ko, Y.-W. Nam, and S.-Y. Sohn, "Geri - bell labs smart grid research focus: Economic modeling, networking, and security privacy," pp. 208 – 213, November 2010.

[6] GSMA, "South korea: Jeju island smart grid test-bed - developing next generation utility networks." `https://www.gsma.com/iot/wp-content/uploads/2012/09/cl_jeju_09_121.pdf`, September 2012. (Accessed on 10/10/2023).

[7] Enerdata, "Residential buildings: Energy efficiency & consumption evolution in europe." `https://www.enerdata.net/publications/executive-briefing/households-energy-efficiency.html#:~:text=At%20the%20EU%20level%2C%20buildings,high%20untapped%20energy%20savings%20potential.`, December 2021. (Accessed on 07/30/2023).

[8] Amt für Kommunikation, "Stadt münster: Solar-pflicht für neue wohngebäude." `https://www.muenster.de/pressemeldungen/web/frontend/output/index.php?offset=/design/standard/page/1719/show/1104973`, June 2022. (Accessed on 10/10/2023).

[9] Presse- und Informationsamt der Bundesregierung , "Mit wärmepumpen tempo machen für die klimawende." `https://www.bundesregierung.de/breg-de/aktuelles/kanzler-viessmann-2070096#:~:text=Ab%20Januar%202024%20gilt%20auch,weitere%20energetische%20Sanierungen%20erforderlich%20sein.`, November 2022. (Accessed on 10/10/2023).

[10] Government of the Netherlands, "Climate policy." `https://www.government.nl/topics/climate-change/climate-policy`. (Accessed on 10/13/2023).

[11] Government of the Netherlands, "Climate agreement." `https://www.klimaatakkoord.nl/documenten/publicaties/2019/06/28/national-climate-agreement-the-netherlands`, June 2019. (Accessed on 10/13/2023).

[12] University of Twente, "Sustainability." `https://www.utwente.nl/en/sustainability/`, August 2023. (Accessed on 10/13/2023).

[13] University of Twente, "Shaping2030." `https://www.utwente.nl/en/organisation/about/shaping2030/`, February 2023. (Accessed on 10/13/2023).

[14] H. Hobbelink, B. Marechal, G. Stam, R. Capperucci, and C. Alderlieste, "Routekaart energietransitie universiteit twente." `https://www.utwente.nl/.uc/fdea11ec50102315ccc005fc02402829f19f161bb0f5700/UT_Routekaart%20gebouwen%202030-2050.pdf`, December 2020. (Accessed on 10/10/2023).

[15] R. Moelard, "Epa-u maatwerkadvies utiliteitsgebouwen." `https://www.utwente.nl/.uc/f230cebfc010208009d015fc024026b1e53956786c7a700/EEP%20-%20EPA%20Zilverling.pdf`, November 2017. (Accessed on 10/16/2023).

[16] R. York and S. E. Bell, "Energy transitions or additions?: Why a transition from fossil fuels requires more than the growth of renewable energy," *Energy Research Social Science*, vol. 51, pp. 40–43, 2019.

[17] BP (British Petroleum), "Bp statistical review of world energy 2022." `https://www.bp.com/content/dam/bp/business-sites/en/global/corporate/pdfs/energy-economics/statistical-review/bp-stats-review-2022-full-report.pdf`, 2022. (Accessed on 11/01/2023).

[18] F. Kern and K. S. Rogge, "The pace of governed energy transitions: Agency, international dynamics and the global paris agreement accelerating decarbonisation processes?," *Energy Research Social Science*, vol. 22, pp. 13–17, 2016.

[19] V. S. Arutyunov and G. V. Lisichkin, "Energy resources of the 21st century: problems and forecasts. can renewable energy sources replace fossil fuels†," *Russian Chemical Reviews*, vol. 86, p. 777, August 2017.

[20] A. Rahman, O. Farrok, and M. M. Haque, "Environmental impact of renewable energy source based electrical power plants: Solar, wind, hydroelectric, biomass, geothermal, tidal, ocean, and osmotic," *Renewable and Sustainable Energy Reviews*, vol. 161, p. 112279, 2022.

[21] A. Ahmed, T. Ge, J. Peng, W.-C. Yan, B. T. Tee, and S. You, "Assessment of the renewable energy generation towards net-zero energy buildings: A review," *Energy and Buildings*, vol. 256, p. 111755, 2022.

[22] B. Rezaie, E. Esmailzadeh, and I. Dincer, "Renewable energy options for buildings: Case studies," *Energy and Buildings*, vol. 43, no. 1, pp. 56–65, 2011.

[23] D. Carli, M. Ruggeri, M. Bottarelli, and M. Mazzer, "Grid-assisted photovoltaic power supply to improve self-sustainability of ground-source heat pump systems," in *2013 IEEE International Conference on Industrial Technology (ICIT)*, pp. 1579–1584, 2013.

[24] N. Kuemple, "Photovoltaik: Kosten einer solaranlage in 2023." https://www.wegatech.de/ratgeber/photovoltaik/kosten-und-wirschaftlichkeit/photovoltaikanlagen/#:~:text=Elektroinstallation%20%26%20Modulmontage,%E2%82%AC%20f%C3%BCr%20die%20Modulmontage%20rechnen., October 2023. (Accessed on 11/28/2023).

[25] R. Croteau and L. Gosselin, "Correlations for cost of ground-source heat pumps and for the effect of temperature on their performance," *International Journal of Energy Research*, vol. 39, March 2015.

[26] F. Culkin, "External wall insulation cost." https://buildtech.ie/blog/external-wall-insulation-cost, August 2023. (Accessed on 01/17/2024).

[27] S. Sabihuddin, A. Kiprakis, and M. Mueller, "A numerical and graphical review of energy storage technologies," *Energies*, vol. 8, pp. 172–216, January 2015.

[28] H. Behabtu, M. Messagie, T. Coosemans, M. Berecibar, K. Fante, A. Alem, and J. Van Mierlo, "A review of energy storage technologies' application potentials in renewable energy sources grid integration," *Sustainability*, vol. 12, p. 10511, December 2020.

[29] A. Baniasadi, D. Habibi, W. Al-Saedi, M. A. Masoum, C. K. Das, and N. Mousavi, "Optimal sizing design and operation of electrical and thermal energy storage systems in smart buildings," *Journal of Energy Storage*, vol. 28, p. 101186, 2020.

[30] N. Munzke, "Sector coupling - pv storage system with heat pump system." https://www.batterietechnikum.kit.edu/english/848.php, July 2023. (Accessed on 11/28/2023).

[31] INTILION, "Indoor energy storage intilion | scalestac." https://intilion.com/en/indoor-energy-storage-intilion-scalestac/. (Accessed on 11/28/2023).

[32] BloombergNEF, "Lithium-ion battery price worldwide from 2013 to 2022." https://www.statista.com/statistics/883118/global-lithium-ion-battery-pack-costs/#:~:text=Lithium%2Dion%20battery%20pack%20price,efficient%20energy%20storage%20devices%20worldwide., January 2023. (Accessed on 11/28/2023).

[33] U.S. Department of Energy, "Commercial battery storage." https://atb.nrel.gov/electricity/2022/commercial_battery_storage, July 2022. (Accessed on 11/28/2023).

[34] L. Pompei, F. Nardecchia, and A. Miliozzi, "Current, projected performance and costs of thermal energy storage," *Processes*, vol. 11, no. 3, 2023.

[35] S. Bespalko, A. Miranda, and O. Halychyi, "Overview of the existing heat storage technologies: sensible heat," *Acta Innovations*, no. 28, p. 82–113, 2018.

[36] EASE - European Association for Storage of Energy, "Thermal hot water storage." https://ease-storage.eu/wp-content/uploads/2016/03/EASE_TD_HotWater.pdf, March 2016. (Accessed on 11/28/2023).

[37] IRENA, "Thermal energy storage: Technology brief." https://www.irena.org/publications/2013/Jan/Thermal-energy-storage, January 2013. (Accessed on 11/28/2023).

[38] G. Hoogsteen, *A Cyber-Physical Systems Perspective on Decentralized Energy Management*. Phd thesis - research ut, graduation ut, University of Twente, Netherlands, December 2017.

[39] C. Shuaixun, H. Gooi, and M. Wang, "Sizing of energy storage for microgrids," *IEEE Trans. Smart Grid*, vol. 3, pp. 142–151, March 2012.

[40] J. Lian, Y. Zhang, C. Ma, Y. Yang, and E. Chaima, "A review on recent sizing methodologies of hybrid renewable energy systems," *Energy Conversion and Management*, vol. 199, p. 112027, 2019.

[41] W. Badr, "6 different ways to compensate for missing values in a dataset (data imputation with examples)." https://towardsdatascience.com/6-different-ways-to-compensate-for-missing-values-data-imputation-with.-examples-6022d9ca0779, January 2019. (Accessed on 10/04/2023).

[42] S. Aguacil, S. Lufkin, and E. Rey, "Active surfaces selection method for building-integrated photovoltaics (bipv) in renovation projects based on self-consumption and self-sufficiency," *Energy and Buildings*, vol. 193, pp. 15–28, 2019.

[43] T. Østergård, R. L. Jensen, and S. E. Maagaard, "Building simulations supporting decision making in early design – a review," *Renewable and Sustainable Energy Reviews*, vol. 61, pp. 187–201, 2016.

[44] S. Attia, L. Beltran, A. Herde, and J. Hensen, ""architect friendly": A comparison of ten different building performance simulation tools," *IBPSA 2009 - International Building Performance Simulation Association 2009*, pp. 204–211, January 2009.

[45] K. Świrydowicz, E. Darve, W. Jones, J. Maack, S. Regev, M. A. Saunders, S. J. Thomas, and S. Peleš, "Linear solvers for power grid optimization problems: A review of gpu-accelerated linear solvers," *Parallel Computing*, vol. 111, p. 102870, 2022.

[46] MathWorks, "Matlab lsqlin: Solve constrained linear least-squares problems." https://www.mathworks.com/help/optim/ug/lsqlin.html. (Accessed on 09/19/2023).

[47] G. Hoogsteen and J. Hurink, "Demkit." https://www.utwente.nl/en/eemcs/energy/demkit/, 2017. (Accessed on 09/19/2023).

[48] European Commission, "JRC Photovoltaic Geographical Information System (PVGIS)." https://re.jrc.ec.europa.eu/pvg_tools/en/. (Accessed on 09/21/2023).

[49] KNMI, "Uurgegevens van het weer in nederland." https://www.knmi.nl/nederland-nu/klimatologie/uurgegevens. (Accessed on 09/25/2023).

[50] B. Badenes, M. Belliardi, B. Bernardi, M. De Carli, M. Di Tuccio, G. Emmi, A. Galgaro, S. Graci, S. Pera, L. Pockelé, *et al.*, "Definition of standardized energy profiles for heating and cooling of buildings," in *Proceedings of Clima*, p. 27, 2016.

[51] W. Sun, P. Hu, F. Lei, N. Zhu, and Z. Jiang, "Case study of performance evaluation of ground source heat pump system based on ann and anfis models," *Applied Thermal Engineering*, vol. 87, pp. 586–594, 2015.

[52] C. A. De Swardt and J. P. Meyer, "A performance comparison between an air-source and a ground-source reversible heat pump," *International Journal of Energy Research*, vol. 25, no. 10, pp. 899–910, 2001.

[53] D. Connolly, D. Drysdale, K. Hansen, and T. Novosel, "Creating hourly profiles to model both demand and supply," *Background Report*, vol. 2, 2015.

[54] B. Homan, *Batteries in Smart Microgrids*. Phd thesis - research ut, graduation ut, University of Twente, Netherlands, November 2020.

[55] The Engineering ToolBox, "Water - specific heat vs. temperature." https://www.engineeringtoolbox.com/specific-heat-capacity-water-d_660.html, 2004. (Accessed on 01/08/2024).

[56] The Engineering ToolBox, "Water - density, specific weight and thermal expansion coefficients." https://www.engineeringtoolbox.com/water-density-specific-weight-d_595.html, 2003. (Accessed on 01/08/2024).

[57] E. Goodarzi, M. Ziaei, and E. Z. Hosseinipour, *Introduction to optimization analysis in hydrosystem engineering*. Springer, 2014.

[58] A. Jahan, K. Edwaeds, and M. Bahraminasab, *Multi-criteria Decision Analysis for Supporting the Selection of Engineering Materials in Product Design: Second Edition*. March 2016.

[59] S. Weber, J. Montero, M. Bleckmann, and K. Paetzold, "Parametric design optimisation of tree-like support structure for the laser-based powder bed fusion of metals," *Journal of Manufacturing Processes*, vol. 84, pp. 660–668, 2022.

[60] University of Twente, "Energy data." https://energydata.utwente.nl/. (Accessed on 10/10/2023).

[61] Current Results, "Annual sunshine in the netherlands." https://www.currentresults.com/Weather/Netherlands/sunshine-annual-average.php. (Accessed on 09/25/2023).

[62] World Weather Online, "Enschede annual weather averages - overijssel, nl." https://www.worldweatheronline.com/enschede-weather-averages/overijssel/nl.aspx. (Accessed on 09/25/2023).

[63] T. Berger, C. Amann, H. Formayer, A. Korjenic, B. Pospichal, C. Neururer, and R. Smutny, "Impacts of external insulation and reduced internal heat loads upon energy demand of offices in the context of climate change in vienna, austria," *Journal of Building Engineering*, vol. 5, pp. 86–95, 2016.

[64] M. Ozel, "Effect of insulation location on dynamic heat-transfer characteristics of building external walls and optimization of insulation thickness," *Energy and Buildings*, vol. 72, pp. 288–295, 2014.

[65] MathWorks, "Matlab movmean: Moving mean." https://www.mathworks.com/help/matlab/ref/movmean.html. (Accessed on 10/27/2023).

[66] European Heat Pump Association (ehpa), "Large scale heat pumps in europe." https://www.ehpa.org/wp-content/uploads/2022/11/Large-heat-pumps-in-Europe-and-industrial-uses_2020.pdf, December 2022. (Accessed on 11/27/2023).

[67] Eurostat, "Prices of electricity for non-household consumers in the netherlands from 2008 to 2022 (in euro cents per kilowatt-hour)." `https://www.statista.com/statistics/596254/electricity-non-household-price-netherlands/`, June 2023. (Accessed on 01/15/2024).

[68] Ennatuurlijk, "Tarievenblad 2024." `https://ennatuurlijk.nl/sites/default/files/2023-12/Tarievenblad%202024%20ENN.pdf`, December 2023. (Accessed on 01/15/2024).

[69] AOS, "How do air source heat pumps work? - the technology in a nutshell." `https://www.aosheatpumps.co.uk/air-source-heat-pumps/how-does-an-ashp-work`, 2022. (Accessed on 01/19/2024).

Chapter 8

Appendix
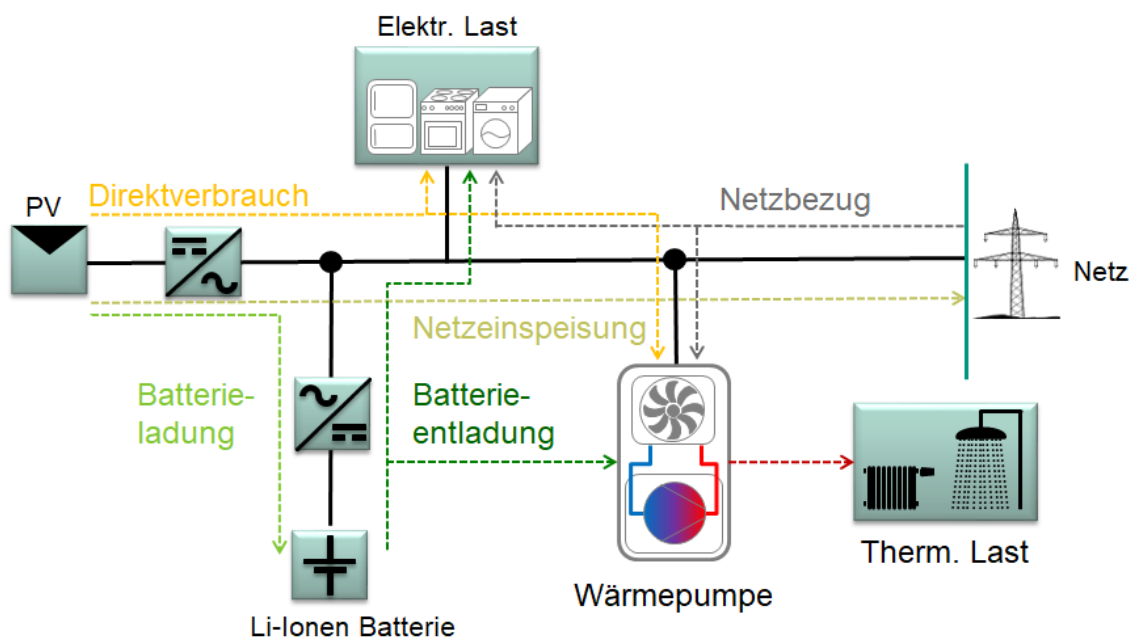
FIGURE 8.1: PV Storage System with Heat Pump System [30]
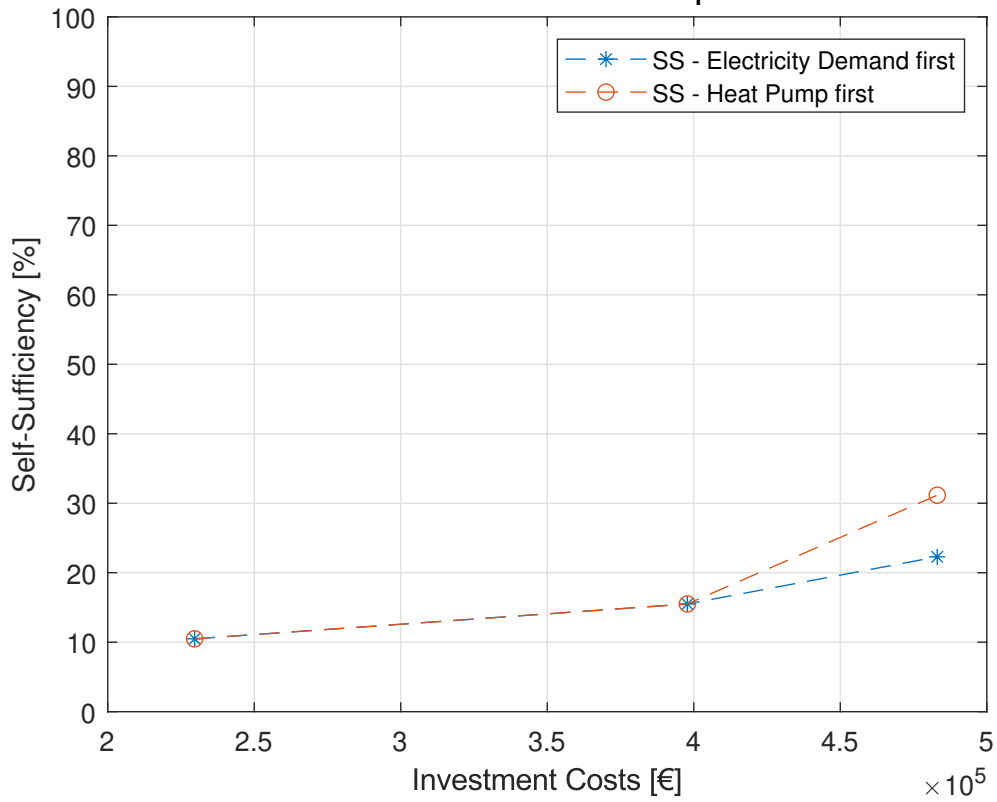
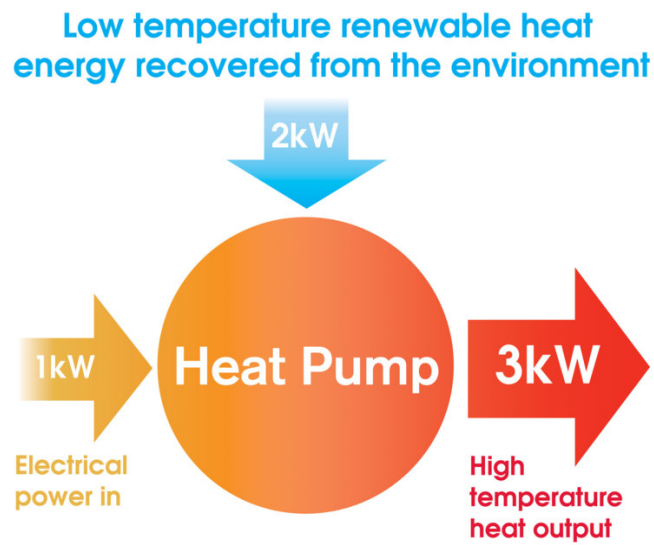FIGURE 8.2: Difference between Prioritization of Electricity Usage

FIGURE 8.3: Principle of a Heat Pump [69]

FIGURE 8.4: Basement and Above-Ground Hot Water Storage Reservoirs in Dessau-Rosslau, Germany [35]